

9-11-2014 12:00 AM

Amyloid β Peptides, Signalling and Trafficking of the $\alpha 7$ Nicotine Receptor

Kirk Young, *The University of Western Ontario*

Supervisor: R. Jane Rylett, *The University of Western Ontario*

A thesis submitted in partial fulfillment of the requirements for the Master of Science degree in Physiology

© Kirk Young 2014

Follow this and additional works at: <https://ir.lib.uwo.ca/etd>

 Part of the [Cellular and Molecular Physiology Commons](#)

Recommended Citation

Young, Kirk, "Amyloid β Peptides, Signalling and Trafficking of the $\alpha 7$ Nicotine Receptor" (2014).
Electronic Thesis and Dissertation Repository. 2588.
<https://ir.lib.uwo.ca/etd/2588>

This Dissertation/Thesis is brought to you for free and open access by Scholarship@Western. It has been accepted for inclusion in Electronic Thesis and Dissertation Repository by an authorized administrator of Scholarship@Western. For more information, please contact wlsadmin@uwo.ca.

AMYLOID β PEPTIDES, SIGNALLING AND TRAFFICKING OF THE $\alpha 7$ NICOTINIC RECEPTOR

(Thesis format: Integrated Article)

by

Kirk F. Young

Graduate Program in Physiology

A thesis submitted in partial fulfilment
of the requirements for the degree of
Master of Science

The School of Graduate and Postdoctoral Studies
The University of Western Ontario
London, Ontario, Canada

© Kirk F. Young 2014

Abstract

The $\alpha 7$ nicotinic acetylcholine receptor (nAChR) is an ionotropic receptor for the neurotransmitter acetylcholine and its precursor, choline. Interestingly, $\alpha 7$ nAChR binds amyloid β 42 (A β 42) peptide, which has a primary role in Alzheimer's disease pathology. A β 42 peptide forms aggregates and different structural forms elicit different physiological outcomes. Oligomeric, fibrillar and non-aggregated preparations of A β 42 were characterized by atomic force microscopy. Immunoblotting of neuronal cells exposed to these preparations determined oligomeric aggregates of A β 42 mediate ERK1/2 intracellular signalling through $\alpha 7$ nAChR. Cell surface ionotropic receptors are regulated through endocytosis to maintain the integrity of neurotransmission. Cellular pathways for endocytosis of $\alpha 7$ nAChR are not fully elucidated. Immunocytochemistry, fluorochrome-labelled proteins, and laser-scanning confocal microscopy identified a clathrin-independent flotillin 1- or caveolin 1 α -associated pathway for $\alpha 7$ nAChR endocytosis. These studies identify a biologically important form of A β 42 relevant to $\alpha 7$ nAChR intracellular signalling and an endocytosis pathway for subcellular regulation of $\alpha 7$ nAChR.

KEYWORDS: nicotinic receptor, amyloid β , amyloid oligomer, amyloid fibril, extracellular signal-regulated kinase mitogen-activated protein kinase, Alzheimer's disease, endocytosis, protein trafficking, lysosome, flotillin, caveolin, α -bungarotoxin

Co-Authorship

The chapter entitled, “Oligomeric Aggregates of Amyloid β Peptide 1-42 Activate ERK/MAPK in SH-SY5Y Cells via the $\alpha 7$ Nicotinic Receptor” is adapted from the manuscript: Young, K.F., Pasternak, S.H., Rylett, R.J. (2009). Oligomeric aggregates of amyloid β peptide 1-42 activate ERK/MAPK in SH-SY5Y cells via the $\alpha 7$ nicotinic receptor. *Neurochemistry International*. 55(8): 796-801. Figures and text are reproduced with permission from the journal, *Neurochemistry International* (Appendix D). All studies were performed by K.F. Young. Experiments were performed in the laboratory of R.J. Rylett. The publication was written by K.F. Young with suggestions from S.H. Pasternak and R.J. Rylett.

The chapter entitled, “The $\alpha 7$ Nicotinic Receptor is Internalized via a Clathrin-Independent, Flotillin- or Caveolin-Associated Endocytic Pathway” was written by K.F. Young with suggestions from R.J. Rylett. All studies were performed by K.F. Young with the assistance of Kathi James. Experiments were performed in the laboratory of R.J. Rylett.

Acknowledgments

I would like to thank my supervisor, Jane Rylett and my advisory committee members, Frank Beier, Stephen Ferguson, Stephen Pasternak, and Andrew Watson for their contributions to the completion of this work. I would also like to thank Tomas Dobransky, for sharing his technical knowledge and wisdom; Ewa Jaworski, for always being very helpful, and Daisy Wong, for filling many a requisition.

Stan Leung, Lina Dagnino, and Andrew Watson, in particular, provided kind and inspiring words. Kem Rogers provided much appreciated guidance and sincerity. I am grateful for the assistance of Peter Simpson.

Table of Contents

Abstract.....	ii
Co-Authorship.....	iii
Acknowledgments.....	iv
Table of Contents.....	v
List of Tables	ix
List of Figures	x
List of Appendices	xii
Abbreviations	xiii
Chapter 1.....	1
1 General Review of the Literature.....	1
1.1 The Cholinergic Neuron	2
1.2 Organization of Cholinergic Neurons in the CNS.....	2
1.3 Nicotinic Receptors of the CNS.....	3
1.4 The $\alpha 7$ nAChR	4
1.5 Localization of the $\alpha 7$ nAChR within the CNS.....	7
1.6 Subcellular Localization and Function of the $\alpha 7$ nAChR within the CNS.....	7
1.7 Signalling of the $\alpha 7$ nAChR	8
1.8 Regulation of the $\alpha 7$ nAChR	8
1.9 The $\alpha 7$ nAChR in Alzheimer's Disease Pathology	9
1.10 Amyloid β Peptides	10
1.11 A β Peptides and the $\alpha 7$ nAChR.....	11
1.12 Objectives and Hypotheses Tested in this Thesis.....	12
1.12.1 Specific Aims:	12

1.12.2	<i>Study One: Oligomeric Aggregates of Amyloid β Peptide 1-42 Activate ERK/MAPK in SH-SY5Y Cells via the $\alpha 7$ Nicotinic Receptor</i>	13
1.12.3	<i>Study Two: The $\alpha 7$ Nicotinic Receptor is Internalized via a Clathrin-Independent, Flotillin- or Caveolin-Associated Endocytic Pathway</i>	14
1.13	References	16
Chapter 2		30
2	Oligomeric Aggregates of Amyloid β Peptide 1-42 Activate ERK/MAPK in SH-SY5Y Cells via the $\alpha 7$ Nicotinic Receptor ^a	30
2.1	Summary	31
2.2	Introduction	32
2.3	Methods	34
2.3.1	Materials	34
2.3.2	A β 42 Preparation and Atomic Force Microscopy	34
2.3.3	Cell Model	37
2.3.4	Cell Culture and Treatments	40
2.3.5	Immunoblotting	40
2.3.6	Statistical Analysis	41
2.4	Results	41
2.4.1	Generation of Oligomeric and Fibrillar Aggregates of A β 42	41
2.4.2	ERK/MAPK Phosphorylation Induced by Oligomeric Aggregates of A β 42	42
2.4.3	Effect of $\alpha 7$ nAChR Antagonist Methyllycaconitine on ERK/MAPK Phosphorylation Induced by Oligomeric A β 42	50
2.5	Discussion	53
2.6	References	59
Chapter 3		71
3	The $\alpha 7$ Nicotinic Receptor is Internalized via a Clathrin-Independent, Flotillin- or Caveolin-Associated Endocytic Pathway	71

3.1	Summary	72
3.2	Introduction	73
3.3	Methods.....	74
3.3.1	Materials	74
3.3.2	DNA Constructs and Site-Directed Mutagenesis	75
3.3.3	Cell Model	76
3.3.4	Cell Culture and Transfection	77
3.3.5	Immunoblotting	78
3.3.6	Fluorescent α -Bungarotoxin Internalization and Co-localization	78
3.3.7	Clathrin and Dynamin Inhibition.....	79
3.3.8	Cytochalasin D Treatment and RhoGTPase Inhibition.....	80
3.3.9	Co-localization with Flotillin 1 and Caveolin 1 α	80
3.3.10	Confocal Microscopy.....	81
3.3.11	Criteria for Selection of Micrographs	81
3.4	Results.....	82
3.4.1	The Chaperone Protein, hRIC3 is Required for Functional Cell Surface Expression of α 7 nAChR in HEK 293 Cells	82
3.4.2	α -Bungarotoxin Induces Internalization of the α 7 nAChR.....	88
3.4.3	α 7 nAChR- α BTX Complexes Traffic Through Late Endosomes to Lysosomes	93
3.4.4	Canonical Endocytic Receptor Trafficking Motifs Do Not Alter Cell Surface Expression or Endocytosis of α 7 nAChR	97
3.4.5	Endocytosis of α 7nAChR- α BTX Complexes is Independent of Clathrin .	102
3.4.6	Inhibition of Actin Dynamics, RhoGTPases or RalGTPase Does Not Block α 7 nAChR Endocytosis	107
3.4.7	α 7 nAChR- α BTX Complexes Endocytose Through Flotillin 1 and Caveolin 1 α Pathways.....	111

3.5	Discussion	117
3.6	References	123
Chapter 4.....		136
4	General Discussion	136
4.1	Conclusions	137
4.1.1	<i>Study One:</i> Oligomeric aggregates of amyloid β peptide 1-42 activate ERK/MAPK in SH-SY5Y cells via the $\alpha 7$ nicotinic receptor	137
4.1.2	<i>Study Two:</i> The $\alpha 7$ nicotinic receptor is internalized via a clathrin- independent, flotillin- or caveolin-associated endocytic pathway	137
4.2	Contributions to the Current State of Knowledge.....	138
4.3	Limitations of Research	142
4.4	Suggestions for Future Studies	143
4.5	Significance of the Research	144
4.6	References	145
Appendices.....		151
Curriculum Vitae		157

List of Tables

Table 3.1 Oligonucleotide primers used in cloning and sub-cloning of the human $\alpha 7$ nAChR subunit and hRIC3 cDNA.	76
--	----

List of Figures

Figure 1.1 Structure of the nAChR.	5
Figure 2.1 Preparation of A β 42 Peptides and Cell Culture Treatments.	35
Figure 2.2 Atomic Force Microscopy and Image Analysis.	38
Figure 2.3 Atomic force microscopy of oligomeric, fibrillar and non-aggregated preparations of A β 42.	43
Figure 2.4 Distribution of aggregate heights within oligomeric preparations of A β 42.	45
Figure 2.5 Phosphorylation of ERK1/2 induced by A β 42 is dependent upon the concentration and structural form of the peptide.	46
Figure 2.6 Phosphorylation of ERK1/2 induced by A β 42 is dependent upon the exposure time and structural form of the peptide.	48
Figure 2.7 Oligomeric A β 42-induced ERK1/2 phosphorylation is dependent upon the α 7 nAChR and the upstream MAPK kinase, MEK1/2.	51
Figure 2.8 A model for oligomeric A β 42 signalling through the α 7 nAChR.	58
Figure 3.1 The chaperone protein, hRIC3 is required for functional cell surface expression of α 7 nAChR in HEK 293 cells.	84
Figure 3.2 Pulse-chase method for investigating α BTX-induced internalization of α 7 nAChR.	89
Figure 3.3 α BTX binding induces internalization of α 7 nAChR.	90
Figure 3.4 α BTX induces internalization of α 7 nAChR in neuronal cells.	94
Figure 3.5 α 7 nAChR- α BTX complexes traffic to late endosomes.	98

Figure 3.6 $\alpha 7$ nAChR- α BTX complexes traffic through late endosomes/lysosomes but not rapidly or slowly recycling endosomes or Rab5 positive early endosomes.	100
Figure 3.7 Canonical endocytic receptor trafficking motifs do not alter cell surface expression or endocytosis of $\alpha 7$ nAChR.	103
Figure 3.8 Endocytosis of $\alpha 7$ nAChR- α BTX complexes is independent of clathrin.....	108
Figure 3.9 Inhibition of actin dynamics, RhoGTPases or RalGTPase does not block $\alpha 7$ nAChR endocytosis.	112
Figure 3.10 $\alpha 7$ nAChR- α BTX complexes internalize through flotillin 1 and caveolin 1 α pathways.	115
Figure 3.11 A Model for α BTX-induced internalization of the $\alpha 7$ nAChR.....	122

List of Appendices

Appendix A. Addition of the FLAG epitope to the $\alpha 7$ nAChR subunit slows receptor-dependent Ca^{2+} responses to the agonist nicotine.	152
Appendix B. Cell surface biotinylation of HEK 293 cells transfected with FLAG- $\alpha 7$ nAChR cDNA with or without co-transfection with HA-hRIC3 cDNA.	154
Appendix C. De novo cell surface $\alpha 7$ nAChR following α BTX-induced receptor internalization.	155
Appendix D. Permission for reproduction from <i>Neurochemistry International</i>	156

Abbreviations

A β	amyloid β
A β 40	amyloid β , 40 amino acid length fragment
A β 42	amyloid β , 42 amino acid length fragment
ACh	acetylcholine
AD	Alzheimer's disease
AFM	atomic force microscopy
α 7 nAChR	nicotinic acetylcholine receptor comprised of α 7 subunits
α BTX	α -bungarotoxin
AMPA	α -amino-3-hydroxy-5-methyl-4-isoxazolepropionic acid receptor
ANOVA	analysis of variance
AP180-C	carboxyl-terminal fragment of adaptor protein 180
APP	amyloid β precursor protein
BSA	bovine serum albumin - fraction V
CD	circular dichroism
CNS	central nervous system
CSF	cerebrospinal fluid
DAPI	4',6-diamidino-2-phenylindole
DMEM	Dulbecco's modified Eagle's medium

DMSO	dimethyl sulfoxide
EEA1	early endosomal autoantigen 1
ER	endoplasmic reticulum
ERK/MAPK	extracellular signal-regulated kinase mitogen-activated protein kinase
ERK1/2	extracellular signal-regulated kinase 1 and 2
FBS	fetal bovine serum
FLAG- $\alpha 7$ nAChR	nicotinic acetylcholine receptor comprised of $\alpha 7$ subunits, each with a FLAG epitope on the extracellular carboxyl-terminus
G418	Geneticin
GABA	γ -aminobutyric acid
GABA _A R	γ -aminobutyric acid type A receptor
GFP	green fluorescent protein
HA	influenza haemagglutinin
HA-hRIC3	human homologue of RIC3, product of the <i>Caenorhabditis elegans</i> gene, resistant to inhibitors of cholinesterase (ric-3), with an influenza haemagglutinin epitope on the carboxyl-terminus
HBSS	HEPES-buffered salt solution
HFIP	hexafluoro-2-propanol
HPLC	high-performance liquid chromatography
hRIC3	human homologue of RIC3, product of the <i>Caenorhabditis elegans</i> gene, resistant to inhibitors of cholinesterase (ric-3)

HRP	horseradish peroxidase
K _d	dissociation constant
LAMP1	lysosomal-associated membrane protein 1
LTP	long-term potentiation
MEK1/2	mitogen-activated protein kinase kinase 1 and 2
MEM	Eagle's minimal essential medium with Earle's salts
MLA	methyllycaconitine
nAChR	nicotinic acetylcholine receptor
NGF	nerve growth factor 2.5S
NMDA	<i>N</i> -methyl <i>D</i> -aspartate receptor
p75NTR	low-affinity neurotrophin receptor
PBS	phosphate-buffered saline
PLP	periodate 0.2%, lysine 1.4%, paraformaldehyde 2%
PNS	peripheral nervous system
PVDF	polyvinylidene fluoride
RIC3	RIC3, product of the <i>Caenorhabditis elegans</i> gene, resistant to inhibitors of cholinesterase (ric-3)
SDS-PAGE	sodium dodecyl sulfate-polyacrylamide gel electrophoresis
SEC	size-exclusion chromatography

SNARE	<i>N</i> -ethylmaleimide-sensitive factor attachment protein receptor
ThT	thioflavin T
TM	transmembrane domain
TrkA	high-affinity neurotrophin tyrosine kinase receptor type 1
VTA	ventral tegmental area
YFP	yellow fluorescent protein

Chapter 1

1 General Review of the Literature

1.1 The Cholinergic Neuron

Acetylcholine (ACh) was the first neurotransmitter described (1), it mediates a broad range of physiological functions in the central (CNS) and peripheral (PNS) nervous systems. Neurons that synthesize and store ACh are defined as cholinergic (2). ACh synthesis is catalyzed by the enzyme choline acetyltransferase in the cytoplasm of the nerve terminal from the substrates choline and acetyl-CoA (3, 4). Newly synthesized ACh is packaged into secretory vesicles by the vesicular ACh transporter (5 - 11). Neuronal membrane depolarization leads to the release of vesicular ACh into the synaptic cleft by a highly-regulated, Ca^{2+} -dependent, complex cascade of events (12 - 14). Upon release from the nerve terminal, ACh may bind its cognate receptors, postsynaptic nicotinic or muscarinic receptors or presynaptic nicotinic and muscarinic autoreceptors (2, 15 - 17). Excess, unbound ACh in the extracellular milieu is cleared by the enzyme acetylcholinesterase, which hydrolyzes ACh into free acetate and choline (18). Free choline can be taken up from the extracellular space by the sodium-dependent high-affinity choline transporter, which resides almost exclusively in cholinergic nerve terminals and facilitates the replenishment of intracellular choline (19, 20). In the PNS, cholinergic neurons innervate skeletal muscle and a number of target tissues of the sympathetic and parasympathetic branches of the autonomic nervous system. In the CNS, cholinergic neurons contribute to learning, memory, arousal, and sleep functions (21).

1.2 Organization of Cholinergic Neurons in the CNS

Cholinergic neurons within the CNS innervate brain structures either intrinsically or extrinsically (22 - 24). Intrinsic innervation arises from cholinergic interneurons within the same brain structure, which project their axons locally (23, 24). Innervation of the striatum and its structures, the islands of Calleja, olfactory tubercle, nucleus accumbens, and caudate-putamen is intrinsic (22 - 25). Extrinsic innervation connects cholinergic regions to other brain structures through efferent projections (23, 24, 26). Cholinergic projection neurons have been divided into two subsystems, the basal forebrain and the

pontomesencephalic complex (23, 24). Axons from the basal forebrain innervate the limbic structures and neocortex, while axons from the pontomesencephalic complex innervate the thalamus and superior colliculus (23, 24). Cholinergic cell groups in the CNS are diffusely organized and are not confined within traditional nuclear groups, but are intermixed with non-cholinergic neurons (24). In particular, the nucleus basalis of Meynert, which provides the primary cholinergic input from the basal forebrain to the neocortex, contains a mixture of cholinergic, GABAergic, peptidergic, and dopaminergic neurons (27 - 32). The major groups of cholinergic neurons within the CNS are designated Ch1 – Ch8 (24). The cholinergic cell groupings within the basal forebrain are the medial septal nucleus (Ch1), nucleus of the diagonal band of Broca (Ch2), nucleus of the horizontal band of Broca (Ch3), and the nucleus basalis of Meynert (Ch4) (24). Ch5 and Ch6 designate cholinergic neurons of the pedunculopontine and lateral dorsal nuclei, respectively; Ch7 designates cholinergic cells of the medial habenula, and Ch8 designates cholinergic neurons in the parabrachial nucleus (24). Ch1 – Ch4 are major sources of cholinergic projections to the hippocampus, olfactory bulb, amygdala and cerebral cortex (24). Ch5 and Ch6 are a source of projections to the thalamic nuclei, Ch7 to the interpeduncular nucleus, and Ch8 to the superior colliculus (24). To a large extent, cholinergic neurons innervate structures of the brain that are involved in learning and memory and other higher order functions. Although considerable research has focused on the role that muscarinic ACh receptors play in cholinergic modulation of the neural network (33), nicotinic ACh receptors (nAChR) may also contribute substantially to synaptic plasticity (34).

1.3 Nicotinic Receptors of the CNS

Neuronal nAChRs are distributed widely throughout the brain, with the majority localized to the pre-synapse or pre-terminal, where they modulate the release of almost all neurotransmitters (35). They share a common structure comprised of five subunits that surround a central gated cation pore, permeable to Na^+ , K^+ , and Ca^{2+} , which is opened upon ligand binding (35, 36). They have distinct pharmacological and functional

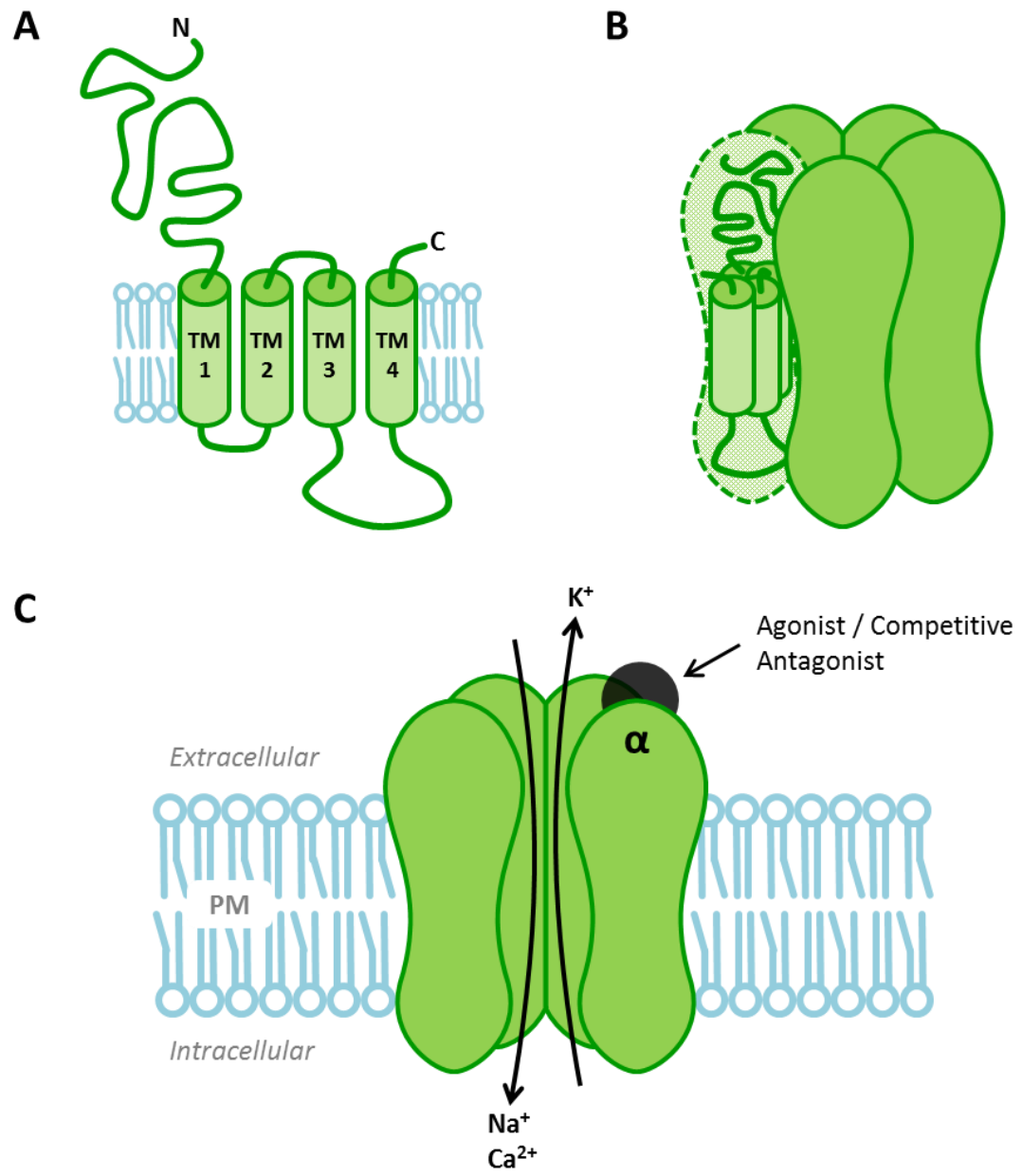
properties that are determined by their subunit composition (35). Nine α ($\alpha 2 - \alpha 10$) and three β ($\beta 2 - \beta 4$) neuronal nAChR subunits have been identified to date (35). The two major subtypes of nAChR found in the mammalian CNS are heteromeric receptors containing $\alpha 4\beta 2$ subunits and homomeric receptors comprised of $\alpha 7$ subunits (35). Each neuronal nAChR subunit has a large hydrophilic extracellular amino-terminus domain that forms the ACh binding site, followed by three transmembrane domains (TM1 - TM3), a large intracellular loop, a fourth transmembrane domain (TM4), and a short extracellular carboxyl-terminus (37) (Figure 1.1). Ligand binding occurs at the interface between α and adjacent subunits, the heteromeric $\alpha 4\beta 2$ nAChR, with two $\alpha 4$ subunits and three $\beta 2$ subunits, binds two ligands and the homomeric $\alpha 7$ nAChR, with five $\alpha 7$ subunits, has five ligand binding sites (35).

1.4 The $\alpha 7$ nAChR

The human $\alpha 7$ nAChR subunit was cloned originally from the SH-SY5Y human neuroblastoma cell line based on sequence homology with the chick and rat homologue α -bungarotoxin (α BTX)-binding receptor (38 - 40). α BTX is a subtype-selective nAChR antagonist isolated from the venom of the Many-banded krait, *Bungarus multicinctus* (36, 41). The $\alpha 7$ nAChR is unique in the brain in that it has low binding affinity for nAChR agonists, such as ACh and nicotine, binds choline as an agonist, and binds α BTX with high affinity (36). The receptor also has unique biophysical properties, exhibiting brief channel open times, a large ion conductance, and a high permeability to Ca^{2+} relative to Na^+ (36). Through high Ca^{2+} conductance, the $\alpha 7$ nAChR is linked to activation of a number of intracellular signalling events (42). Although the $\alpha 7$ nAChR was originally thought to exist only as a homomer in the mammalian CNS, evidence from heterologous expression studies demonstrate the $\alpha 7$ subunit can also form functional heteromeric receptors with $\alpha 5$, $\beta 2$, or $\beta 3$ subunits (43 - 47). Only very recently has biochemical evidence emerged in support of the existence of an $\alpha 7\beta 2$ -containing heteromeric nAChR in the brain (48). The $\alpha 7\beta 2$ nAChR has a pharmacological profile similar to the $\alpha 7$ nAChR in that its ligand binding properties reflect that of the

Figure 1.1 Structure of the nAChR.

The neuronal nAChR is a macromolecule comprised of subunit proteins of similar tertiary structure. **(A)** Each nAChR subunit contains a large hydrophilic extracellular amino-terminus, followed by three transmembrane domains (TM1 - TM3), a large intracellular loop, a fourth transmembrane domain (TM4), and a short extracellular carboxyl-terminus. **(B)** Five subunits combine to form a functional receptor pentamer. **(C)** The five subunits surround a central cation pore that is permeable to Na^+ , K^+ , and Ca^{2+} ; gating of the cation pore occurs in response to agonist binding at the interface between α and adjacent subunits. PM, plasma membrane. Adapted from (35 - 37).



interface between adjacent $\alpha 7$ subunits (46, 48). While the $\alpha 7$ nAChR is expressed throughout the brain, the $\alpha 7\beta 2$ nAChR appears to be localized exclusively to basal forebrain cholinergic neurons (48). This thesis will focus on signalling and molecular regulation of the homomeric $\alpha 7$ nAChR. Altered $\alpha 7$ nAChR activity is implicated in cholinergic dysfunction in a number of neurological and psychiatric disorders, including Alzheimer's disease (AD) and schizophrenia (34). A 2-base pair deletion polymorphism in the partial duplication of the $\alpha 7$ nAChR gene has been linked to schizophrenia (49, 50).

1.5 Localization of the $\alpha 7$ nAChR within the CNS

In situ hybridization studies in monkey brain demonstrate widespread expression of $\alpha 7$ nAChR subunit mRNA throughout the brain, including the neocortex, basal ganglia and the ventral tegmental area (VTA), with the highest levels found in the hippocampus, particularly the dentate gyrus (51). [125 I]- α BTX binding in adult rat brain provides similar localization, with moderate binding throughout the cerebral cortex and a high level of binding in the hippocampus (52). It is evident that the $\alpha 7$ nAChR has a role in mediating cholinergic input to several brain regions and may have an important role in cholinergic modulation of synaptic plasticity in the hippocampus (52).

1.6 Subcellular Localization and Function of the $\alpha 7$ nAChR within the CNS

The subcellular localization and function of $\alpha 7$ nAChR in the brain has largely been determined through electrophysiology studies and the use of receptor-selective antagonists. Although there are some examples of $\alpha 7$ nAChR-mediated fast-synaptic transmission to interneurons in the hippocampus (53 - 55), to a greater extent, the $\alpha 7$ nAChR serves a modulatory role in the brain by regulating the release of other neurotransmitters. Presynaptic $\alpha 7$ nAChR directly modulate the release of glutamate in the hippocampus and VTA, as well as excitatory amino acids in the prefrontal cortex (56 - 58). Evidence that the $\alpha 7$ nAChR participates in cholinergic volume transmission, as

opposed to synaptic transmission, stems from studies of $\alpha 7$ nAChR localization in the VTA, where cholinergic terminals are located remotely from α BTX labelling of the receptor (57). Presynaptic $\alpha 7$ nAChR is also involved in indirect release of dopamine from the striatum and prefrontal cortex and noradrenaline from the hippocampus (59 - 61). This can occur through the triggering of glutamate release and/or γ -aminobutyric acid (GABA) release and GABAergic disinhibition (61). Somatodendritic $\alpha 7$ nAChR in the hippocampus can depolarize pyramidal neurons to facilitate short- and long-term potentiation within the hippocampus (62 - 64).

1.7 Signalling of the $\alpha 7$ nAChR

The modulatory role of the $\alpha 7$ nAChR in the CNS likely reflects the permeability of the ion channel to Ca^{2+} and local activation of Ca^{2+} -dependent signalling pathways. Modulation of neurotransmitter release may involve receptor-dependent activation of ryanodine-sensitive intracellular Ca^{2+} stores and extracellular signal-regulated kinase 1 and 2 (ERK1/2)-dependent phosphorylation of synapsin-1 (58). Additionally, activity of the receptor has been linked to the phosphorylation of cyclic adenosine monophosphate response element binding protein through protein kinase A-dependent activation of ERK1/2 (65, 66), which may result in the expression of genes that are important for synaptic plasticity (42, 67). The $\alpha 7$ nAChR may also play a role in neuroprotection through the phosphatidylinositol 3-kinase-dependent signalling pathway (68, 69).

1.8 Regulation of the $\alpha 7$ nAChR

A number of factors that regulate function of the $\alpha 7$ nAChR have been identified. Through primary amino acid sequence analysis, several amino acid residues within the large intracellular loop of the $\alpha 7$ nAChR appear to be important for cell surface expression in *Xenopus laevis* (70). These residues may act in a manner similar to the endoplasmic reticulum (ER) retention motif identified on the $\alpha 1$ nAChR subunit, which is conserved among heteromeric-receptor forming nAChR subunits (71). Post-

translational modification of the $\alpha 7$ nAChR in the form of palmitoylation appears to be required for the assembly of $\alpha 7$ nAChR subunits into functional receptors in PC12 cells (72). It is apparent that host-cell specific subcellular proteins are required for functional expression of $\alpha 7$ nAChR, as $\alpha 7$ nAChR subunits heterologously expressed in HEK 293 cells do not form functional α BTX-binding channels unless they are co-expressed with the chaperone protein RIC3 (73 - 75), the product of the *Caenorhabditis elegans* gene, resistant to inhibitors of cholinesterase (*ric-3*), an ER protein that co-ordinates efficient assembly of $\alpha 7$ nAChR subunits into receptor pentamers (76). Receptor activity can be regulated by Src-family tyrosine kinases directly through phosphorylation of tyrosine residues on the large intracellular loop of the $\alpha 7$ nAChR subunit (77) and indirectly in a manner that does not involve phosphorylation of the receptor, but is mediated by *N*-ethylmaleimide-sensitive factor attachment protein receptors (SNAREs) (78). SNAREs are also involved in the activity dependent recycling of cell surface $\alpha 7$ nAChR in response to nicotine stimulation (79). Additionally, somatodendritic localization of $\alpha 7$ nAChR on hippocampal neurons is regulated by a tyrosine motif in the large intracellular loop of the subunit (63). Although several of these studies focused on factors that are involved in the assembly and insertion of $\alpha 7$ nAChR into the plasma membrane, few have described mechanisms involved in its removal from the cell surface and receptor down-regulation. Chapter 3 of this thesis demonstrates that binding of the competitive antagonist α BTX leads to receptor internalization through a unique endocytic mechanism and trafficking of the receptor to a degradative compartment in the cell.

1.9 The $\alpha 7$ nAChR in Alzheimer's Disease Pathology

Positron emission tomography studies employing ^{11}C -nicotine to measure nAChR levels in the brains of AD subjects have demonstrated a global reduction in nAChRs in the brain that correlate with cognitive impairment (80). However, more recent investigations with the $\alpha 7$ nAChR-selective ligand [^3H]-methyllycaconitine (MLA) suggest that the $\alpha 7$ nAChR may not change during the progression of cognitive decline (81).

With the development of transgenic mouse models that express proteins linked to familial or early-onset AD, investigators have determined that $\alpha 7$ nAChR in hippocampus may be up-regulated in response to increased amyloid β peptide production (82). Critically, knockout of the $\alpha 7$ nAChR gene from an AD mouse model protects against the synaptic dysfunction and learning and memory deficits associated with expression of the AD-related transgene (83)

1.10 Amyloid β Peptides

The proteolysis of the integral membrane protein amyloid β precursor protein (APP), resulting in the generation of amyloid β ($A\beta$) peptides, is hypothesized to be an initiating event in AD pathology (84). $A\beta$ peptides are generated from the sequential cleavage of APP, first by β -secretase activity of the β -site APP-cleaving enzyme (85), resulting in shedding of the APP ectodomain, then by intra-membrane cleavage of the remaining transmembrane fragment of APP by the γ -secretase complex, resulting in the secretion of $A\beta$ peptide and the release of the APP intracellular domain (86, 87). The γ -secretase complex is composed of four proteins, presenilin-1 (PS1) or PS2, nicastrin, APH1 and PEN2 (85, 88 - 90). β - and γ -secretase cleavage of APP can generate multiple $A\beta$ peptide fragments, with the most abundant being 40 ($A\beta 40$) or 42 ($A\beta 42$) amino acids in length, depending on the site of cleavage (84). Each contains a small portion of the APP transmembrane domain (84). Mutations in APP, PS1 and PS2 are linked to early onset familial AD, resulting from an increased ratio of $A\beta 42/A\beta 40$ generation (84). $A\beta 42$ contains two additional hydrophobic amino acid residues, increasing its potential for aggregation into soluble oligomeric forms which can bind receptors and interfere with synaptic transmission, or form insoluble fibrillar aggregates found at the core of amyloid plaques in the end stages of AD (84). Measures of the levels of soluble $A\beta$ in the brain are a better correlate with the presence and degree of cognitive deficits than the burden of $A\beta$ plaques, suggesting soluble $A\beta$ is a causative factor in AD pathology (91 - 94).

1.11 A β Peptides and the α 7 nAChR

Initial studies that investigated the interaction between A β and α 7 nAChR were based on observations that α 7 nAChR expression correlated with brain areas that exhibited A β plaques, particularly the hippocampus and cerebral cortex (95). The α 7 nAChR was found to co-immunoprecipitate with A β 42 from human AD brain tissue and localize to A β plaques in the hippocampus (95). Subsequent studies determined that A β 42 binds with high affinity to the α 7 nAChR (96) and that cell surface expression of α 7 nAChR can facilitate intracellular accumulation of the peptide (97). Electrophysiology experiments determined A β 42 could either activate α 7 nAChR responses in heterologous expression systems (98) or inhibit ACh-evoked receptor responses in the same systems (99, 100) or from native α 7 nAChR in hippocampus (101). These observations are not without controversy, as it is apparent that A β 42 can activate Ca²⁺ signalling independent of receptor binding (102) and that A β 42 may interact directly with plasma membrane lipids (103). An important caveat that may explain these differences is that the A β peptides used in these experiments have largely been uncharacterized in terms of the different structural forms present or the state of aggregation of the peptide. Given the propensity for A β 42 to aggregate in solution, it is difficult to make comparisons between studies that have not characterized the aggregation state of the peptide because different aggregates may yield different physiological outcomes. In Chapter 2 of this thesis, I examined the effects of different structural forms of A β 42 peptides upon extracellular signal-regulated kinase mitogen-activated protein kinase (ERK/MAPK) signalling through the α 7 nAChR and identify oligomeric aggregates as the biologically relevant form.

1.12 Objectives and Hypotheses Tested in this Thesis

My research interests lie in characterizing the structural forms of A β 42 peptide capable of activating α 7 nAChR-dependent intracellular signalling pathways. There is evidence A β 42 peptide binds the α 7 nAChR to activate the receptor ion channel (95) and receptor-dependent signalling pathways (82). However, the state of aggregation of A β 42 peptide in these experiments has not been fully characterized, and the structural forms of the peptide capable of activating the α 7 nAChR have yet to be determined. I am also interested in investigating subcellular mechanisms that may be involved in regulating cell surface levels of the α 7 nAChR. A number of cell surface receptors undergo regulated endocytosis in response to ligand binding as a means of modulating receptor-dependent signalling. I would like to determine if ligand binding induces internalization of the α 7 nAChR and elucidate the subcellular mechanisms involved in this process.

1.12.1 Specific Aims:

- 1) To identify the structural form of A β 42 peptide aggregates that signal through the α 7 nAChR and characterize their effects with dose and time.
- 2) To identify factors that affect cell surface expression of the α 7 nAChR and elucidate the subcellular mechanisms involved.

1.12.2 *Study One: Oligomeric Aggregates of Amyloid β Peptide 1-42 Activate ERK/MAPK in SH-SY5Y Cells via the $\alpha 7$ Nicotinic Receptor*

Rationale: Previous studies have shown that A β 42 peptide activates the ERK/MAPK intracellular signalling pathway through the $\alpha 7$ nAChR (82, 104). However, A β 42 peptide readily aggregates in solution to take on different structural forms with different biological consequences and the structural form of the peptide in these studies was not characterized. Thus, the aim of this study was to determine the structural form of A β 42 peptide aggregates capable of activating ERK/MAPK signalling through the $\alpha 7$ nAChR.

Hypothesis: A β 42-dependent ERK/MAPK signalling through the $\alpha 7$ nAChR is independent of the structural form or aggregation state of the peptide.

Outcome: Using atomic force microscopy, I characterized A β 42 peptide that had been pre-incubated under different solution conditions to yield either oligomeric or fibrillar aggregates. When these were added to human neuroblastoma cells in culture and changes in ERK1/2 phosphorylation were measured by immunoblotting, oligomeric aggregates of A β 42 acutely increased phosphorylation of ERK1/2 in a concentration- and time-dependent manner. Fibrillar aggregates of A β 42 or A β 42 that had not been pre-incubated to induce aggregate formation did not significantly change the level ERK1/2 phosphorylation. Importantly, MLA, a competitive antagonist selective for the $\alpha 7$ nAChR, inhibited oligomeric A β 42-induced ERK1/2 phosphorylation. Thus, oligomeric aggregates of A β 42 are the structural form of the peptide that activates ERK/MAPK through the $\alpha 7$ nAChR.

1.12.3 *Study Two: The $\alpha 7$ Nicotinic Receptor is Internalized via a Clathrin-Independent, Flotillin- or Caveolin-Associated Endocytic Pathway*

Rationale: Some ionotropic neurotransmitter receptors undergo regulated clathrin-dependent endocytosis in response to ligand binding, a process that maintains the integrity of neurotransmission (105, 106). Primary amino acid sequence analysis of the large intracellular loop of the $\alpha 7$ nAChR subunit revealed two clathrin adaptor-protein binding motifs that could regulate trafficking of the receptor from the cell surface. The aim of this study was to determine if the $\alpha 7$ nAChR undergoes endocytosis in response to ligand binding and to determine the subcellular mechanisms involved.

Hypothesis: Cell surface expression of the $\alpha 7$ nAChR is not regulated by clathrin and dynamin and is independent of adaptor protein binding motifs within the large intracellular loop of the receptor subunit.

Outcome: Confocal microscopy of cells fixed following pulse-chase with fluorochrome-labelled α BTX revealed binding α BTX caused internalization of the $\alpha 7$ nAChR. Following internalization, $\alpha 7$ nAChR- α BTX complexes trafficked to early and late endosomes and lysosomes, subcellular membrane compartments identified by antibody labelling of endogenous and heterologous expression of fluorescent protein-tagged compartmental markers. Null mutation of clathrin adaptor-protein binding motifs within the large intracellular loop of the $\alpha 7$ nAChR subunit did not prevent α BTX-induced receptor internalization. Over-expression of dominant negative proteins that block clathrin-dependent endocytosis determined internalization did not occur through a clathrin-dependent mechanism. Inhibition of actin cytoskeleton polymerization, and over-expression of dominant negative proteins that block actin dynamics, determined internalization did not occur through common clathrin-independent mechanisms. Rather, internalized $\alpha 7$ nAChR- α BTX complexes localized with fluorescent protein-tagged flotillin 1 and caveolin 1 α , markers for specialized plasma membrane regions associated with clathrin-independent endocytosis. Thus, I demonstrate α BTX binding to

the $\alpha 7$ nAChR causes internalization through a clathrin-independent flotillin 1- or caveolin 1 α -associated pathway, and trafficking through early and late endosomes to the lysosomal compartment.

1.13 References

1. Loewi, O. (1921) Über humorale Übertragbarkeit der Herznervenwirkung - I. Mitteilung. *Pflügers Archiv für die Gesamte Physiologie des Menschen und der Tiere* **189**: 239-242.
2. Blusztajn, J.K. and Berse, B. (2000) The cholinergic neuronal phenotype in Alzheimer's disease. *Metab. Brain Dis.* **15**: 45-64.
3. Tucek, S. (1983) Acetylcoenzyme A and the synthesis of acetylcholine in neurones: review of recent progress. *Gen. Physiol. Biophys.* **2**: 313-324.
4. Fulton, J.F. and Nachmansohn, D. (1943) Acetylcholine and the Physiology of the Nervous System. *Science* **97**: 569-571.
5. Alfonso, A., Grundahl, K., Duerr, J.S., Han, H.P., Rand, J.B. (1993) The *Caenorhabditis elegans* unc-17 gene: a putative vesicular acetylcholine transporter. *Science* **261**: 617-619.
6. Bahr, B.A., Clarkson, E.D., Rogers, G.A., Noremborg, K., Parsons, S.M. (1992) A kinetic and allosteric model for the acetylcholine transporter-vesamicol receptor in synaptic vesicles. *Biochemistry* **31**: 5752-5762.
7. Bahr, B.A., Noremborg, K., Rogers, G.A., Hicks, B.W., Parsons, S.M. (1992) Linkage of the acetylcholine transporter-vesamicol receptor to proteoglycan in synaptic vesicles. *Biochemistry* **31**: 5778-5784.
8. Bejanin, S., Cervini, R., Mallet, J., Berrard, S. (1994) A unique gene organization for two cholinergic markers, choline acetyltransferase and a putative vesicular transporter of acetylcholine. *J. Biol. Chem.* **269**: 21944-21947.
9. Erickson, J.D., Varoqui, H., Schafer, M.K., Modi, W., Diebler, M.F., Weihe, E., Rand, J., Eiden, L.E., Bonner, T.I., Usdin, T.B. (1994) Functional identification of a

- vesicular acetylcholine transporter and its expression from a "cholinergic" gene locus. *J. Biol. Chem.* **269**: 21929-21932.
10. Parsons, S.M., Bahr, B.A., Gracz, L.M., Kaufman, R., Kornreich, W.D., Nilsson, L., Rogers, G.A. (1987) Acetylcholine transport: fundamental properties and effects of pharmacologic agents. *Ann. N. Y. Acad. Sci.* **493**: 220-233.
 11. Roghani, A., Feldman, J., Kohan, S.A., Shirzadi, A., Gundersen, C.B., Brecha, N., Edwards, R.H. (1994) Molecular cloning of a putative vesicular transporter for acetylcholine. *Proc. Natl. Acad. Sci. U. S. A.* **91**: 10620-10624.
 12. Bauerfeind, R., Galli, T., De Camilli, P. (1996) Molecular mechanisms in synaptic vesicle recycling. *J. Neurocytol.* **25**: 701-715.
 13. Fernandez-Chacon, R. and Sudhof, T.C. (1999) Genetics of synaptic vesicle function: toward the complete functional anatomy of an organelle. *Annu. Rev. Physiol.* **61**: 753-776.
 14. Sudhof, T.C. (1995) The synaptic vesicle cycle: a cascade of protein-protein interactions. *Nature* **375**: 645-653.
 15. Lapchak, P.A., Araujo, D.M., Quirion, R., Collier, B. (1989) Presynaptic cholinergic mechanisms in the rat cerebellum: evidence for nicotinic, but not muscarinic autoreceptors. *J. Neurochem.* **53**: 1843-1851.
 16. Wilkie, G.I., Hutson, P., Sullivan, J.P., Wonnacott, S. (1996) Pharmacological characterization of a nicotinic autoreceptor in rat hippocampal synaptosomes. *Neurochem. Res.* **21**: 1141-1148.
 17. Vizi, E.S. and Somogyi, G.T. (1989) Prejunctional modulation of acetylcholine release from the skeletal neuromuscular junction: link between positive (nicotinic)- and negative (muscarinic)-feedback modulation. *Br. J. Pharmacol.* **97**: 65-70.

18. Augustinsson, K.B. and Nachmansohn, D. (1949) Distinction between Acetylcholine-Esterase and Other Choline Ester-splitting Enzymes. *Science* **110**: 98-99.
19. Suszkiw, J.B. and Pilar, G. (1976) Selective localization of a high affinity choline uptake system and its role in ACh formation in cholinergic nerve terminals. *J. Neurochem.* **26**: 1133-1138.
20. Okuda, T. and Haga, T. (2000) Functional characterization of the human high-affinity choline transporter. *FEBS Lett.* **484**: 92-97.
21. Oda, Y. (1999) Choline acetyltransferase: the structure, distribution and pathologic changes in the central nervous system. *Pathol. Int.* **49**: 921-937.
22. Woolf, N.J. and Butcher, L.L. (1981) Cholinergic neurons in the caudate-putamen complex proper are intrinsically organized: a combined Evans blue and acetylcholinesterase analysis. *Brain Res. Bull.* **7**: 487-507.
23. Woolf, N.J. (1991) Cholinergic systems in mammalian brain and spinal cord. *Prog. Neurobiol.* **37**: 475-524.
24. Mesulam, M.M. (1990) Human brain cholinergic pathways. *Prog. Brain Res.* **84**: 231-241.
25. Mesulam, M.M., Mash, D., Hersh, L., Bothwell, M., Geula, C. (1992) Cholinergic innervation of the human striatum, globus pallidus, subthalamic nucleus, substantia nigra, and red nucleus. *J. Comp. Neurol.* **323**: 252-268.
26. Bigl, V., Woolf, N.J., Butcher, L.L. (1982) Cholinergic projections from the basal forebrain to frontal, parietal, temporal, occipital, and cingulate cortices: a combined fluorescent tracer and acetylcholinesterase analysis. *Brain Res. Bull.* **8**: 727-749.

27. Henderson, Z. (1987) A small proportion of cholinergic neurones in the nucleus basalis magnocellularis of ferret appear to stain positively for tyrosine hydroxylase. *Brain Res.* **412**: 363-369.
28. Mesulam, M.M., Geula, C., Bothwell, M.A., Hersh, L.B. (1989) Human reticular formation: cholinergic neurons of the pedunculo-pontine and laterodorsal tegmental nuclei and some cytochemical comparisons to forebrain cholinergic neurons. *J. Comp. Neurol.* **283**: 611-633.
29. Walker, L.C., Koliatsos, V.E., Kitt, C.A., Richardson, R.T., Rokaeus, A., Price, D.L. (1989) Peptidergic neurons in the basal forebrain magnocellular complex of the rhesus monkey. *J. Comp. Neurol.* **280**: 272-282.
30. Gouras, G.K., Rance, N.E., Young, W.S., 3rd, Koliatsos, V.E. (1992) Tyrosine-hydroxylase-containing neurons in the primate basal forebrain magnocellular complex. *Brain Res.* **584**: 287-293.
31. Wisniewski, L., Ridley, R.M., Baker, H.F., Fine, A. (1992) Tyrosine hydroxylase-immunoreactive neurons in the nucleus basalis of the common marmoset (*Callithrix jacchus*). *J. Comp. Neurol.* **325**: 379-387.
32. Gritti, I., Mainville, L., Jones, B.E. (1993) Codistribution of GABA- with acetylcholine-synthesizing neurons in the basal forebrain of the rat. *J. Comp. Neurol.* **329**: 438-457.
33. Krnjevic, K. (1993) Central cholinergic mechanisms and function. *Prog. Brain Res.* **98**: 285-292.
34. Dani, J.A. and Bertrand, D. (2007) Nicotinic acetylcholine receptors and nicotinic cholinergic mechanisms of the central nervous system. *Annu. Rev. Pharmacol. Toxicol.* **47**: 699-729.

35. Gotti, C., Clementi, F., Fornari, A., Gaimarri, A., Guiducci, S., Manfredi, I., Moretti, M., Pedrazzi, P., Pucci, L., Zoli, M. (2009) Structural and functional diversity of native brain neuronal nicotinic receptors. *Biochem. Pharmacol.* **78**: 703-711.
36. Albuquerque, E.X., Pereira, E.F., Alkondon, M., Rogers, S.W. (2009) Mammalian nicotinic acetylcholine receptors: from structure to function. *Physiol. Rev.* **89**: 73-120.
37. Unwin, N. (2005) Refined structure of the nicotinic acetylcholine receptor at 4Å resolution. *J. Mol. Biol.* **346**: 967-989.
38. Peng, X., Katz, M., Gerzanich, V., Anand, R., Lindstrom, J. (1994) Human alpha 7 acetylcholine receptor: cloning of the alpha 7 subunit from the SH-SY5Y cell line and determination of pharmacological properties of native receptors and functional alpha 7 homomers expressed in *Xenopus* oocytes. *Mol. Pharmacol.* **45**: 546-554.
39. Schoepfer, R., Conroy, W.G., Whiting, P., Gore, M., Lindstrom, J. (1990) Brain alpha-bungarotoxin binding protein cDNAs and MAbs reveal subtypes of this branch of the ligand-gated ion channel gene superfamily. *Neuron* **5**: 35-48.
40. Couturier, S., Bertrand, D., Matter, J.M., Hernandez, M.C., Bertrand, S., Millar, N., Valera, S., Barkas, T., Ballivet, M. (1990) A neuronal nicotinic acetylcholine receptor subunit (alpha 7) is developmentally regulated and forms a homo-oligomeric channel blocked by alpha-BTX. *Neuron* **5**: 847-856.
41. Changeux, J.P., Kasai, M., Lee, C.Y. (1970) Use of a snake venom toxin to characterize the cholinergic receptor protein. *Proc. Natl. Acad. Sci. U. S. A.* **67**: 1241-1247.
42. Dajas-Bailador, F. and Wonnacott, S. (2004) Nicotinic acetylcholine receptors and the regulation of neuronal signalling. *Trends Pharmacol Sci* **25**: 317-24.

43. Girod, R., Crabtree, G., Ernstrom, G., Ramirez-Latorre, J., McGehee, D., Turner, J., Role, L. (1999) Heteromeric complexes of alpha 5 and/or alpha 7 subunits. Effects of calcium and potential role in nicotine-induced presynaptic facilitation. *Ann. N. Y. Acad. Sci.* **868**: 578-590.
44. Khiroug, S.S., Harkness, P.C., Lamb, P.W., Sudweeks, S.N., Khiroug, L., Millar, N.S., Yakel, J.L. (2002) Rat nicotinic ACh receptor alpha7 and beta2 subunits co-assemble to form functional heteromeric nicotinic receptor channels. *J. Physiol.* **540**: 425-434.
45. Liu, Q., Huang, Y., Xue, F., Simard, A., DeChon, J., Li, G., Zhang, J., Lucero, L., Wang, M., Sierks, M., Hu, G., Chang, Y., Lukas, R.J., Wu, J. (2009) A novel nicotinic acetylcholine receptor subtype in basal forebrain cholinergic neurons with high sensitivity to amyloid peptides. *J. Neurosci.* **29**: 918-929.
46. Murray, T.A., Bertrand, D., Papke, R.L., George, A.A., Pantoja, R., Srinivasan, R., Liu, Q., Wu, J., Whiteaker, P., Lester, H.A., Lukas, R.J. (2012) Alpha7beta2 Nicotinic Acetylcholine Receptors Assemble, Function, and are Activated Primarily Via their Alpha7-Alpha7 Interfaces. *Mol. Pharmacol.* **81**: 175-188.
47. Palma, E., Maggi, L., Barabino, B., Eusebi, F., Ballivet, M. (1999) Nicotinic acetylcholine receptors assembled from the alpha7 and beta3 subunits. *J. Biol. Chem.* **274**: 18335-18340.
48. Moretti, M., Zoli, M., George, A.A., Lukas, R.J., Pistillo, F., Maskos, U., Whiteaker, P., Gotti, C. (2014) The novel alpha7beta2-nicotinic acetylcholine receptor subtype is expressed in mouse and human basal forebrain: biochemical and pharmacological characterization. *Mol. Pharmacol.* **86**: 306-317.
49. Sinkus, M.L., Lee, M.J., Gault, J., Logel, J., Short, M., Freedman, R., Christian, S.L., Lyon, J., Leonard, S. (2009) A 2-base pair deletion polymorphism in the partial duplication of the alpha7 nicotinic acetylcholine gene (CHRFAM7A) on chromosome 15q14 is associated with schizophrenia. *Brain Res.* **1291**: 1-11.

50. Wang, Y., Xiao, C., Indersmitten, T., Freedman, R., Leonard, S., Lester, H.A. (2014) The duplicated alpha7 subunits assemble and form functional nicotinic receptors with the full-length alpha7. *J. Biol. Chem.*
51. Quik, M., Polonskaya, Y., Gillespie, A., Jakowec, M., Lloyd, G.K., Langston, J.W. (2000) Localization of nicotinic receptor subunit mRNAs in monkey brain by in situ hybridization. *J. Comp. Neurol.* **425**: 58-69.
52. Tribollet, E., Bertrand, D., Marguerat, A., Raggenbass, M. (2004) Comparative distribution of nicotinic receptor subtypes during development, adulthood and aging: an autoradiographic study in the rat brain. *Neuroscience* **124**: 405-420.
53. Alkondon, M., Pereira, E.F., Albuquerque, E.X. (1998) Alpha-Bungarotoxin- and Methyllaconitine-Sensitive Nicotinic Receptors Mediate Fast Synaptic Transmission in Interneurons of Rat Hippocampal Slices. *Brain Res.* **810**: 257-263.
54. Frazier, C.J., Buhler, A.V., Weiner, J.L., Dunwiddie, T.V. (1998) Synaptic potentials mediated via alpha-bungarotoxin-sensitive nicotinic acetylcholine receptors in rat hippocampal interneurons. *J. Neurosci.* **18**: 8228-8235.
55. Hefft, S., Hulo, S., Bertrand, D., Muller, D. (1999) Synaptic transmission at nicotinic acetylcholine receptors in rat hippocampal organotypic cultures and slices. *J. Physiol.* **515 (Pt 3)**: 769-776.
56. Gray, R., Rajan, A.S., Radcliffe, K.A., Yakehiro, M., Dani, J.A. (1996) Hippocampal synaptic transmission enhanced by low concentrations of nicotine. *Nature* **383**: 713-716.
57. Jones, I.W., Barik, J., O'Neill, M.J., Wonnacott, S. (2004) Alpha bungarotoxin-1.4 nm gold: a novel conjugate for visualising the precise subcellular distribution of alpha 7* nicotinic acetylcholine receptors. *J. Neurosci. Methods* **134**: 65-74.

58. Dickinson, J.A., Kew, J.N., Wonnacott, S. (2008) Presynaptic alpha 7- and beta 2-containing nicotinic acetylcholine receptors modulate excitatory amino acid release from rat prefrontal cortex nerve terminals via distinct cellular mechanisms. *Mol. Pharmacol.* **74**: 348-359.
59. Quarta, D., Naylor, C.G., Barik, J., Fernandes, C., Wonnacott, S., Stolerman, I.P. (2009) Drug discrimination and neurochemical studies in alpha7 null mutant mice: tests for the role of nicotinic alpha7 receptors in dopamine release. *Psychopharmacology (Berl)* **203**: 399-410.
60. Livingstone, P.D., Srinivasan, J., Kew, J.N., Dawson, L.A., Gotti, C., Moretti, M., Shoaib, M., Wonnacott, S. (2009) Alpha7 and Non-Alpha7 Nicotinic Acetylcholine Receptors Modulate Dopamine Release in Vitro and in Vivo in the Rat Prefrontal Cortex. *Eur. J. Neurosci.* **29**: 539-550.
61. Barik, J. and Wonnacott, S. (2006) Indirect modulation by alpha7 nicotinic acetylcholine receptors of noradrenaline release in rat hippocampal slices: interaction with glutamate and GABA systems and effect of nicotine withdrawal. *Mol. Pharmacol.* **69**: 618-628.
62. Khiroug, L., Giniatullin, R., Klein, R.C., Fayuk, D., Yakel, J.L. (2003) Functional mapping and Ca²⁺ regulation of nicotinic acetylcholine receptor channels in rat hippocampal CA1 neurons. *J. Neurosci.* **23**: 9024-9031.
63. Xu, J., Zhu, Y., Heinemann, S.F. (2006) Identification of sequence motifs that target neuronal nicotinic receptors to dendrites and axons. *J. Neurosci.* **26**: 9780-9793.
64. Ji, D., Lape, R., Dani, J.A. (2001) Timing and location of nicotinic activity enhances or depresses hippocampal synaptic plasticity. *Neuron* **31**: 131-141.
65. Dajas-Bailador, F.A., Soliakov, L., Wonnacott, S. (2002) Nicotine activates the extracellular signal-regulated kinase 1/2 via the alpha7 nicotinic acetylcholine

- receptor and protein kinase A, in SH-SY5Y cells and hippocampal neurones. *J Neurochem* **80**: 520-30.
66. Hu, M., Liu, Q.S., Chang, K.T., Berg, D.K. (2002) Nicotinic regulation of CREB activation in hippocampal neurons by glutamatergic and nonglutamatergic pathways. *Mol. Cell. Neurosci.* **21**: 616-625.
 67. Berg, D.K. and Conroy, W.G. (2002) Nicotinic alpha 7 receptors: synaptic options and downstream signaling in neurons. *J. Neurobiol.* **53**: 512-523.
 68. Kihara, T., Shimohama, S., Sawada, H., Honda, K., Nakamizo, T., Shibasaki, H., Kume, T., Akaike, A. (2001) alpha 7 nicotinic receptor transduces signals to phosphatidylinositol 3-kinase to block A beta-amyloid-induced neurotoxicity. *J Biol Chem* **276**: 13541-6.
 69. Inestrosa, N.C., Godoy, J.A., Vargas, J.Y., Arrazola, M.S., Rios, J.A., Carvajal, F.J., Serrano, F.G., Farias, G.G. (2013) Nicotine prevents synaptic impairment induced by amyloid-beta oligomers through alpha7-nicotinic acetylcholine receptor activation. *Neuromolecular Med.* **15**: 549-569.
 70. Dineley, K.T. and Patrick, J.W. (2000) Amino acid determinants of alpha 7 nicotinic acetylcholine receptor surface expression. *J. Biol. Chem.* **275**: 13974-13985.
 71. Wang, J.M., Zhang, L., Yao, Y., Viroonchatapan, N., Rothe, E., Wang, Z.Z. (2002) A transmembrane motif governs the surface trafficking of nicotinic acetylcholine receptors. *Nat. Neurosci.* **5**: 963-970.
 72. Drisdel, R.C., Manzana, E., Green, W.N. (2004) The role of palmitoylation in functional expression of nicotinic alpha7 receptors. *J. Neurosci.* **24**: 10502-10510.
 73. Williams, M.E., Burton, B., Urrutia, A., Shcherbatko, A., Chavez-Noriega, L.E., Cohen, C.J., Aiyar, J. (2005) Ric-3 promotes functional expression of the

- nicotinic acetylcholine receptor alpha7 subunit in mammalian cells. *J. Biol. Chem.* **280**: 1257-1263.
74. Lansdell, S.J., Gee, V.J., Harkness, P.C., Doward, A.I., Baker, E.R., Gibb, A.J., Millar, N.S. (2005) RIC-3 enhances functional expression of multiple nicotinic acetylcholine receptor subtypes in mammalian cells. *Mol. Pharmacol.* **68**: 1431-1438.
 75. Mukherjee, J., Kuryatov, A., Moss, S.J., Lindstrom, J.M., Anand, R. (2009) Mutations of cytosolic loop residues impair assembly and maturation of alpha7 nicotinic acetylcholine receptors. *J. Neurochem.* **110**: 1885-1894.
 76. Valles, A.S. and Barrantes, F.J. (2012) Chaperoning alpha7 neuronal nicotinic acetylcholine receptors. *Biochim. Biophys. Acta* **1818**: 718-729.
 77. Charpantier, E., Wiesner, A., Huh, K.H., Ogier, R., Hoda, J.C., Allaman, G., Raggenbass, M., Feuerbach, D., Bertrand, D., Fuhrer, C. (2005) Alpha7 neuronal nicotinic acetylcholine receptors are negatively regulated by tyrosine phosphorylation and Src-family kinases. *J. Neurosci.* **25**: 9836-9849.
 78. Cho, C.H., Song, W., Leitzell, K., Teo, E., Meleth, A.D., Quick, M.W., Lester, R.A. (2005) Rapid upregulation of alpha7 nicotinic acetylcholine receptors by tyrosine dephosphorylation. *J. Neurosci.* **25**: 3712-3723.
 79. Liu, Z., Tearle, A.W., Nai, Q., Berg, D.K. (2005) Rapid activity-driven SNARE-dependent trafficking of nicotinic receptors on somatic spines. *J. Neurosci.* **25**: 1159-1168.
 80. Nordberg, A. (2001) Nicotinic receptor abnormalities of Alzheimer's disease: therapeutic implications. *Biol Psychiatry* **49**: 200-10.
 81. Ikonomic, M.D., Wecker, L., Abrahamson, E.E., Wu, J., Counts, S.E., Ginsberg, S.D., Mufson, E.J., Dekosky, S.T. (2009) Cortical alpha7 nicotinic acetylcholine

- receptor and beta-amyloid levels in early Alzheimer disease. *Arch. Neurol.* **66**: 646-651.
82. Dineley, K.T., Westerman, M., Bui, D., Bell, K., Ashe, K.H., Sweatt, J.D. (2001) Beta-amyloid activates the mitogen-activated protein kinase cascade via hippocampal $\alpha 7$ nicotinic acetylcholine receptors: In vitro and in vivo mechanisms related to Alzheimer's disease. *J Neurosci* **21**: 4125-33.
83. Dziewczapolski, G., Glogowski, C.M., Masliah, E., Heinemann, S.F. (2009) Deletion of the $\alpha 7$ nicotinic acetylcholine receptor gene improves cognitive deficits and synaptic pathology in a mouse model of Alzheimer's disease. *J. Neurosci.* **29**: 8805-8815.
84. Haass, C. and Selkoe, D.J. (2007) Soluble protein oligomers in neurodegeneration: lessons from the Alzheimer's amyloid beta-peptide. *Nat Rev Mol Cell Biol* **8**: 101-12.
85. Haass, C. (2004) Take five--BACE and the gamma-secretase quartet conduct Alzheimer's amyloid beta-peptide generation. *EMBO J* **23**: 483-8.
86. Wolfe, M.S., Xia, W., Moore, C.L., Leatherwood, D.D., Ostaszewski, B., Rahmati, T., Donkor, I.O., Selkoe, D.J. (1999) Peptidomimetic probes and molecular modeling suggest that Alzheimer's gamma-secretase is an intramembrane-cleaving aspartyl protease. *Biochemistry* **38**: 4720-4727.
87. Steiner, H. and Haass, C. (2000) Intramembrane proteolysis by presenilins. *Nat. Rev. Mol. Cell Biol.* **1**: 217-224.
88. Kimberly, W.T., LaVoie, M.J., Ostaszewski, B.L., Ye, W., Wolfe, M.S., Selkoe, D.J. (2003) Gamma-secretase is a membrane protein complex comprised of presenilin, nicastrin, Aph-1, and Pen-2. *Proc. Natl. Acad. Sci. U. S. A.* **100**: 6382-6387.

89. Takasugi, N., Tomita, T., Hayashi, I., Tsuruoka, M., Niimura, M., Takahashi, Y., Thinakaran, G., Iwatsubo, T. (2003) The role of presenilin cofactors in the gamma-secretase complex. *Nature* **422**: 438-441.
90. Edbauer, D., Winkler, E., Regula, J.T., Pesold, B., Steiner, H., Haass, C. (2003) Reconstitution of gamma-secretase activity. *Nat. Cell Biol.* **5**: 486-488.
91. Lue, L.F., Kuo, Y.M., Roher, A.E., Brachova, L., Shen, Y., Sue, L., Beach, T., Kurth, J.H., Rydel, R.E., Rogers, J. (1999) Soluble amyloid beta peptide concentration as a predictor of synaptic change in Alzheimer's disease. *Am J Pathol* **155**: 853-62.
92. McLean, C.A., Cherny, R.A., Fraser, F.W., Fuller, S.J., Smith, M.J., Beyreuther, K., Bush, A.I., Masters, C.L. (1999) Soluble pool of Abeta amyloid as a determinant of severity of neurodegeneration in Alzheimer's disease. *Ann Neurol* **46**: 860-6.
93. Naslund, J., Haroutunian, V., Mohs, R., Davis, K.L., Davies, P., Greengard, P., Buxbaum, J.D. (2000) Correlation between elevated levels of amyloid beta-peptide in the brain and cognitive decline. *JAMA* **283**: 1571-1577.
94. Wang, Z., Wang, L., Xie, H. (1999) Cerebral amyloid angiopathy with dementia: clinicopathological studies of 17 cases. *Chin. Med. J. (Engl)* **112**: 238-241.
95. Wang, H.Y., Lee, D.H., D'Andrea, M.R., Peterson, P.A., Shank, R.P., Reitz, A.B. (2000) beta-Amyloid(1-42) binds to alpha7 nicotinic acetylcholine receptor with high affinity. Implications for Alzheimer's disease pathology. *J Biol Chem* **275**: 5626-32.
96. Wang, H.Y., Lee, D.H., Davis, C.B., Shank, R.P. (2000) Amyloid peptide Abeta(1-42) binds selectively and with picomolar affinity to alpha7 nicotinic acetylcholine receptors. *J Neurochem* **75**: 1155-61.

97. Nagele, R.G., D'Andrea, M.R., Anderson, W.J., Wang, H.Y. (2002) Intracellular accumulation of beta-amyloid(1-42) in neurons is facilitated by the alpha 7 nicotinic acetylcholine receptor in Alzheimer's disease. *Neuroscience* **110**: 199-211.
98. Dineley, K.T., Bell, K.A., Bui, D., Sweatt, J.D. (2002) beta -Amyloid peptide activates alpha 7 nicotinic acetylcholine receptors expressed in *Xenopus* oocytes. *J Biol Chem* **277**: 25056-61.
99. Grassi, F., Palma, E., Tonini, R., Amici, M., Ballivet, M., Eusebi, F. (2003) Amyloid beta(1-42) peptide alters the gating of human and mouse alpha-bungarotoxin-sensitive nicotinic receptors. *J Physiol* **547**: 147-57.
100. Lee, D.H. and Wang, H.Y. (2003) Differential physiologic responses of alpha7 nicotinic acetylcholine receptors to beta-amyloid1-40 and beta-amyloid1-42. *J. Neurobiol.* **55**: 25-30.
101. Pettit, D.L., Shao, Z., Yakel, J.L. (2001) beta-Amyloid(1-42) peptide directly modulates nicotinic receptors in the rat hippocampal slice. *J. Neurosci.* **21**: RC120.
102. Demuro, A., Mina, E., Kaye, R., Milton, S.C., Parker, I., Glabe, C.G. (2005) Calcium dysregulation and membrane disruption as a ubiquitous neurotoxic mechanism of soluble amyloid oligomers. *J. Biol. Chem.* **280**: 17294-17300.
103. Small, D.H., Maksud, D., Kerr, M.L., Ng, J., Hou, X., Chu, C., Mehrani, H., Unabia, S., Azari, M.F., Loiacono, R., Aguilar, M.I., Chebib, M. (2007) The beta-amyloid protein of Alzheimer's disease binds to membrane lipids but does not bind to the alpha7 nicotinic acetylcholine receptor. *J Neurochem* **101**: 1527-38.
104. Bell, K.A., O'Riordan, K.J., Sweatt, J.D., Dineley, K.T. (2004) MAPK recruitment by beta-amyloid in organotypic hippocampal slice cultures depends on physical state and exposure time. *J Neurochem* **91**: 349-61.

105. Nong, Y., Huang, Y.Q., Ju, W., Kalia, L.V., Ahmadian, G., Wang, Y.T., Salter, M.W. (2003) Glycine binding primes NMDA receptor internalization. *Nature* **422**: 302-307.
106. Ehlers, M.D. (2000) Reinsertion or degradation of AMPA receptors determined by activity-dependent endocytic sorting. *Neuron* **28**: 511-525.

Chapter 2

2 Oligomeric Aggregates of Amyloid β Peptide 1-42 Activate ERK/MAPK in SH-SY5Y Cells via the $\alpha 7$ Nicotinic Receptor^a

^aA version of this chapter has been published.

Young K.F., Pasternak S.H., and Rylett R.J. (2009) Oligomeric aggregates of amyloid β peptide 1-42 activate ERK/MAPK in SH-SY5Y cells via the $\alpha 7$ nicotinic receptor. *Neurochemistry International* 55: 796-801.

<http://dx.doi.org/10.1016/j.neuint.2009.08.002>

Acknowledgements

This research was supported by grants to RJR from the Ontario Mental Health Foundation and the Canadian Institutes for Health Research (CIHR). KFY was the recipient of an Ontario Graduate Scholarship in Science and Technology (OGSST). We thank Kathy deJong, Nils Peterson, and Peter Norton for their assistance with atomic force microscopy.

2.1 Summary

The production and aggregation of amyloid β peptides is linked to the development and progression of Alzheimer's disease. It is apparent that the various structural forms of A β can affect cell signalling pathways and the activity of neurons differently. In this study, we investigated the effects of oligomeric and fibrillar aggregates of A β 42 and non-aggregated peptide upon activation of the ERK/MAPK signalling pathway. In SH-SY5Y cells, acute exposure to oligomeric A β 42 led to phosphorylation of ERK1/2 at concentrations as low as 1 nM and up to 100 nM. These changes were detected as early as 5 min following exposure to 100 nM oligomeric A β 42, reaching a maximum level after 10 min. Phosphorylation of ERK1/2 subsequently declined to and remained at basal levels after 30 min, for up to 2 h of exposure. Fibrillar aggregates of A β 42 did not significantly induce phosphorylation of ERK1/2 and non-aggregated A β 42 did not activate the pathway. The effects of oligomeric A β 42 to increase ERK1/2 phosphorylation above basal levels were inhibited by MLA, a selective antagonist of the α 7nAChR. U0126, an inhibitor of MEK1/2, the upstream activator of ERK1/2, completely blocked induction of ERK1/2 phosphorylation. Oligomeric aggregates of A β 42 were the principal structural form of the peptide that activated ERK/MAPK in SH-SY5Y cells and these effects were mediated by the α 7 nAChR.

2.2 Introduction

Alzheimer's disease is a common form of progressive neurodegeneration that manifests itself as impaired learning and memory and disordered cognitive function (1). Although AD can occur sporadically with a prevalence that increases with age, it has also been linked genetically to the overproduction and aggregation of A β peptides (1). A β peptides are derived from the proteolytic degradation of a type I integral membrane protein, amyloid precursor protein (APP) (2). Cleavage of APP by β - and γ -secretase activity results in the production of peptides that are predominantly either 40 or 42 amino acids in length (A β 40 or A β 42) (2). Familial AD-causing mutations in APP or the γ -secretase protein presenilin result in either the increased production of A β peptides and/or an increase in the relative amount of A β 42 versus A β 40 produced (2). A β 42 contains two additional hydrophobic amino acid residues than A β 40 and aggregates more readily in solution (3, 4). Fibrillar aggregates of A β 42 are found at the core of amyloid plaques in the brain and A β 42 accounts for the majority of A β found within these plaques (5). However, the appearance, number, and distribution of plaques does not correlate well with measures of clinical dementia; rather it is the levels of soluble A β peptides that correlate more strongly with the loss of synaptic terminals and dementia in AD (6 - 9). These small soluble aggregates of A β peptides are detectable in extracts from AD brain, the media of cell cultures and in synthetic preparations of A β peptides (9 - 14). These oligomeric aggregates of A β can inhibit long-term potentiation (LTP; a classical model of synaptic plasticity and learning and memory) in *in vitro* and in *in vivo* models at nanomolar concentrations (15). Recent evidence from studies using a genetically modified mouse model of AD revealed that senile plaques can serve as a reservoir for the release of oligomeric A β and that this can be toxic to synapses at some distance from the plaque (16).

LTP is dependent upon intracellular signalling, particularly activation of the ERK/MAPK signal transduction pathway (17 - 19). The α 7 nAChR plays a role in the formation of LTP in the hippocampus and this can involve signalling through ERK/MAPK (20 - 22). An

interaction between A β 42 and the α 7 nAChR has been implicated in the activation of ERK/MAPK in the hippocampus where disjunctive A β 42- α 7 nAChR-ERK/MAPK signalling may disrupt ERK/MAPK signalling important for the formation of LTP (23, 24).

The findings of some, but not all studies suggest that A β 42 binds the α 7 nAChR with high affinity and can alter gating of the receptor, either by activating the receptor as an agonist or antagonizing receptor activity (25 - 31). The effects of A β 42 binding to the α 7 nAChR and the ability of the peptide to activate receptor-linked intracellular signalling pathways are likely affected by the state of aggregation and structural form of the peptide. Previous studies have addressed the possible role of A β 42 in activation of downstream signalling pathways engaged by the α 7 nAChR, but those studies did not involve documentation of the aggregation state or structural forms of A β 42 peptides responsible for mediating these effects (24).

In the present study, activation of the ERK/MAPK signalling pathway by well-characterized oligomeric and fibrillar aggregates of A β 42 and non-aggregated A β 42 was compared in the SH-SY5Y human neuroblastoma cell line. Synthetic A β 42 peptides were treated to remove any pre-existing structural forms and subsequently incubated under conditions that promoted the formation of either oligomeric or fibrillar aggregates. Alternatively, the peptides were not incubated prior to their application to cultured neuronal cells to prevent the formation of these aggregates and to retain the peptides in monomeric form. The preparations were applied to SH-SY5Y cells *in vitro* and the acute effects upon phosphorylation of ERK1/2 were monitored to obtain a dose-response and time-course for oligomeric, fibrillar or non-aggregated forms of A β 42. The involvement of the α 7 nAChR was assessed with the use of a competitive antagonist selective for the receptor, MLA.

2.3 Methods

2.3.1 Materials

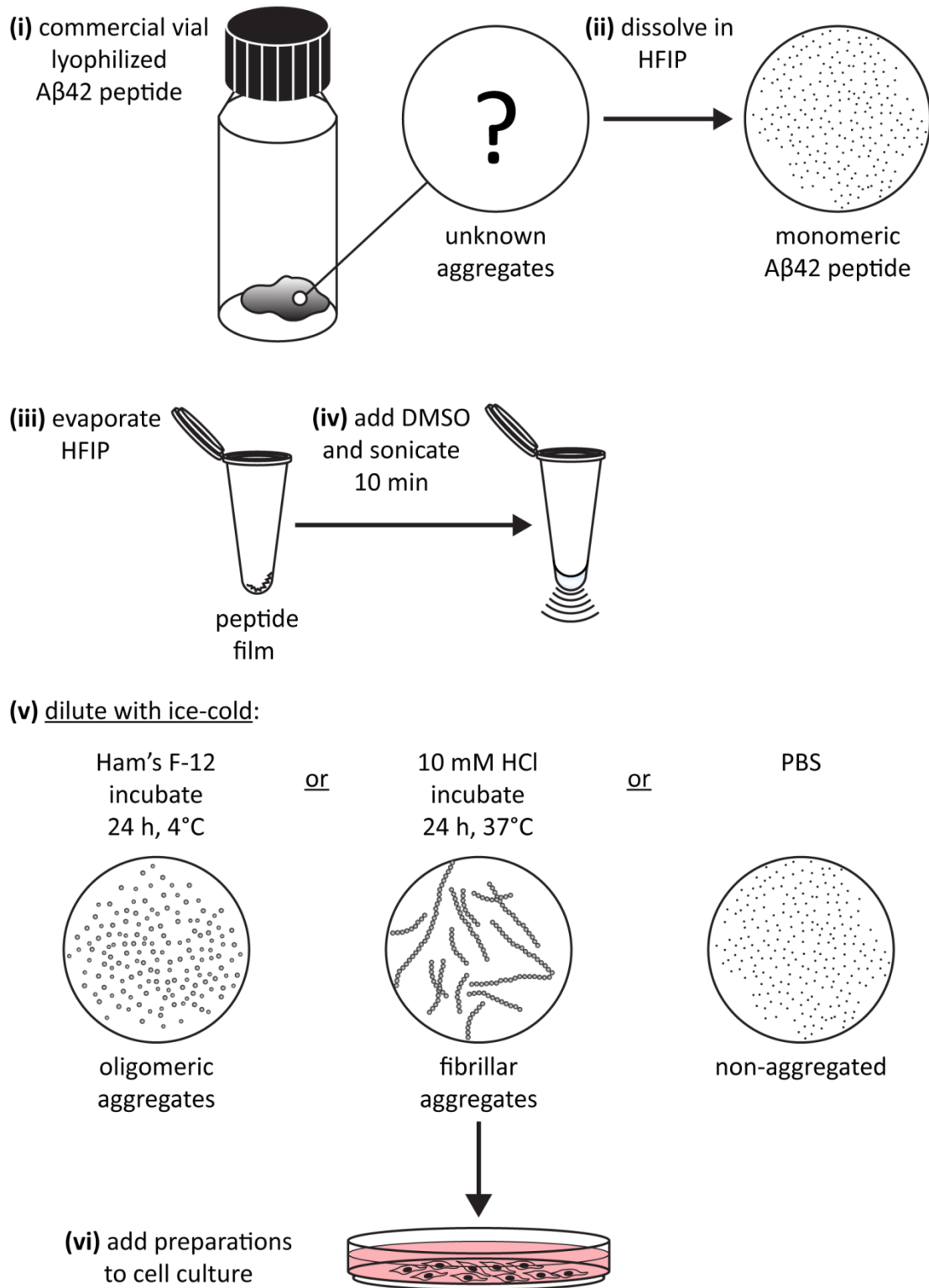
SH-SY5Y cells were purchased from American Type Tissue Culture (Manassas, VA). Dulbecco's modified Eagle's medium (DMEM), fetal bovine serum (FBS) and Ham's F-12 nutrient mixture (phenol red-free) were obtained from Invitrogen (Burlington, ON). A β 42 peptides were from Bachem (Torrance, CA) and California Peptide Research (Napa, CA); no differences were found in experimental measures made between the two peptide sources. Nerve growth factor 2.5S (NGF) was from Harlan Bioproducts (Indianapolis, IN). U0126 was from Calbiochem (Gibbstown, NJ). MLA, 1,1,1,3,3,3-hexafluoro-2-propanol (HFIP), dimethyl sulfoxide (DMSO) and bovine serum albumin - fraction V (BSA) were from Sigma-Aldrich (Oakville, ON). Polyclonal antibodies against dually phosphorylated ERK1/2 and monoclonal and polyclonal antibodies against ERK1/2 were from Cell Signaling Technology (Danvers, MA). Polyclonal antibody against the C-terminus of actin was from Santa Cruz Biotechnology Inc. (Santa Cruz, CA). Horseradish peroxidase (HRP)-conjugated goat anti-rabbit antibody was from Jackson Immuno-Research Laboratories (West Grove, PA). HRP-conjugated sheep anti-mouse antibody, ECL western blotting detection reagent and Hybond-C Extra nitrocellulose membrane were from GE Healthcare (Baie d'Urfé, QC). X-OMAT LS film was from Eastman Kodak (Toronto, ON).

2.3.2 A β 42 Preparation and Atomic Force Microscopy

Oligomeric and fibrillar forms of A β 42 were prepared as described previously (14, 32). The preparation of A β 42 peptides and treatment of cells in culture is illustrated (Figure 2.1). Briefly, lyophilized A β 42 peptides were dissolved in HFIP and aliquoted into polypropylene micro-centrifuge tubes. HFIP was removed by evaporation and the resulting A β 42 peptide films were stored at - 80 °C. Prior to use, these peptide films were reconstituted to give an A β 42 stock solution at a concentration of 1 mM in DMSO, sonicated for 10 min, then subsequently diluted to 100 μ M with ice-cold Ham's F-12 (phenol red-free) and incubated for 24 h at 4 °C to facilitate the formation of A β 42

Figure 2.1 Preparation of A β 42 Peptides and Cell Culture Treatments.

(i) Chemically synthesized A β 42 peptide was obtained from a commercial source as a lyophilized product. **(ii)** To ensure that the starting material was in a homogenous non-aggregated monomeric state, the lyophilized peptide was dissolved in HFIP and aliquoted into micro-centrifuge tubes. **(iii)** HFIP was removed by evaporation in a vacuum centrifuge to yield a peptide film. **(iv)** Peptide films were reconstituted in DMSO to a concentration of 1 mM and sonicated for 10 min immediately prior to **(v)** dilution to 100 μ M in ice-cold Ham's F-12, 10 mM HCl, or PBS, pH 7.4. DMSO solutions diluted in Ham's F-12 were incubated for 24 h at 4 °C to form oligomeric aggregates and solutions diluted in 10 mM HCl were incubated for 24 h at 37 °C to form fibrillar aggregates. Solutions diluted in PBS were not incubated to prevent the formation of aggregates and yield a non-aggregated form of A β 42. **(vi)** The resulting stock solutions were serially diluted on ice prior to being added to cells in culture.



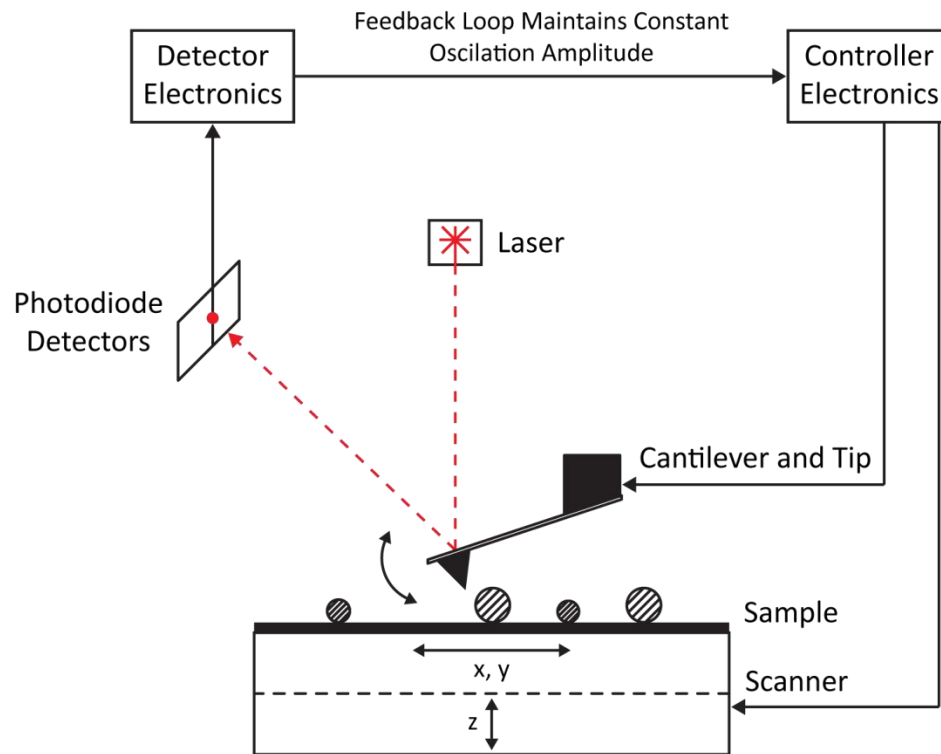
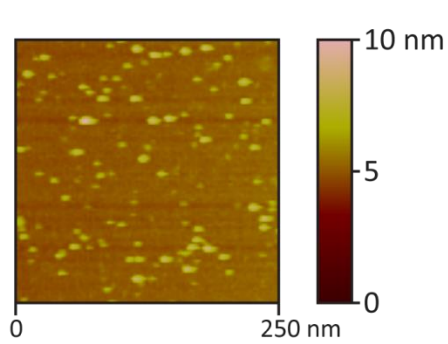
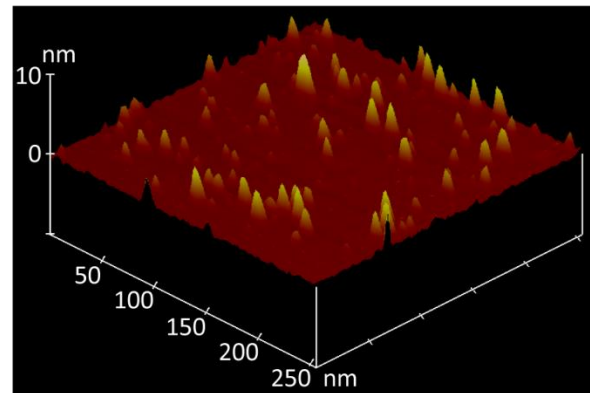
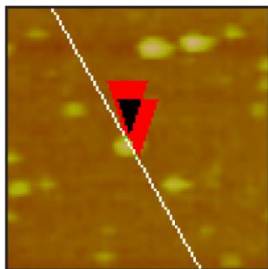
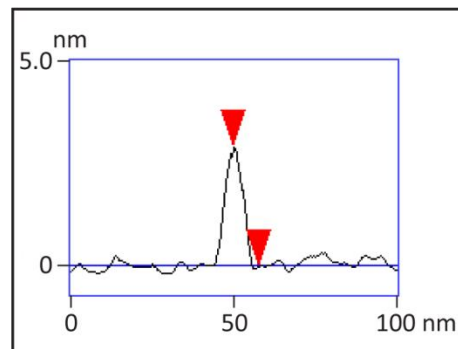
oligomers. Alternatively, the DMSO stock solution was diluted to 100 μ M with 10 mM HCl and incubated for 24 h at 37 °C to facilitate the formation of A β 42 fibrils. For non-aggregated A β 42, DMSO stock solutions were diluted to 100 μ M with ice-cold phosphate-buffered saline (PBS) (138 mM NaCl, 2.7 mM KCl), pH 7.4. Peptide preparations were either stored at - 80 °C or used immediately for treatment of cells or atomic force microscopy (AFM). Non-aggregated A β 42 preparations in PBS were used immediately. A β 42 aggregates were characterized by TappingMode™ AFM using a Multimode SPM with a NanoScope™ IIIa controller and J-series scanner (Digital Instruments) (Figure 2.2). AFM probes were Tap 300 silicon cantilevers with 40 N/m spring constants and 300 kHz resonant frequencies (Nanodevices). A β 42 solutions at 10 μ M were spotted onto freshly-cleaved mica, incubated for 1 min, then rinsed twice with high performance liquid chromatography (HPLC)-grade H₂O and blown dry with compressed air. Images of bare mica were captured from freshly-cleaved mica spotted with an equivalent volume of HPLC-grade H₂O and blown dry. Samples were imaged at scan rates from 0.5 to 5 Hz with drive amplitude and contact force kept to a minimum. Section analysis of images was performed to measure the height of A β 42 aggregates on the surface of mica substrate (Figure 2.2 D and E). Aggregate heights were measured individually in images captured from three to four independent preparations of A β 42 for each form of the peptide; oligomeric, fibrillar, or non-aggregated. The periodicity of fibrils was determined by measuring the distance between peaks of subunits.

2.3.3 Cell Model

The SH-SY5Y cell line is a human cell line sub-cloned from the SK-N-SH cell line (33) originally isolated from a human metastatic neuroblastoma (34). SH-SY5Y cells endogenously express α 7 nAChR (35, 36) and they have been successfully employed in several studies to investigate subcellular signalling the α 7 nAChR (37 - 41). A signalling pathway for activation of ERK/MAPK through α 7 nAChR has been characterized in SH-SY5Y cells (42), making them a candidate model for investigating ERK/MAPK activation

Figure 2.2 Atomic Force Microscopy and Image Analysis.

(A) AFM is a form of scanning probe microscopy that generates very high resolution topographic images by monitoring the interaction of a physical probe with a sample surface. In TappingMode™ AFM, a cantilever and tip integrated on a single silicon crystal is oscillated at or near its resonance frequency at a set amplitude and lightly taps across a sample surface during scanning. Laser light reflected off the back of the cantilever is detected by two closely spaced photodiodes. Displacement of the cantilever as it scans across the sample surface alters the amount of light reflected into each photodiode. The amount of light received by each photodiode is proportional to the deflection of the cantilever. A feedback loop maintains the constant oscillation amplitude by vertically moving the scanner in the (z) at each (x,y) data point. The distance the scanner moves vertically at each (x,y) data point is recorded to create a topographic image of the sample surface. Adapted from (43). **(B)** Data sets can be presented as an image in two-dimensions with a vertical colour scale, or **(C)** visualized in three-dimensions as a perspective. **(D)** Section analysis performed on images in which cross-sections (white line) through aggregates were examined to measure the height of each aggregate individually. **(E)** Profile of cross-section from D, measurement indicated by red arrowheads is a height of 2.9 nm. B, C, D, and E are from the same data set.

A**B****C****D****E**

as an endpoint to discriminate between the signalling capability of different structural forms of A β 42 peptide in relation to the α 7 nAChR.

2.3.4 Cell Culture and Treatments

SH-SY5Y cells were maintained in 75 cm² flasks using DMEM supplemented with 10% FBS and 0.05 mg/ml gentamycin at 37 °C in humidified air with 5% CO₂. Cells were plated onto 35 mm dishes two days prior to experimentation, with media changed to serum-free media containing 0.1% BSA 24 h prior to experiments. Treatment groups included 50 ng/mL NGF for 5 min; 5 min incubation with 0.01, 0.1, 1, 10, or 100 nM oligomeric, fibrillar or non-aggregated A β 42, or 100 nM oligomeric, fibrillar or non-aggregated A β 42 for 2, 5, 10, 30, 60 or 120 min. The inhibitors MLA (10 nM) or U0126 (50 mM) were added 30 min prior to the addition of 100 nM oligomeric A β 42. Stock solutions of MLA at 10 mM in distilled H₂O were stored at - 80 °C and activity was tested in Ca²⁺ fluorimetry experiments in which 10 μ M MLA, diluted from stock, blocked 1 mM nicotine induced increases in intracellular Ca²⁺ in SH-SY5Y cells loaded with the Ca²⁺-sensitive dye fura-2. The concentration of A β 42, whether oligomeric, fibrillar, or non-aggregated, was estimated based on dilution from that of the starting material, originally reconstituted from peptide films to 1 mM in DMSO.

2.3.5 Immunoblotting

At the end of the specified treatment periods, cells were washed twice with ice-cold PBS, scraped into lysis buffer comprised of 50 mM Tris-HCl, pH 7.5, 150 mM NaCl, 0.1% Triton X-100, 1 mM AEBSF, 10 mM NaF, 500 mM NaVO₄, 10 mg/ml leupeptin, 25 mg/ml aprotinin and 10 mg/ml pepstatin-A and incubated on ice for 30 min. The protein concentration of each lysate was determined by the method of Bradford (44). Equal amounts of protein (50 mg per sample) were resolved on 10% polyacrylamide gels by sodium dodecyl sulfate-polyacrylamide gel electrophoresis (SDS-PAGE) according to the method of Laemmli (45). To limit the overexposure of immunoblots caused by the intensity of NGF-induced bands, 50% less protein (25 mg per sample) from cells treated with NGF was loaded onto each SDS-PAGE gel. Proteins were transferred to

nitrocellulose membranes and immunoblotted with phosphorylation-specific (anti-phosphorylated p44/42 ERK1/2; 1:1000) or phosphorylation state independent (anti-p44/42 ERK1/2; 1:1000) anti-ERK1/2 antibodies. Immunoblotting with anti-actin antibody (1:5000) was used to demonstrate equal loading and transfer of SDS-PAGE gels. Anti-rabbit or anti-mouse IgG HRP-conjugated secondary antibodies (1:20,000 or 1:5000, respectively), followed by ECL reagent were used to detect immunoreactive protein bands. Immunoblots were quantified by densitometry with Quantity One software, version 4.6 (Bio-Rad, Mississauga, ON). The density of phosphorylated ERK1 and phosphorylated ERK2 proteins, resolving as two separate immunoreactive bands, were quantified as a single value.

2.3.6 Statistical Analysis

Results from the densitometric analysis of immunoblots are presented as a percentage of control responses and the data are given as mean \pm SEM from three or more separate experiments where indicated. Statistical significance was determined by one-way analysis of variance (ANOVA), followed by post hoc Dunnett analysis. A value of $p \leq 0.05$ was considered to be statistically significant.

2.4 Results

2.4.1 Generation of Oligomeric and Fibrillar Aggregates of A β 42

A β 42 in aqueous solution spontaneously assembles into aggregates of various sizes and conformations that have been determined to have unique biological properties (46). To differentiate between the effects of these different forms of A β 42 in our studies, it was important that we produce solutions of A β 42 that could be documented in terms of the structural forms of peptides present and demonstrated to be enriched in specific A β 42 conformations. We chose to follow a method previously established to produce specific structural forms of A β 42 (14, 32). We employed AFM to evaluate the aggregation state of our peptide preparations and were able to consistently produce small oligomeric or

fibrillar aggregates of A β 42 that were distinct from non-aggregated A β 42 and the surface of bare mica (Figure 2.3).

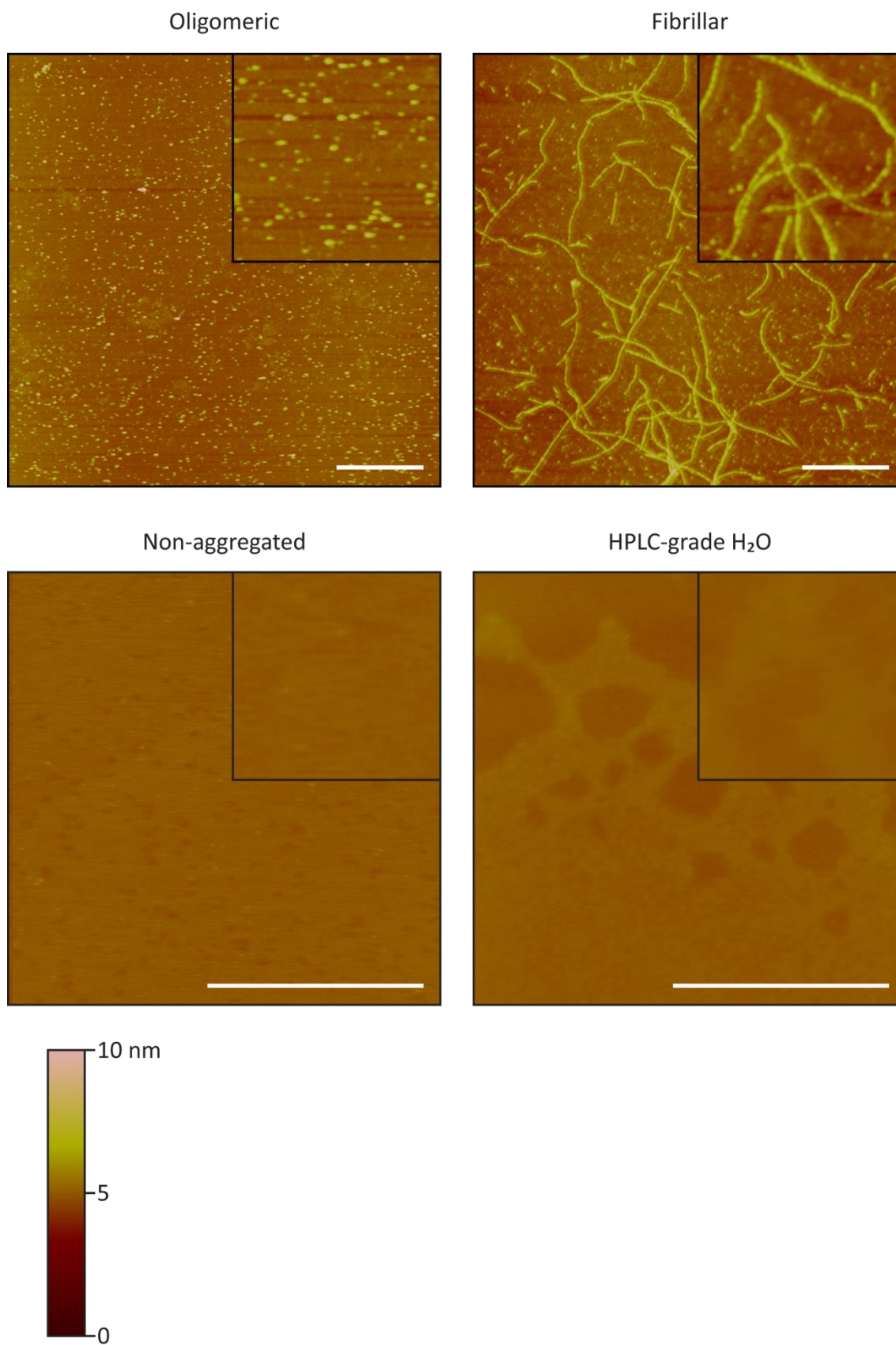
Oligomeric preparations of A β 42 contained small round globular structures with an average height of 3.1 ± 0.7 nm ($n = 100$), ranging in size from 1.3 to 4.4 nm. Oligomeric aggregates 3.0 - 3.8 nm in height were in the greatest frequency and there appeared to be a second smaller population circa 2 nm in height (Figure 2.4). Fibrillar preparations of A β 42 contained elongated fibrils that extended in length from tens of nanometres to micrometres. These fibrils appeared to be comprised of oligomeric-like subunits with an average height of 2.5 ± 0.3 nm ($n = 50$) that exhibited a distinct periodicity of 36 ± 3 nm ($n = 20$). Some small round globular aggregates were also present in fibrillar preparations, and these structures had an average height of 1.9 ± 0.5 nm ($n = 50$), ranging from 1.1 to 3.2 nm, with 80% of the population 1.4 - 2.6 nm in height. We observed that the majority of the peptide material in fibrillar preparations of A β 42 was confined to elongated fibrils. Non-aggregated preparations of A β 42 contained relatively small infrequent globular structures with an average height of 0.5 ± 0.4 nm ($n = 50$), ranging in size from 0.2 to 2.0 nm, with 90% of the population 0.2 - 1.0 nm in height. Thus, the forms of A β 42 used in our experiments were either oligomeric aggregates, predominantly fibrillar aggregates, or a non-aggregated form of the peptide containing smaller and less abundant aggregate structures.

2.4.2 ERK/MAPK Phosphorylation Induced by Oligomeric Aggregates of A β 42

Acute exposure of SH-SY5Y cells for 5 min to oligomeric aggregates of A β 42 induced ERK1/2 phosphorylation that was greater than that observed in cells treated with either fibrillar or non-aggregated A β 42 (Figure 2.5). However, the oligomeric A β 42-induced ERK1/2 phosphorylation was less than that mediated by NGF (Figure 2.5 A). The levels of total ERK1/2 and actin were unaffected by treatment of cells with A β 42. Oligomeric A β 42 induced ERK1/2 phosphorylation in a dose-dependent manner when cells were exposed to concentrations between 0.01 and 100 nM, with the maximum effect

Figure 2.3 Atomic force microscopy of oligomeric, fibrillar and non-aggregated preparations of A β 42.

Lyophilized A β 42 was dissolved in HFIP, dried, re-suspended in DMSO, sonicated, and then incubated for 24 h following dilution in either fresh cell culture medium at 4 °C to yield **Oligomeric** or 10 mM HCl at 37 °C to yield **Fibrillar** aggregates. For **Non-aggregated** A β 42, DMSO solutions were diluted in ice-cold PBS, pH 7.4. **HPLC-grade H₂O** was used in the place of A β 42-containing preparations to image the surface of bare mica. A β 42-containing samples were mounted on freshly-cleaved mica at a concentration of 10 μ M for AFM. Images are representative 5 μ m \times 5 μ m x-y (Oligomeric and Fibrillar) or 2 μ m \times 2 μ m x-y (Non-aggregated and HPLC-grade H₂O), 10 nm z-range taken from AFM; insets are 250 nm \times 250 nm x-y, 10 nm z-range. Images are representative of samples taken from independent preparations (oligomeric A β 42, n = 4; fibrillar A β 42, n = 3; non-aggregated A β 42, n = 3; HPLC-grade H₂O, n = 3). Bar, 1 μ m.



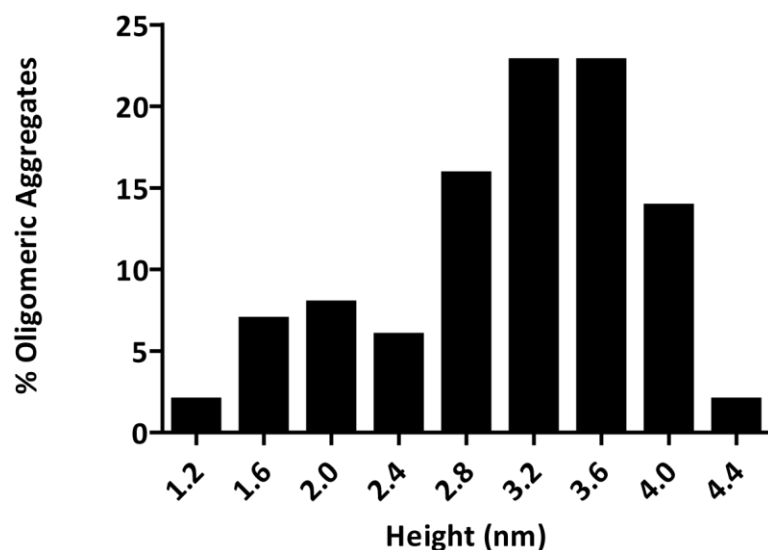


Figure 2.4 Distribution of aggregate heights within oligomeric preparations of A β 42.

Section analysis was performed on images captured by AFM from four independent oligomeric preparations of A β 42 peptide. Cross-sections through aggregates were examined individually to measure their heights, 25 aggregates were examined per image. The distribution of aggregate heights within oligomeric preparations of A β 42 are represented as a percentage of the total population ($n = 100$).

achieved at a concentration of 100 nM. When SH-SY5Y cells were treated with fibrillar A β 42 in the same concentration range as oligomeric A β 42, ERK1/2 phosphorylation was increased slightly above basal levels, but this did not increase at higher concentrations as was observed for the oligomeric form of the peptide. Non-aggregated A β 42 did not activate ERK1/2 under these conditions. At concentrations of 0.1, 1 and 100 nM, oligomeric A β 42 significantly activated ERK1/2 when compared to the basal level of ERK1/2 phosphorylation in untreated SH-SY5Y cells (Figure 2.5 B). In these experiments, NGF treatment of cells was used as a well-characterized positive control for ERK/MAPK activation. NGF induced ERK1/2 phosphorylation to a level at least twice that observed for oligomeric A β 42.

Oligomeric aggregates of A β 42, at a concentration of 100 nM, induced ERK1/2 phosphorylation in a time-dependent manner (Figure 2.6). When SH-SY5Y cells were treated with oligomeric A β 42, the level of ERK1/2 phosphorylation increased from 2 to

Figure 2.5 Phosphorylation of ERK1/2 induced by A β 42 is dependent upon the concentration and structural form of the peptide.

(A) SH-SY5Y cells were treated with oligomeric or fibrillar aggregates of A β 42 or non-aggregated A β 42 at concentrations of 0.01, 0.1, 1, 10, and 100 nM, or 50 ng/mL NGF for 5 min. Cells were lysed and proteins were resolved by SDS-PAGE and transferred to nitrocellulose membrane for immunoblotting for phosphorylated ERK1/2, total ERK1/2 or actin. Representative immunoblots are shown. **(B)** Immunoblots were analyzed by densitometry, the density of phosphorylated ERK1 and phosphorylated ERK2 bands were quantified together as a single value. Values were expressed as a percentage of the basal level of phosphorylated ERK1/2 measured in untreated control cells. Oligomeric A β 42 significantly induced phosphorylation of ERK1/2 at concentrations of 1, 10, and 100 nM when compared to control cells (* $p < 0.05$), as determined by one-way ANOVA and post hoc Dunnett analysis. Fibrillar or non-aggregated A β 42 did not significantly affect phosphorylation of ERK1/2. Data are mean \pm SEM (bars) values (oligomeric A β 42, $n = 6$; fibrillar A β 42, $n = 6$; non-aggregated A β 42, $n = 4$).

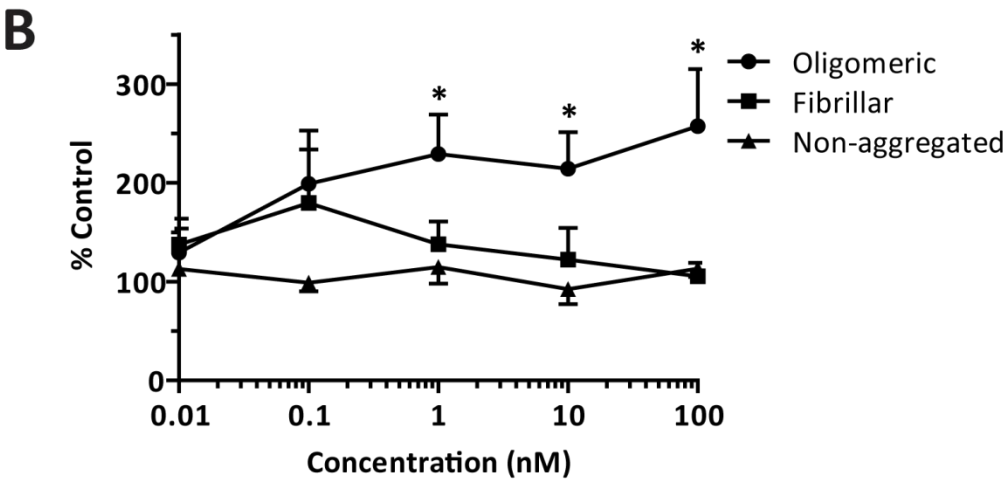
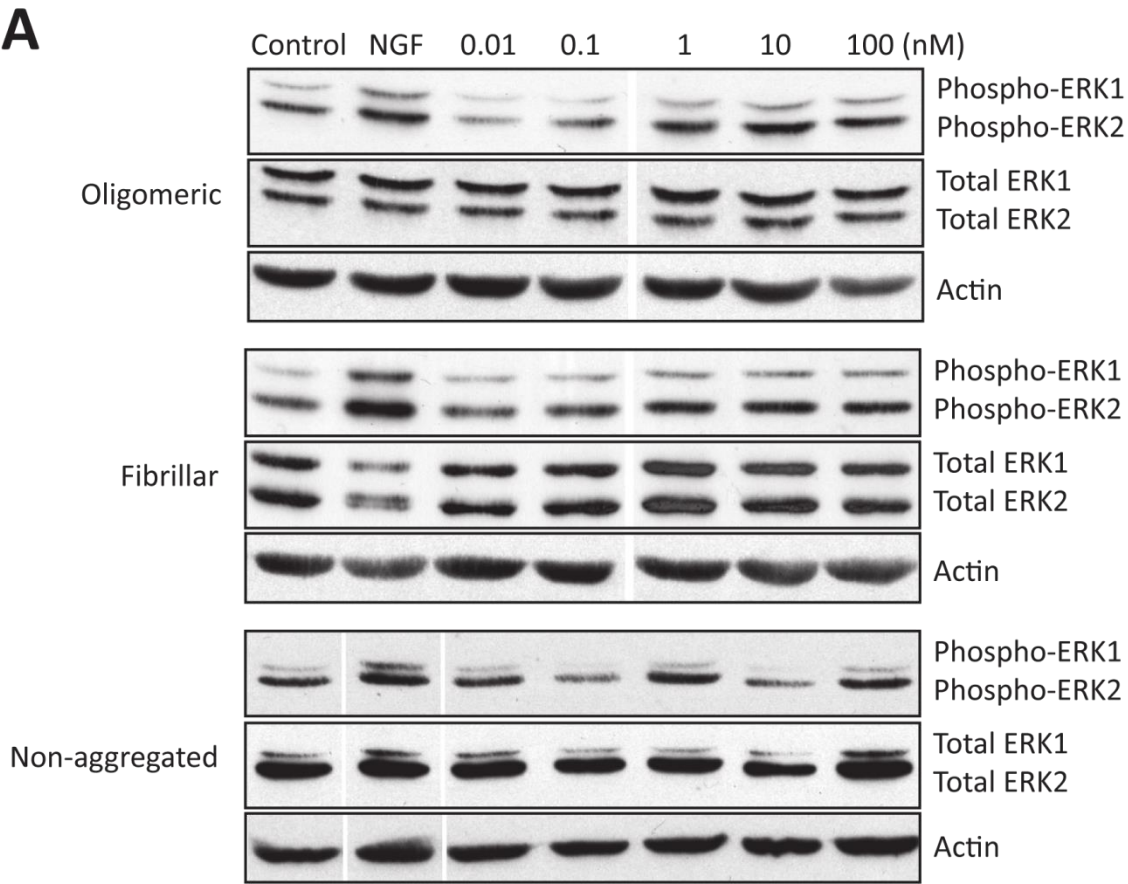
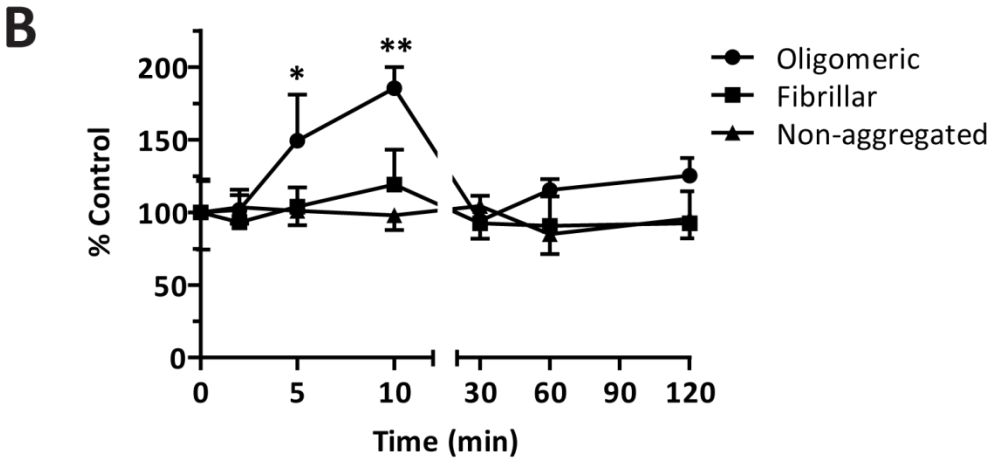
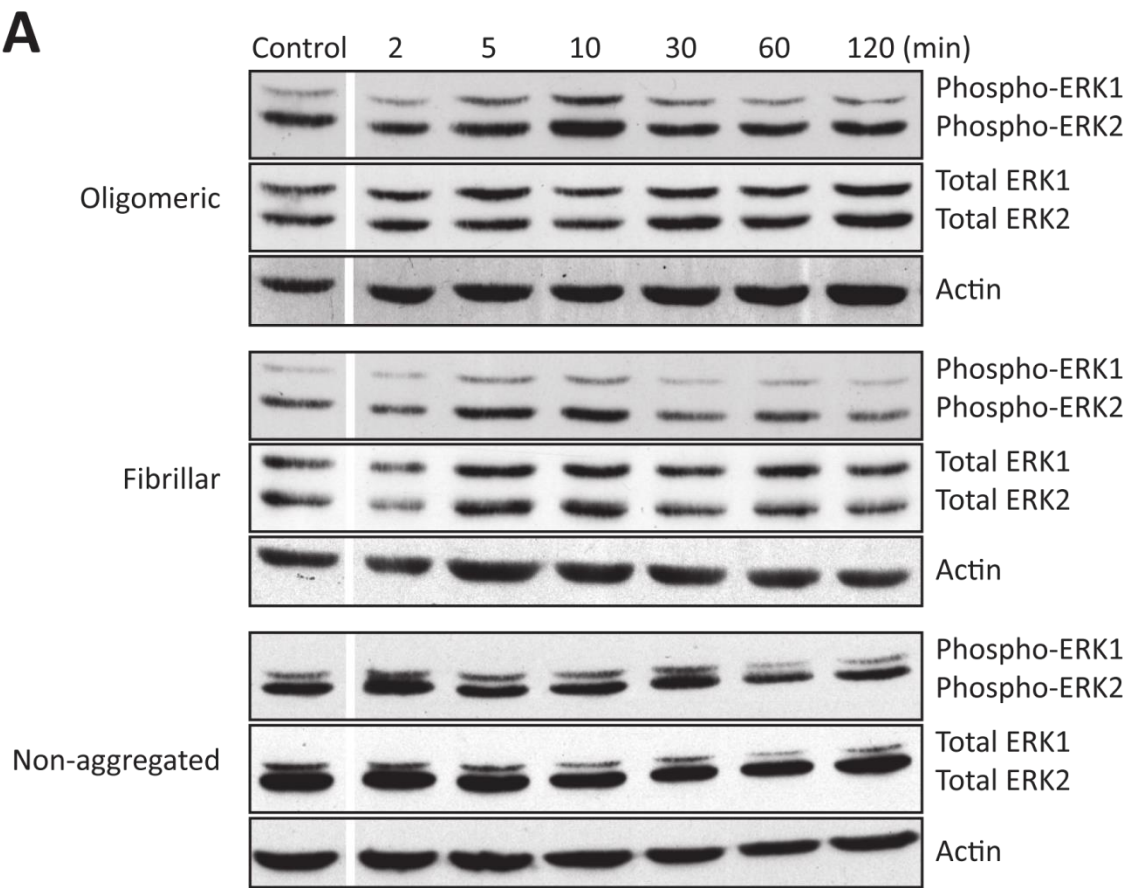


Figure 2.6 Phosphorylation of ERK1/2 induced by A β 42 is dependent upon the exposure time and structural form of the peptide.

(A) SH-SY5Y cells were exposed to oligomeric or fibrillar aggregates of A β 42 or non-aggregated A β 42 at a concentration of 100 nM for 2, 5, 10, 30, 60, or 120 min. Cells were lysed and proteins were resolved by SDS-PAGE and transferred to nitrocellulose membrane for immunoblotting for phosphorylated ERK1/2, total ERK1/2 or actin. Representative immunoblots are shown. **(B)** Immunoblots were analyzed by densitometry, the density of phosphorylated ERK1 and phosphorylated ERK2 bands were quantified together as a single value. Values were expressed as a percentage of the basal level of phosphorylated ERK1/2 measured in untreated control cells. 100 nM oligomeric A β 42 significantly induced phosphorylation of ERK1/2 after 5 min (* $p < 0.05$) and maximally affected ERK1/2 phosphorylation after 10 min of exposure (** $p < 0.01$). Fibrillar or non-aggregated A β 42 did not significantly affect phosphorylation of ERK1/2 with time. Significance was determined by one-way ANOVA and post hoc Dunnett analysis, data are mean \pm SEM (bars) values (oligomeric A β 42, $n = 6$; fibrillar A β 42, $n = 3$; non-aggregated A β 42, $n = 4$).



5 min and reached a maximum after 10 min of exposure, before returning to basal levels at 30 to 120 min after the initiation of treatment (Figure 2.6 A). Although 100 nM fibrillar A β 42 appeared to induce slight ERK1/2 phosphorylation in a time-dependent manner similar to oligomeric A β 42, the level of ERK1/2 phosphorylation was much less than that caused by oligomeric A β 42 and only slightly above the basal level of ERK1/2 phosphorylation in untreated SH-SY5Y cells. At the same concentration, non-aggregated A β 42 did not alter ERK1/2 phosphorylation over the time frame examined. When these effects were quantified, 100 nM oligomeric A β 42 significantly induced ERK1/2 activation in SH-SY5Y cells after 5 and 10 min of exposure (Figure 2.6 B).

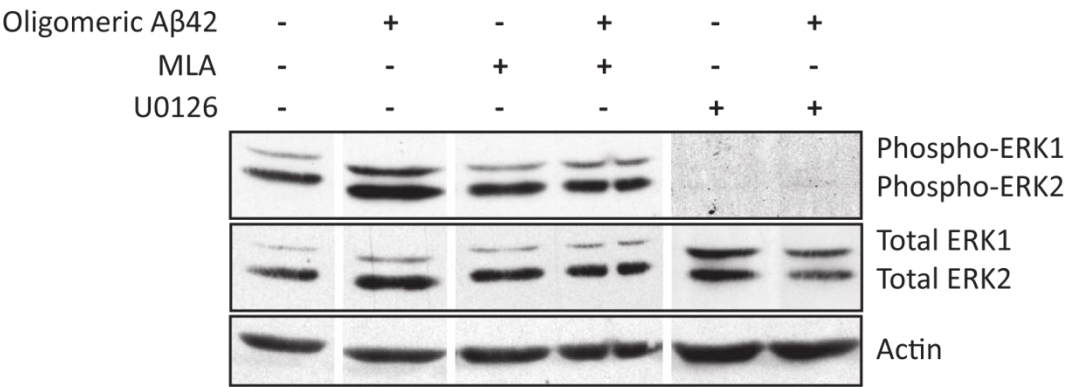
2.4.3 Effect of α 7 nAChR Antagonist Methyllaconitine on ERK/MAPK Phosphorylation Induced by Oligomeric A β 42

To investigate whether the α 7 nAChR was involved in oligomeric A β 42-induced ERK1/2 phosphorylation in SH-SY5Y cells, we examined the effect of the α 7 nAChR-selective competitive antagonist, MLA (Figure 2.7). In the absence of MLA, ERK1/2 phosphorylation induced by 100 nM oligomeric A β 42 was elevated approximately two-fold when compared to that of the basal level in untreated SH-SY5Y cells (Figure 2.7 B). Pre-incubation of cells with 10 nM MLA prior to the addition of oligomeric A β 42 attenuated the increase in ERK1/2 phosphorylation to near basal levels (Figure 2.7). When MLA was added to cells alone, it did not affect basal ERK1/2 phosphorylation (Figure 2.7). This suggests that oligomeric A β 42 may be acting, at least in part, through the α 7 nAChR to induce ERK1/2 phosphorylation in SH-SY5Y cells. Next, we determined the effect of inhibition of MAPK kinase 1 and 2 (MEK1/2) upon oligomeric A β 42-induced ERK1/2 phosphorylation. MEK1/2 resides directly upstream of ERK1/2 in the ERK/MAPK cascade (47) and is required for the activation of this pathway in SH-SY5Y cells by nicotine (42). In the presence of the MEK1/2 inhibitor U0126, ERK1/2 phosphorylation was completely abolished in both untreated cells and cells that were treated with oligomeric A β 42 (Figure 2.7 A).

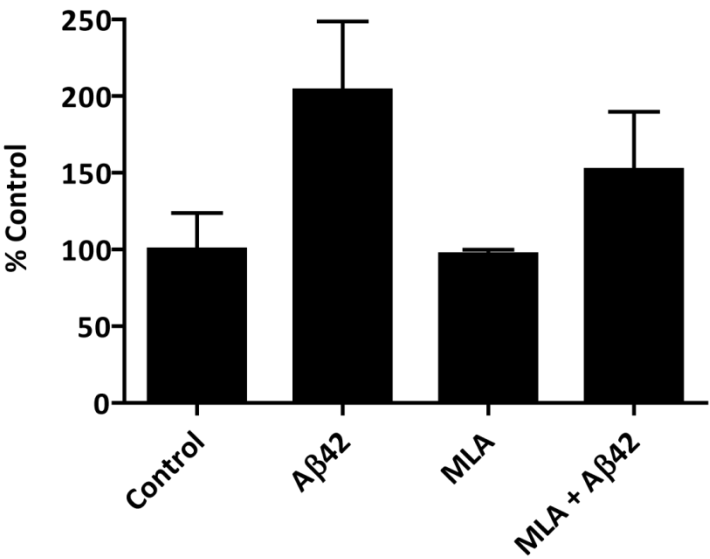
Figure 2.7 Oligomeric A β 42-induced ERK1/2 phosphorylation is dependent upon the α 7 nAChR and the upstream MAPK kinase, MEK1/2.

SH-SY5Y cells were exposed to 100 nM oligomeric A β 42 alone, or pre-incubated with 10 nM MLA or 50 mM U0126 for 30 min prior to the addition of 100 nM oligomeric A β 42. **(A)** Cells were lysed and proteins were resolved by SDS-PAGE and transferred to nitrocellulose membrane for immunoblotting for phosphorylated ERK1/2, total ERK1/2 or actin as outlined in the Methods. U0126, an inhibitor of MEK1/2, completely abolished ERK1/2 phosphorylation compared to untreated cells and cells that were exposed to oligomeric A β 42. MLA, a specific antagonist of the α 7 nAChR, did not alter ERK1/2 phosphorylation on its own, but prevented the phosphorylation of ERK1/2 induced by oligomeric A β 42. Representative immunoblots are shown from six independent experiments. **(B)** Immunoblots were analyzed by densitometry, the density of phosphorylated ERK1 and phosphorylated ERK2 bands were quantified together as a single value. Values were expressed as a percentage of the basal level of phosphorylated ERK1/2 measured in untreated control cells. Data are mean \pm SEM values (n = 6).

A



B



2.5 Discussion

In the present study, we demonstrate that oligomeric aggregates of A β 42 are the principal structural form of A β 42 peptides responsible for activation of the ERK/MAPK signalling pathway. Oligomeric aggregates of A β 42 activate ERK/MAPK in a concentration and time-dependent manner in SH-SY5Y cells. Phosphorylation of ERK1/2 induced by oligomeric A β 42 is blocked by MLA, a competitive antagonist selective for the α 7 nAChR, and occurs through a mechanism that requires MEK1/2 as an upstream mediator of ERK1/2 activity.

To differentiate between the biological effects of fibrillar and soluble oligomeric forms of A β 42, we followed a protocol established by Stine and colleagues that defined conditions for the aggregation of A β 42 into either oligomeric or fibrillar structures (14, 32). In the absence of incubation under these conditions, non-aggregated A β 42, that lacked the structural complexity of oligomeric or fibrillar preparations, was obtained. The oligomeric aggregates that we generated were in the 2 - 4 nm height range of oligomers (mean 3.1 ± 0.7 nm) reported by Stine et al., and the images that we obtained by AFM support their findings that the conditions they describe yield predominantly either oligomeric or fibrillar aggregates of A β 42 (32). These oligomeric aggregates are structurally similar in size and appearance to the A β -derived diffusible ligands generated by others, analogues of which have been detected in the cerebrospinal fluid (CSF) of AD subjects at higher levels than non-demented control subjects (48 - 50).

AFM is an established method for characterizing and visually distinguishing between non-aggregated, oligomeric, and fibrillar preparations of A β 42 peptide (32, 49). Other methods used to assess the aggregation state of A β 42 include thioflavin T (ThT) fluorescence, circular dichroism (CD), SDS-PAGE, and size-exclusion chromatography (SEC), but their application, with the exception of SEC, was of limited value in the context of the current study. Ultraviolet CD is a method for determining the secondary structure of proteins through the analysis of dynamic light scattering (51). Both oligomeric and fibrillar aggregates of A β 42 elicit CD spectra indicative of a β -sheet

secondary structure, while HFIP treatment yields monomeric A β 42, which exhibits an α -helical conformation (52). Incorporation of the benzothiazole dye ThT into the β -sheet structure of A β 42 aggregates results in an increase and spectral shift in its fluorescent emission, making it ideal for amyloid plaque histology of AD brain and measuring the rate of A β aggregation (53, 54). ThT fluorescence and CD can discriminate between solutions containing non-aggregated and aggregated forms of A β 42, but can not be used to differentiate between solutions containing oligomeric and fibrillar aggregates due to their common secondary structure. SDS-PAGE, although widely used to characterize A β 42 aggregates, produces nearly identical electrophoretic profiles regardless of preparation, either non-aggregated, oligomeric, or fibrillar A β 42, and the presence of SDS alters the distribution of the peptide amongst different molecular weight aggregates (49). SEC, in combination with a method for cross-linking and therefore stabilizing oligomeric aggregates of A β 42 of specific n-mer would have been useful for extending the current study. High-resolution SEC, coupled with multiangle laser light scattering analysis allows for the separation and precise determination of the molecular weight of A β 42 oligomers (49). Photo- and chemically-induced cross-linking of A β 42 oligomers has been performed successfully (55, 56). The combination of photo- or chemically-induced cross-linking and SEC would have potentially allowed for the isolation and identification of oligomeric species of A β 42 responsible for the activation of ERK/MAPK.

Oligomeric aggregates of A β 42, but neither fibrillar aggregates of A β 42 or non-aggregated A β 42, led to activation of the ERK/MAPK signalling pathway in SH-SY5Y cells. Although ERK1/2 phosphorylation was not as robust in response to oligomeric A β 42 as to NGF, this study demonstrates phosphorylation of ERK1/2 in response to oligomeric A β 42 as a consequence of dose and time, at concentrations of A β 42 within the range measured in the CSF of AD subjects (57 - 59). NGF activates ERK/MAPK through its cognate receptors, the low-affinity neurotrophin receptor, p75NTR (60) and the high-affinity neurotrophin tyrosine kinase receptor type 1, TrkA (61). The concentration of NGF in CSF is circa 1 pg/mL (62). SH-SY5Y cells express both TrkA and p75NTR (63, 64)

and will respond to 100 ng/mL NGF to activate ERK/MAPK (65). We treated SH-SY5Y cells with 50 ng/mL of NGF as a positive control for phosphorylation of ERK1/2 and were required to reduce the amount of protein resolved by SDS-PAGE by half, compared to A β 42 treated and control cells, to avoid over-exposure of immunoblots due to the intensity of NGF-stimulated phosphorylated-ERK1/2 bands. The concentration of A β 42 in the CSF of individuals diagnosed with AD, as measured by enzyme-linked immunosorbent assay, is 50 – 200 nM (57 - 59). In SH-SY5Y cells, oligomeric A β 42 acutely induced phosphorylation of ERK1/2 at a concentration of 100 nM, which peaked after 10 min incubation. These results are similar to those of Dineley et al. when they examined ERK/MAPK activation in hippocampal slice cultures in response to A β 42 peptides (23). They observed maximal induction of ERK1/2 phosphorylation at an earlier time point, after 5 min incubation with 100 nM A β 42. However, this study was performed with solutions of synthetic A β 42 peptides that were not characterized in terms of the different structural forms or aggregates of A β 42 that may have been present to contribute to these effects. Our findings of A β 42-induced activation of ERK1/2 differ from those of Townsend et al. and Ma et al. in which they observed inhibition of the ERK/MAPK signalling pathway through insulin receptor- or insulin-like growth factor receptor-dependent mechanisms, respectively (66, 67). Several critical factors could account for the differences between experimental responses, most notably the time frames from the exposure to A β prior to monitoring for ERK1/2 activation and the aggregation state and concentrations of A β tested.

In our analysis, oligomers 3.0 - 3.8 nm in height comprised the majority of the aggregates in oligomeric preparations of A β 42. We noted the presence of a second smaller population of aggregates on the order of 2 nm in height, an aggregate species that was also apparent, to a small degree, as oligomers within fibrillar preparations. The presence of oligomers within fibrillar preparations may have been responsible for the slight activation of ERK/MAPK observed in our experiments. However, since we did not observe significant changes in the phosphorylation of ERK1/2 in response to the application of fibrillar preparations of A β 42, this suggests the aggregate species which

are capable of activating ERK1/2 were absent from this preparation. Oligomers of A β 42 in the range of 3.0 - 3.8 nm in height, which appeared with the greatest frequency in oligomeric preparations and were absent from fibrillar preparations, may represent the structural form of the peptide responsible for the activation of ERK1/2 in SH-SY5Y cells.

The sensitivity of oligomeric A β 42-induced phosphorylation of ERK1/2 to MLA suggests a role for the α 7 nAChR in mediating activation of this pathway. SH-SY5Y cells express functional α 7 nAChR (36, 68) and have been previously used to elucidate the role of the α 7 nAChR in activation of the ERK/MAPK signalling pathway by the nAChR agonist nicotine (42). MLA is a competitive antagonist selective for the α 7 nAChR (69, 70). Incubation of SH-SY5Y cells with 10 nM MLA prior to the addition of oligomeric A β 42 mitigated the peptide-stimulated increase in phosphorylation of ERK1/2 above basal levels. These findings are in support of those made by Bell et al. that 1 μ M MLA blocked A β 42-induced activation of ERK/MAPK in hippocampal slice cultures (24). The dissociation constant (K_d) of MLA for the α 7 nAChR is approximately 2 nM (70). If a higher concentration of MLA, on the order of 100 to 1000-fold K_d (0.2 - 2 μ M) to ensure maximal receptor binding, had been used in our experiments, we may have observed significant blockade of oligomeric A β 42-induced phosphorylation of ERK1/2 and our results would have perhaps been more in line with that of Bell and colleagues. These results demonstrate that the α 7 nAChR is a mechanism through which A β 42 oligomers can activate the ERK/MAPK signalling pathway. The p75NTR has also been identified as a receptor for oligomeric aggregates of A β 42 and subsequent activation of ERK/MAPK. A low concentration, 25 nM of low n-mer A β 42 aggregates induces acute phosphorylation of ERK1/2 within 5 min in cells stably transfected with p75NTR (71). As SH-SY5Y cells endogenously express p75NTR (64) and interaction between oligomeric A β 42 and p75NTR could have affected our investigation, antisense silencing of α 7 nAChR mRNA through transfection of SH-SY5Y cells with small interfering RNA (72, 73) prior to cell treatments would have been useful for determining the contribution of α 7 nAChR to phosphorylation of ERK1/2 in oligomeric A β 42 treated cells. Directly upstream of ERK1/2 in the ERK/MAPK pathway, activation of MEK1/2 is required for

phosphorylation and activation of ERK1/2 (47). U0126 is an inhibitor of MEK1/2 that prevents phosphorylation of ERK1/2 (74). Blockade of oligomeric A β 42-induced phosphorylation of ERK1/2 by U0126 suggests that oligomeric aggregates of A β 42 are capable of activating ERK/MAPK in SH-SY5Y cells through the upstream activator MEK1/2. Based on these findings, we would propose a signalling pathway for oligomeric A β 42 that leads from α 7 nAChR to the phosphorylation of ERK1/2 through MEK1/2, involving an undetermined mechanism that transduces signals from α 7 nAChR to MEK1/2 (Figure 2.8).

Our findings reinforce the widely held hypothesis that small oligomers of A β 42, rather than A β 42 fibrils or non-aggregated A β 42, represent the biologically active form of the peptide. This relationship to the activity of oligomeric A β 42 extends to effects on a wide variety of other important cellular processes (75), including regulation of calcineurin activity (76); production of brain-derived neurotrophic factor (77); protein kinase C activity (78); MAPK kinase 6 expression (79); ERK/MAPK-dependent neuronal differentiation of bone marrow-derived mesenchymal stem cells (80), and cellular prion protein signalling and trafficking (81 - 83). Activation of ERK/MAPK by soluble diffusible oligomers of A β 42, similar to those we observed in oligomeric preparations of synthetic A β 42, may play a role in the disruption of cognitive function in AD. Oligomeric aggregates of A β 42 acutely activate the ERK/MAPK signalling pathway through a mechanism that involves the α 7 nAChR and is dependent upon MEK1/2 activity. The α 7 nAChR has an emerging role in learning and memory processes (84). Given the increasing relevance of the α 7 nAChR to cognitive function and the importance of ERK/MAPK to these processes, the results of this study place an emphasis on identifying the structural forms of A β 42 peptides which may interact with the α 7 nAChR and the signalling consequences that result.

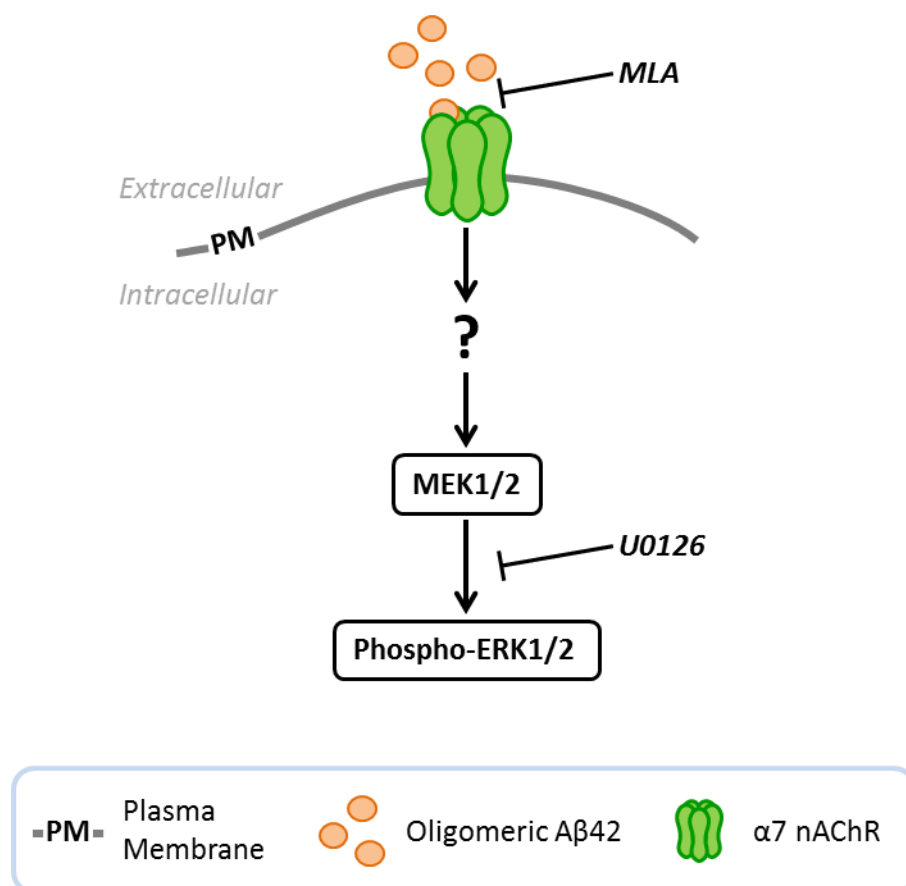


Figure 2.8 A model for oligomeric Aβ42 signalling through the α7 nAChR.

Oligomeric Aβ42, but neither non-aggregated or fibrillar Aβ42, induces phosphorylation of ERK1/2 through the α7 nAChR. Phosphorylation of ERK1/2 is mitigated by the α7 nAChR-selective antagonist, MLA, and completely blocked by U0126, an inhibitor of MEK1/2. MEK1/2 acts directly upstream of ERK1/2 in the ERK/MAPK signal transduction pathway. An undetermined signal transduction mechanism lies between α7 nAChR and MEK1/2. Legend, inset.

2.6 References

1. Selkoe, D.J. and Podlisny, M.B. (2002) Deciphering the genetic basis of Alzheimer's disease. *Annu Rev Genomics Hum Genet* **3**: 67-99.
2. Haass, C. (2004) Take five--BACE and the gamma-secretase quartet conduct Alzheimer's amyloid beta-peptide generation. *EMBO J* **23**: 483-8.
3. Jarrett, J.T., Berger, E.P., T., L.P., Jr. (1993) The carboxy terminus of the beta amyloid protein is critical for the seeding of amyloid formation: implications for the pathogenesis of Alzheimer's disease. *Biochemistry* **32**: 4693-7.
4. Burdick, D., Soreghan, B., Kwon, M., Kosmoski, J., Knauer, M., Henschen, A., Yates, J., Cotman, C., Glabe, C. (1992) Assembly and aggregation properties of synthetic Alzheimer's A4/beta amyloid peptide analogs. *J Biol Chem* **267**: 546-54.
5. Iwatsubo, T., Odaka, A., Suzuki, N., Mizusawa, H., Nukina, N., Ihara, Y. (1994) Visualization of A beta 42(43) and A beta 40 in senile plaques with end-specific A beta monoclonals: evidence that an initially deposited species is A beta 42(43). *Neuron* **13**: 45-53.
6. Dickson, D.W., Crystal, H.A., Bevona, C., Honer, W., Vincent, I., Davies, P. (1995) Correlations of synaptic and pathological markers with cognition of the elderly. *Neurobiol Aging* **16**: 285-98; discussion 298-304.
7. Terry, R.D., Masliah, E., Salmon, D.P., Butters, N., DeTeresa, R., Hill, R., Hansen, L.A., Katzman, R. (1991) Physical basis of cognitive alterations in Alzheimer's disease: synapse loss is the major correlate of cognitive impairment. *Ann Neurol* **30**: 572-80.
8. Lue, L.F., Kuo, Y.M., Roher, A.E., Brachova, L., Shen, Y., Sue, L., Beach, T., Kurth, J.H., Rydel, R.E., Rogers, J. (1999) Soluble amyloid beta peptide concentration as a predictor of synaptic change in Alzheimer's disease. *Am J Pathol* **155**: 853-62.

9. McLean, C.A., Cherny, R.A., Fraser, F.W., Fuller, S.J., Smith, M.J., Beyreuther, K., Bush, A.I., Masters, C.L. (1999) Soluble pool of Abeta amyloid as a determinant of severity of neurodegeneration in Alzheimer's disease. *Ann Neurol* **46**: 860-6.
10. Walsh, D.M., Tseng, B.P., Rydel, R.E., Podlisny, M.B., Selkoe, D.J. (2000) The oligomerization of amyloid beta-protein begins intracellularly in cells derived from human brain. *Biochemistry* **39**: 10831-9.
11. Lambert, M.P., Barlow, A.K., Chromy, B.A., Edwards, C., Freed, R., Liosatos, M., Morgan, T.E., Rozovsky, I., Trommer, B., Viola, K.L., Wals, P., Zhang, C., Finch, C.E., Krafft, G.A., Klein, W.L. (1998) Diffusible, nonfibrillar ligands derived from Abeta1-42 are potent central nervous system neurotoxins. *Proc Natl Acad Sci U S A* **95**: 6448-53.
12. Podlisny, M.B., Ostaszewski, B.L., Squazzo, S.L., Koo, E.H., Rydel, R.E., Teplow, D.B., Selkoe, D.J. (1995) Aggregation of secreted amyloid beta-protein into sodium dodecyl sulfate-stable oligomers in cell culture. *J Biol Chem* **270**: 9564-70.
13. Morishima-Kawashima, M. and Ihara, Y. (1998) The presence of amyloid beta-protein in the detergent-insoluble membrane compartment of human neuroblastoma cells. *Biochemistry* **37**: 15247-53.
14. Dahlgren, K.N., Manelli, A.M., B., S.W., Jr, Baker, L.K., Krafft, G.A., LaDu, M.J. (2002) Oligomeric and fibrillar species of amyloid-beta peptides differentially affect neuronal viability. *J Biol Chem* **277**: 32046-53.
15. Walsh, D.M., Klyubin, I., Fadeeva, J.V., Cullen, W.K., Anwyl, R., Wolfe, M.S., Rowan, M.J., Selkoe, D.J. (2002) Naturally secreted oligomers of amyloid beta protein potently inhibit hippocampal long-term potentiation in vivo. *Nature* **416**: 535-9.
16. Koffie, R.M., Meyer-Luehmann, M., Hashimoto, T., Adams, K.W., Mielke, M.L., Garcia-Alloza, M., Micheva, K.D., Smith, S.J., Kim, M.L., Lee, V.M., Hyman,

- B.T., Spires-Jones, T.L. (2009) Oligomeric amyloid beta associates with postsynaptic densities and correlates with excitatory synapse loss near senile plaques. *Proc. Natl. Acad. Sci. U. S. A.* **106**: 4012-4017.
17. Adams, J.P., Roberson, E.D., English, J.D., Selcher, J.C., Sweatt, J.D. (2000) MAPK regulation of gene expression in the central nervous system. *Acta Neurobiol. Exp. (Wars)* **60**: 377-394.
 18. Waltereit, R. and Weller, M. (2003) Signaling from cAMP/PKA to MAPK and synaptic plasticity. *Mol. Neurobiol.* **27**: 99-106.
 19. Smolen, P., Baxter, D.A., Byrne, J.H. (2006) A model of the roles of essential kinases in the induction and expression of late long-term potentiation. *Biophys J* **90**: 2760-75.
 20. Hunter, B.E., de Fiebre, C.M., Papke, R.L., Kem, W.R., Meyer, E.M. (1994) A novel nicotinic agonist facilitates induction of long-term potentiation in the rat hippocampus. *Neurosci. Lett.* **168**: 130-134.
 21. Matsuyama, S., Matsumoto, A., Enomoto, T., Nishizaki, T. (2000) Activation of nicotinic acetylcholine receptors induces long-term potentiation in vivo in the intact mouse dentate gyrus. *Eur. J. Neurosci.* **12**: 3741-3747.
 22. Welsby, P.J., Rowan, M.J., Anwyl, R. (2009) Intracellular mechanisms underlying the nicotinic enhancement of LTP in the rat dentate gyrus. *Eur. J. Neurosci.* **29**: 65-75.
 23. Dineley, K.T., Westerman, M., Bui, D., Bell, K., Ashe, K.H., Sweatt, J.D. (2001) Beta-amyloid activates the mitogen-activated protein kinase cascade via hippocampal $\alpha 7$ nicotinic acetylcholine receptors: In vitro and in vivo mechanisms related to Alzheimer's disease. *J Neurosci* **21**: 4125-33.

24. Bell, K.A., O'Riordan, K.J., Sweatt, J.D., Dineley, K.T. (2004) MAPK recruitment by beta-amyloid in organotypic hippocampal slice cultures depends on physical state and exposure time. *J Neurochem* **91**: 349-61.
25. Wang, H.Y., Lee, D.H., Davis, C.B., Shank, R.P. (2000) Amyloid peptide Abeta(1-42) binds selectively and with picomolar affinity to alpha7 nicotinic acetylcholine receptors. *J Neurochem* **75**: 1155-61.
26. Wang, H.Y., Lee, D.H., D'Andrea, M.R., Peterson, P.A., Shank, R.P., Reitz, A.B. (2000) beta-Amyloid(1-42) binds to alpha7 nicotinic acetylcholine receptor with high affinity. Implications for Alzheimer's disease pathology. *J Biol Chem* **275**: 5626-32.
27. Dineley, K.T., Bell, K.A., Bui, D., Sweatt, J.D. (2002) beta -Amyloid peptide activates alpha 7 nicotinic acetylcholine receptors expressed in *Xenopus* oocytes. *J Biol Chem* **277**: 25056-61.
28. Wang, H.Y., Li, W., Benedetti, N.J., Lee, D.H. (2003) Alpha 7 nicotinic acetylcholine receptors mediate beta-amyloid peptide-induced tau protein phosphorylation. *J Biol Chem* **278**: 31547-53.
29. Lee, D.H. and Wang, H.Y. (2003) Differential physiologic responses of alpha7 nicotinic acetylcholine receptors to beta-amyloid1-40 and beta-amyloid1-42. *J Neurobiol.* **55**: 25-30.
30. Grassi, F., Palma, E., Tonini, R., Amici, M., Ballivet, M., Eusebi, F. (2003) Amyloid beta(1-42) peptide alters the gating of human and mouse alpha-bungarotoxin-sensitive nicotinic receptors. *J Physiol* **547**: 147-57.
31. Small, D.H., Maksel, D., Kerr, M.L., Ng, J., Hou, X., Chu, C., Mehrani, H., Unabia, S., Azari, M.F., Loiacono, R., Aguilar, M.I., Chebib, M. (2007) The beta-amyloid protein of Alzheimer's disease binds to membrane lipids but does not bind to the alpha7 nicotinic acetylcholine receptor. *J Neurochem* **101**: 1527-38.

32. B., S.W., Jr, Dahlgren, K.N., Krafft, G.A., LaDu, M.J. (2003) In vitro characterization of conditions for amyloid-beta peptide oligomerization and fibrillogenesis. *J Biol Chem* **278**: 11612-22.
33. Ross, R.A., Spengler, B.A., Biedler, J.L. (1983) Coordinate morphological and biochemical interconversion of human neuroblastoma cells. *J. Natl. Cancer Inst.* **71**: 741-747.
34. Biedler, J.L., Helson, L., Spengler, B.A. (1973) Morphology and growth, tumorigenicity, and cytogenetics of human neuroblastoma cells in continuous culture. *Cancer Res.* **33**: 2643-2652.
35. Peng, X., Katz, M., Gerzanich, V., Anand, R., Lindstrom, J. (1994) Human alpha 7 acetylcholine receptor: cloning of the alpha 7 subunit from the SH-SY5Y cell line and determination of pharmacological properties of native receptors and functional alpha 7 homomers expressed in *Xenopus* oocytes. *Mol. Pharmacol.* **45**: 546-554.
36. Ridley, D.L., Rogers, A., Wonnacott, S. (2001) Differential effects of chronic drug treatment on alpha3* and alpha7 nicotinic receptor binding sites, in hippocampal neurones and SH-SY5Y cells. *Br. J. Pharmacol.* **133**: 1286-1295.
37. Dajas-Bailador, F.A., Mogg, A.J., Wonnacott, S. (2002) Intracellular Ca²⁺ signals evoked by stimulation of nicotinic acetylcholine receptors in SH-SY5Y cells: contribution of voltage-operated Ca²⁺ channels and Ca²⁺ stores. *J. Neurochem.* **81**: 606-614.
38. Mousavi, M. and Hellstrom-Lindahl, E. (2009) Nicotinic receptor agonists and antagonists increase sAPPalpha secretion and decrease Abeta levels in vitro. *Neurochem. Int.* **54**: 237-244.
39. Del Barrio, L., Martin-de-Saavedra, M.D., Romero, A., Parada, E., Egea, J., Avila, J., McIntosh, J.M., Wonnacott, S., Lopez, M.G. (2011) Neurotoxicity induced by

okadaic acid in the human neuroblastoma SH-SY5Y line can be differentially prevented by $\alpha 7$ and $\beta 2^*$ nicotinic stimulation. *Toxicol. Sci.* **123**: 193-205.

40. Parada, E., Egea, J., Romero, A., del Barrio, L., Garcia, A.G., Lopez, M.G. (2010) Poststress treatment with PNU282987 can rescue SH-SY5Y cells undergoing apoptosis via $\alpha 7$ nicotinic receptors linked to a Jak2/Akt/HO-1 signaling pathway. *Free Radic. Biol. Med.* **49**: 1815-1821.
41. Qi, X.L., Ou-Yang, K., Ren, J.M., Wu, C.X., Xiao, Y., Li, Y., Guan, Z.Z. (2013) Preventing expression of the nicotinic receptor subunit $\alpha 7$ in SH-SY5Y cells with interference RNA indicates that this receptor may protect against the neurotoxicity of A β . *Neurochem. Res.* **38**: 943-950.
42. Dajas-Bailador, F.A., Soliakov, L., Wonnacott, S. (2002) Nicotine activates the extracellular signal-regulated kinase 1/2 via the $\alpha 7$ nicotinic acetylcholine receptor and protein kinase A, in SH-SY5Y cells and hippocampal neurones. *J Neurochem* **80**: 520-30.
43. Thornton, J.T. 1998. Scanning Probe Microscopy Training Notebook, Version 3.0. Digital Instruments Veeco Metrology Group.
44. Bradford, M.M. (1976) A rapid and sensitive method for the quantitation of microgram quantities of protein utilizing the principle of protein-dye binding. *Anal. Biochem.* **72**: 248-254.
45. Laemmli, U.K. (1970) Cleavage of structural proteins during the assembly of the head of bacteriophage T4. *Nature* **227**: 680-685.
46. Walsh, D.M. and Selkoe, D.J. (2007) A β oligomers - a decade of discovery. *J Neurochem* **101**: 1172-84.

47. Sweatt, J.D. (2001) The neuronal MAP kinase cascade: a biochemical signal integration system subserving synaptic plasticity and memory. *J Neurochem* **76**: 1-10.
48. Shekhawat, G.S., Lambert, M.P., Sharma, S., Velasco, P.T., Viola, K.L., Klein, W.L., Dravid, V.P. (2009) Soluble state high resolution atomic force microscopy study of Alzheimer's beta-amyloid oligomers. *Appl. Phys. Lett.* **95**: 183701.
49. Hepler, R.W., Grimm, K.M., Nahas, D.D., Breese, R., Dodson, E.C., Acton, P., Keller, P.M., Yeager, M., Wang, H., Shughrue, P., Kinney, G., Joyce, J.G. (2006) Solution state characterization of amyloid beta-derived diffusible ligands. *Biochemistry* **45**: 15157-67.
50. Georganopoulou, D.G., Chang, L., Nam, J.M., Thaxton, C.S., Mufson, E.J., Klein, W.L., Mirkin, C.A. (2005) Nanoparticle-based detection in cerebral spinal fluid of a soluble pathogenic biomarker for Alzheimer's disease. *Proc. Natl. Acad. Sci. U. S. A.* **102**: 2273-2276.
51. Kelly, S.M. and Price, N.C. (1997) The application of circular dichroism to studies of protein folding and unfolding. *Biochim. Biophys. Acta* **1338**: 161-185.
52. Barrow, C.J., Yasuda, A., Kenny, P.T., Zagorski, M.G. (1992) Solution conformations and aggregational properties of synthetic amyloid beta-peptides of Alzheimer's disease. Analysis of circular dichroism spectra. *J. Mol. Biol.* **225**: 1075-1093.
53. LeVine, H.,3rd. (1999) Quantification of beta-sheet amyloid fibril structures with thioflavin T. *Methods Enzymol.* **309**: 274-284.
54. Yang, Y. and Cui, M. (2014) Radiolabeled bioactive benzoheterocycles for imaging beta-amyloid plaques in Alzheimer's disease. *Eur. J. Med. Chem.* **87C**: 703-721.

55. Rahimi, F., Maiti, P., Bitan, G. (2009) Photo-induced cross-linking of unmodified proteins (PICUP) applied to amyloidogenic peptides. *J. Vis. Exp.* **(23)**. pii: 1071. doi: 10.3791/1071.
56. Moore, B.D., Rangachari, V., Tay, W.M., Milkovic, N.M., Rosenberry, T.L. (2009) Biophysical analyses of synthetic amyloid-beta(1-42) aggregates before and after covalent cross-linking. Implications for deducing the structure of endogenous amyloid-beta oligomers. *Biochemistry* **48**: 11796-11806.
57. Smach, M.A., Charfeddine, B., Lammouchi, T., Harrabi, I., Ben Othman, L., Dridi, H., Bennamou, S., Limem, K. (2008) CSF beta-amyloid 1-42 and tau in Tunisian patients with Alzheimer's disease: the effect of APOE epsilon4 allele. *Neurosci Lett* **440**: 145-9.
58. Sluimer, J.D., Bouwman, F.H., Vrenken, H., Blankenstein, M.A., Barkhof, F., van der Flier, W.M., Scheltens, P. (2008) Whole-brain atrophy rate and CSF biomarker levels in MCI and AD: A longitudinal study. *Neurobiol Aging*
59. Bouwman, F.H., Schoonenboom, N.S., Verwey, N.A., van Elk, E.J., Kok, A., Blankenstein, M.A., Scheltens, P., van der Flier, W.M. (2009) CSF biomarker levels in early and late onset Alzheimer's disease. *Neurobiol. Aging* **30**: 1895-1901.
60. Susen, K., Heumann, R., Blochl, A. (1999) Nerve growth factor stimulates MAPK via the low affinity receptor p75(LNTR). *FEBS Lett.* **463**: 231-234.
61. Roux, P.P. and Barker, P.A. (2002) Neurotrophin signaling through the p75 neurotrophin receptor. *Prog. Neurobiol.* **67**: 203-233.
62. Hock, C., Heese, K., Muller-Spahn, F., Huber, P., Riesen, W., Nitsch, R.M., Otten, U. (2000) Increased CSF levels of nerve growth factor in patients with Alzheimer's disease. *Neurology* **54**: 2009-2011.

63. Lavenius, E., Gestblom, C., Johansson, I., Nanberg, E., Pahlman, S. (1995)
Transfection of TRK-A into human neuroblastoma cells restores their ability to differentiate in response to nerve growth factor. *Cell Growth Differ.* **6**: 727-736.
64. Ehrhard, P.B., Ganter, U., Schmutz, B., Bauer, J., Otten, U. (1993) Expression of low-affinity NGF receptor and trkB mRNA in human SH-SY5Y neuroblastoma cells. *FEBS Lett.* **330**: 287-292.
65. Olsson, A.K., Vadhammar, K., Nanberg, E. (2000) Activation and protein kinase C-dependent nuclear accumulation of ERK in differentiating human neuroblastoma cells. *Exp. Cell Res.* **256**: 454-467.
66. Townsend, M., Mehta, T., Selkoe, D.J. (2007) Soluble Abeta inhibits specific signal transduction cascades common to the insulin receptor pathway. *J Biol Chem* **282**: 33305-12.
67. Ma, Q.L., Harris-White, M.E., Ubeda, O.J., Simmons, M., Beech, W., Lim, G.P., Teter, B., Frautschy, S.A., Cole, G.M. (2007) Evidence of Abeta- and transgene-dependent defects in ERK-CREB signaling in Alzheimer's models. *J. Neurochem.* **103**: 1594-1607.
68. Dajas-Bailador, F.A., Mogg, A.J., Wonnacott, S. (2002) Intracellular Ca²⁺ signals evoked by stimulation of nicotinic acetylcholine receptors in SH-SY5Y cells: contribution of voltage-operated Ca²⁺ channels and Ca²⁺ stores. *J. Neurochem.* **81**: 606-614.
69. Gopalakrishnan, M., Buisson, B., Touma, E., Giordano, T., Campbell, J.E., Hu, I.C., Donnelly-Roberts, D., Arneric, S.P., Bertrand, D., Sullivan, J.P. (1995) Stable expression and pharmacological properties of the human alpha 7 nicotinic acetylcholine receptor. *Eur. J. Pharmacol.* **290**: 237-246.
70. Davies, A.R., Hardick, D.J., Blagbrough, I.S., Potter, B.V., Wolstenholme, A.J., Wonnacott, S. (1999) Characterisation of the binding of [3H]methyllycaconitine: a

new radioligand for labelling alpha 7-type neuronal nicotinic acetylcholine receptors. *Neuropharmacology* **38**: 679-690.

71. Susen, K. and Blochl, A. (2005) Low concentrations of aggregated beta-amyloid induce neurite formation via the neurotrophin receptor p75. *J. Mol. Med.* **83**: 720-735.
72. Arredondo, J., Chernyavsky, A.I., Jolkovsky, D.L., Pinkerton, K.E., Grando, S.A. (2006) Receptor-mediated tobacco toxicity: cooperation of the Ras/Raf-1/MEK1/ERK and JAK-2/STAT-3 pathways downstream of alpha7 nicotinic receptor in oral keratinocytes. *FASEB J.* **20**: 2093-2101.
73. Qi, X.L., Nordberg, A., Xiu, J., Guan, Z.Z. (2007) The consequences of reducing expression of the alpha7 nicotinic receptor by RNA interference and of stimulating its activity with an alpha7 agonist in SH-SY5Y cells indicate that this receptor plays a neuroprotective role in connection with the pathogenesis of Alzheimer's disease. *Neurochem. Int.* **51**: 377-383.
74. DeSilva, D.R., Jones, E.A., Favata, M.F., Jaffee, B.D., Magolda, R.L., Trzaskos, J.M., Scherle, P.A. (1998) Inhibition of mitogen-activated protein kinase kinase blocks T cell proliferation but does not induce or prevent anergy. *J Immunol* **160**: 4175-81.
75. Kirkitadze, M.D., Bitan, G., Teplow, D.B. (2002) Paradigm shifts in Alzheimer's disease and other neurodegenerative disorders: the emerging role of oligomeric assemblies. *J. Neurosci. Res.* **69**: 567-577.
76. Reese, L.C., Zhang, W., Dineley, K.T., Kaye, R., Taglialatela, G. (2008) Selective induction of calcineurin activity and signaling by oligomeric amyloid beta. *Aging Cell.* **7**: 824-835.
77. Garzon, D.J. and Fahnstock, M. (2007) Oligomeric amyloid decreases basal levels of brain-derived neurotrophic factor (BDNF) mRNA via specific downregulation of

- BDNF transcripts IV and V in differentiated human neuroblastoma cells. *J. Neurosci.* **27**: 2628-2635.
78. Kim, H.J., Kim, J.H., Chae, S.C., Park, Y.C., Kwon, K.S., Hong, S.T. (2004) Soluble oligomeric A β disrupts the protein kinase C signaling pathway. *Neuroreport* **15**: 503-507.
79. Joerchel, S., Raap, M., Bigl, M., Eschrich, K., Schliebs, R. (2008) Oligomeric beta-amyloid(1-42) induces the expression of Alzheimer disease-relevant proteins in cholinergic SN56.B5.G4 cells as revealed by proteomic analysis. *Int. J. Dev. Neurosci.* **26**: 301-308.
80. Jin, H.K., Bae, J.S., Furuya, S., Carter, J.E. (2009) Amyloid beta-derived neuroplasticity in bone marrow-derived mesenchymal stem cells is mediated by NPY and 5-HT_{2B} receptors via ERK1/2 signalling pathways. *Cell Prolif.* **42**: 571-586.
81. Lauren, J., Gimbel, D.A., Nygaard, H.B., Gilbert, J.W., Strittmatter, S.M. (2009) Cellular prion protein mediates impairment of synaptic plasticity by amyloid-beta oligomers. *Nature* **457**: 1128-1132.
82. Ostapchenko, V.G., Beraldo, F.H., Mohammad, A.H., Xie, Y.F., Hirata, P.H., Magalhaes, A.C., Lamour, G., Li, H., Maciejewski, A., Belrose, J.C., Teixeira, B.L., Fahnestock, M., Ferreira, S.T., Cashman, N.R., Hajj, G.N., Jackson, M.F., Choy, W.Y., MacDonald, J.F., Martins, V.R., Prado, V.F., Prado, M.A. (2013) The prion protein ligand, stress-inducible phosphoprotein 1, regulates amyloid-beta oligomer toxicity. *J. Neurosci.* **33**: 16552-16564.
83. Caetano, F.A., Beraldo, F.H., Hajj, G.N., Guimaraes, A.L., Jurgensen, S., Wasilewska-Sampaio, A.P., Hirata, P.H., Souza, I., Machado, C.F., Wong, D.Y., De Felice, F.G., Ferreira, S.T., Prado, V.F., Rylett, R.J., Martins, V.R., Prado, M.A. (2011) Amyloid-beta oligomers increase the localization of prion protein at the cell surface. *J. Neurochem.* **117**: 538-553.

84. Bitner, R.S., Bunnelle, W.H., Anderson, D.J., Briggs, C.A., Buccafusco, J., Curzon, P., Decker, M.W., Frost, J.M., Gronlien, J.H., Gubbins, E., Li, J., Malysz, J., Markosyan, S., Marsh, K., Meyer, M.D., Nikkel, A.L., Radek, R.J., Robb, H.M., Timmermann, D., Sullivan, J.P., Gopalakrishnan, M. (2007) Broad-spectrum efficacy across cognitive domains by alpha7 nicotinic acetylcholine receptor agonism correlates with activation of ERK1/2 and CREB phosphorylation pathways. *J. Neurosci.* **27**: 10578-10587.

Chapter 3

3 The $\alpha 7$ Nicotinic Receptor is Internalized via a Clathrin-Independent, Flotillin- or Caveolin-Associated Endocytic Pathway

Acknowledgements

This research was supported by grants to RJR from the Ontario Mental Health Foundation and the Canadian Institutes for Health Research (CIHR). KFY was the recipient of an Ontario Graduate Scholarship in Science and Technology (OGSST). We thank Stephen Sims and Tom Chrones for their assistance with calcium fluorimetry.

3.1 Summary

The $\alpha 7$ nicotinic acetylcholine receptor is a ligand-gated ion channel expressed at pre- and postsynaptic as well as somatodendritic sites throughout the brain, where it can modulate activity within the neural network. The regulated endocytosis of ligand-gated ion channels from the plasma membrane is an important mechanism for maintaining the integrity of neurotransmission. We demonstrate that binding of the competitive antagonist α BTX causes internalization of the $\alpha 7$ nAChR in HEK 293 cells and an SH-SY5Y human neuroblastoma cell line that stably express FLAG epitope-tagged $\alpha 7$ nAChR. α BTX-induced internalization of the receptor is clathrin- and dynamin-independent, and is unaffected by putative clathrin adaptor protein binding motifs within the large intracellular loop of the $\alpha 7$ nAChR subunit. Internalization is not blocked by inhibition of actin polymerization or over-expression of dominant negative RhoGTPases or dominant negative RalGTPase, mechanisms of clathrin-independent endocytosis. Rather, α BTX may lead to endocytosis of $\alpha 7$ nAChR- α BTX complexes through alternate flotillin 1 or caveolar 1α pathways that traffic through early and late endosomes to the lysosome.

3.2 Introduction

The $\alpha 7$ nAChR is an important neuronal nAChR that modulates synaptic plasticity underlying learning and memory processes (1). It is localized at presynaptic locations (2 - 5) as well as postsynaptic and somatodendritic sites (6 - 12). At postsynaptic locations, it can convey cholinergic synaptic input to inhibitory interneurons in the hippocampus (8, 9, 13) to elicit GABA release, inhibit the hippocampal network (14, 15) and block short- and long-term potentiation (16). Alternatively, at presynaptic or somatodendritic locations, the $\alpha 7$ nAChR can enhance glutamate release (3, 17) or membrane depolarization to facilitate short- and long-term potentiation within the hippocampus (16).

The $\alpha 7$ nAChR functions as a ligand-gated ion channel and exerts its modulatory effects through calcium signalling (1). To maintain the integrity of neurotransmission, a number of neurotransmitter receptors that function as ligand-gated ion channels undergo regulated trafficking to control the number of cell surface receptors, and hence the response of neurons to the surrounding neural network. The most thoroughly studied are γ -aminobutyric acid type A receptors (GABA_ARs), α -amino-3-hydroxy-5-methyl-4-isoxazolepropionic acid receptors (AMPA_Rs), and *N*-methyl *D*-aspartate receptors (NMDARs). Plasma membrane levels of GABA_ARs, AMPARs, and NMDARs are each regulated by binding of clathrin adaptor protein AP2 and clathrin and dynamin mediated endocytosis (18 - 20). GABA_ARs and AMPARs undergo constitutive recycling, with receptor turnover occurring within minutes (18, 19), while NMDAR as well as AMPAR endocytosis occurs in response to ligand binding (20, 21).

In this study, we demonstrate ligand-induced internalization of the $\alpha 7$ nAChR transiently expressed in HEK 293 human embryonic kidney cells and stably expressed in SH-SY5Y human neuroblastoma cells. The competitive antagonist, α BTX induces endocytosis of $\alpha 7$ nAChR in both HEK 293 and SH-SY5Y cells. The endocytic pathway of $\alpha 7$ nAChR- α BTX complexes differs from clathrin-dependent endocytosis because internalization of the receptor is not blocked by expression of a dominant negative isoform of dynamin or

disruption of the clathrin-coat. Endocytosis is unaffected by inhibition of actin polymerization or by dominant negative isoforms of RhoGTPases. α BTX appears to induce internalization of the $\alpha 7$ nAChR through flotillin 1 or caveolin 1 α -positive pathways that traffic the receptor through late endosomes to lysosomes.

3.3 Methods

3.3.1 Materials

HEK 293 cells and SH-SY5Y cells were provided by American Type Culture Collection (Manassas, VA). DMEM, Eagle's minimal essential medium with Earle's salts (MEM), FBS, the pcDNA3.1(+) mammalian expression vector, Lipofectamine 2000, Geneticin (G418), α BTX, Alexa Fluor 647-conjugated α BTX, Alexa Fluor 546-conjugated goat anti-rabbit IgG antibody, Alexa Fluor 546-conjugated donkey anti-mouse IgG antibody, Alexa Fluor 633 transferrin, 4',6-diamidino-2-phenylindole (DAPI) dilactate, and cytochalasin D were obtained from Invitrogen (Burlington, ON). DMSO and polyclonal rabbit anti-FLAG antibody were obtained from Sigma-Aldrich Canada (Oakville, ON). Monoclonal mouse anti-EEA1 antibody was from BD Biosciences (Mississauga, ON). Monoclonal mouse anti-LAMP1 (H4A3) was from Abcam (Cambridge, MA). Monoclonal mouse anti-HA antibody (12CA5) was from Roche (Laval, QC). Polyclonal rabbit anti- $\alpha 7$ nAChR antibody (H-302) was from Santa Cruz Biotechnology (Santa Cruz, CA). HRP-conjugated goat anti-rabbit IgG secondary antibody was from Jackson ImmunoResearch Laboratories (West Grove, PA). HRP-conjugated sheep anti-mouse IgG secondary antibody and ECL western blotting detection reagent were from GE Healthcare (Baie d'Urfé, QC). Immuno-Blot polyvinylidene fluoride (PVDF) membrane was from Bio-Rad Laboratories (Mississauga, ON). X-OMAT LS film was from Eastman Kodak (Toronto, ON). Shandon Immu-mount, EZ-Link sulfo-NHS-SS-biotin and NeutrAvidin Agarose were from Thermo Fisher Scientific (Waltham, MA).

3.3.2 DNA Constructs and Site-Directed Mutagenesis

All recombinant cDNA procedures were carried out following standard protocols. The sequence for each oligonucleotide primer is listed in Table 3.1. The cDNA for the $\alpha 7$ nAChR subunit was cloned from a QUICK-Clone™ human universal cDNA library (Clontech Laboratories, Mountain View, CA) by PCR using 5'-oligonucleotide primers ($\alpha 7$ -*fwd*) and 3'-oligonucleotide primers ($\alpha 7$ -*rev*) designed from the NCBI Reference Sequence NM_000746.3 in the GenBank database. 5'-Oligonucleotide primers ($\alpha 7$ -*BamHI-fwd*) introduced an amino-terminal BamHI restriction site, and 3'-oligonucleotide primers ($\alpha 7$ -*XbaI-rev*) introduced a carboxyl-terminal Xba I site to allow sub-cloning of the PCR product into pcDNA3.1(+). 3'-Oligonucleotide primers ($\alpha 7$ -*FLAG-rev*) introduced a FLAG epitope (DYKDDDDK) to the carboxyl-terminal of the PCR product for sub-cloning of a FLAG epitope-tagged $\alpha 7$ nAChR subunit cDNA (FLAG- $\alpha 7$ nAChR) into pcDNA3.1(+). The cDNA for human RIC3, matching the GenBank NCBI Reference Sequence NM_024557, was purchased from Origene (Rockville, MD). 5'-Oligonucleotide primers (*hRIC3-KpnI-fwd*) introduced an amino-terminal Kpn I restriction site, and 3'-oligonucleotide primers (*hRIC3-NotI-HA-rev*) introduced a carboxyl-terminal influenza haemagglutinin (HA) epitope tag (YPYDVPDYA) and Not I restriction site to allow sub-cloning of an HA epitope-tagged hRIC3 (HA-hRIC3) cDNA into pcDNA5/FRT (Invitrogen, Burlington, ON). Mutant isoforms of FLAG- $\alpha 7$ nAChR, Y386A/F389A, Y386F/F389A, L420A/L421A, and D417A/L420A/L421A were generated by sequential PCR (22). GFP-Rab4, GFP-Rab5, GFP-Rab7, GFP-Rab11, YFP-RhoA T19N, YFP-Rac1 T17N, GFP-Cdc42 T17N, YFP-RalA S28N, dynamin 1 K44A, and AP180-C constructs were kindly provided by Stephen Ferguson. Flotillin 1-GFP and caveolin 1 α -GFP constructs were a generous gift from Marco Prado. All plasmids were confirmed by DNA sequencing to ensure the presence of restriction sites, fluorescent or epitope tags, and mutations; that cDNA sequences were in the correct orientation for expression, and no other mutations had been introduced by PCR.

Table 3.1 Oligonucleotide primers used in cloning and sub-cloning of the human $\alpha 7$ nAChR subunit and hRIC3 cDNA.

Primer	Sequence (5' – 3')
$\alpha 7$ -fwd	CGACAGCCGAGACGTGGA
$\alpha 7$ -rev	CCGATGGTACGGATGTGC
$\alpha 7$ -BamHI-fwd	GCCGGGATCCGCCACCGGGACTCAACATGCGCTG
$\alpha 7$ -XbaI-rev	AGACTTTGCGTAACCACGCCTCTAGAGCCG
$\alpha 7$ -FLAG-rev	CGGCTCTAGATTACTTGTCGTCGTCGTCCTTATAGTCCGCAAAGTCTTTGGACA CGGCC
hRIC3-KpnI-fwd	CGGCGGTACCGCCACCATGGCGTACTCCACAGTGCAGAGAGTC
hRIC3-NotI-HA-rev	GCGGCCGCCAACTCACGCATAATCCGGCACATCATACGGATACTCTAAACCCT GGGGGTTACGCTTCCT

3.3.3 Cell Model

Human embryonic kidney 293 (HEK-293) cells present a flat surface area conducive to transfection as well as a large area of cytoplasm relative to their nuclei beneficial for the observation of intracellular proteins by confocal microscopy. The HEK 293 cell line was developed by transforming primary cultures of human embryonic kidney cells with adenovirus (23). HEK-293 cells have been used extensively in studies requiring transfection and heterologous expression of proteins (24), including the endocytosis and trafficking of transmembrane proteins (25, 26). HEK 293 cells are limited by their inability to heterologously express functional $\alpha 7$ nAChR, this is overcome by co-transfection with cDNA for the nAChR chaperone protein RIC3 (27).

The SH-SY5Y cell line is a human cell line sub-cloned from the SK-N-SH cell line (28), originally isolated from a human metastatic neuroblastoma (29). SH-SY5Y cells endogenously express $\alpha 3$, $\alpha 5$, $\alpha 7$, $\beta 2$ and $\beta 4$ nAChR subunits (30, 31) as well as the chaperone protein RIC3 (27). SH-SY5Y cells have small, round cell bodies with little cytoplasm (28) making them difficult to transfect, requiring isolation of stably transfected clones for studies involving heterologously expressed proteins and limiting their use for confocal microscopy.

3.3.4 Cell Culture and Transfection

HEK 293 cells were grown in MEM containing 10% (v/v) FBS at 37 °C in humidified air with 5% CO₂. Cells were seeded at a density of 2.5×10^6 per 100 mm dish and transiently transfected by a modified calcium phosphate method (32) with the cDNA expression plasmids described in the figure legends. Following transfection (approximately 18 h), cells were pooled and collected for immunoblotting or reseeded onto 15 mm collagen-coated glass cover slips in 12-well plates for receptor internalization experiments or immunocytochemistry. SH-SY5Y-FLAG- α 7 cells, expressing FLAG- α 7 nAChR protein and the neomycin resistance gene, and SH-SY5Y-Neo cells, expressing only the neomycin resistance gene, were generated by transfecting SH-SY5Y cells with FLAG- α 7 nAChR cDNA in pcDNA3.1(+) and empty vector pcDNA3.1(+) DNA, respectively, with Lipofectamine 2000, following the manufacturer's protocols. Briefly, SH-SY5Y cells, 70% confluent in 35 mm dishes, were transfected as described and cultured for 48 h prior to being diluted 1:8 into 100 mm dishes and subsequently cultured in the presence of 2 mg/mL G418 until individual foci of neomycin resistant clonal cells had grown. Isolated foci were transferred to single wells of a 48-well plate and each was separately cultured up to a 75 cm² flask upon which clones were selected based on growth rate and protein expression. Positive clones were maintained in DMEM, 10% (v/v) FBS, 0.2 mg/mL G418 at 37 °C in humidified air with 5% CO₂. SH-SY5Y-FLAG- α 7 cells were identified by binding of Alexa Fluor 647-conjugated α BTX. Stable integration of the neomycin resistance gene into the genome of SH-SY5Y-Neo cells was determined by reverse-transcriptase PCR amplification of a neomycin resistance gene 795 bp fragment using 5'-oligonucleotide (5'-ATGATTGAACAAGATGGATTCCACGC-3') and 3'-oligonucleotide (5'-TCAGAAGAACTCGTCAAGAAGGCG-3') primers. The same clone, of either SH-SY5Y-FLAG- α 7 cells or SH-SY5Y-Neo cells, was used throughout experiments.

3.3.5 Immunoblotting

Cells were collected following transfection, washed with PBS (138 mM NaCl, 2.7 mM KCl, pH 7.4), lysed in lysis buffer (50 mM Tris-HCl, pH 7.5, 150 mM NaCl, 0.1% Triton X-100, 1 mM AEBSF, 10 mM NaF, 500 nM NaVO₄, 10 mg/mL leupeptin, 25 mg/mL aprotinin, and 10 mg/mL pepstatin A) and rotated at 4 °C for 30 min. The protein concentration of each lysate was determined by the method of Bradford (33). Equal amounts of protein (50 µg per sample) were resolved on 10% polyacrylamide gels by SDS-PAGE according to the method of Laemmli (34). Separate sets of protein samples were resolved for each antibody to be blotted and transferred to separate PVDF membranes. Membranes were probed with primary anti-FLAG antibody (1:1000), anti- $\alpha 7$ nAChR antibody (1:200), or anti-HA antibody (1:1000) and HRP-conjugated anti-rabbit or anti-mouse IgG secondary antibodies (1:20,000 or 1:5000), followed by detection of immunoreactive protein bands with ECL reagent and film.

3.3.6 Fluorescent α -Bungarotoxin Internalization and Co-localization

For labelling and internalization of FLAG- $\alpha 7$ nAChR expressed in HEK 293 and SH-SY5Y-FLAG- $\alpha 7$ cells, cells were reseeded onto collagen-coated glass cover slips, then washed with chilled HEPES-buffered salt solution (HBSS) (1.2 mM KH₂PO₄, 5 mM NaHCO₃, 20 mM HEPES, 11 mM D-glucose, 116 mM NaCl, 4.7 mM KCl, 1.2 mM MgSO₄, 2.5 mM CaCl₂, pH 7.4) and incubated with 500 nM of Alexa Fluor 647-conjugated α BTX in HBSS 0.1% BSA for 1 h on ice. The K_d of α BTX is 0.4 - 0.6 nM for the $\alpha 7$ nAChR (35, 36), and a concentration of 500 nM, roughly 1000-fold K_d, was deemed sufficient to saturate receptor binding sites present on HEK 293 and SH-SY5Y cells. Cover slips were washed with HBSS to remove excess unbound fluorescent α BTX and transferred to cell culture medium at 37 °C for the specified time. At the end of the incubation period, cover slips were washed with chilled HBSS containing 0.1% BSA and incubated in the same with rabbit anti-FLAG antibody (1:1000) for 1 h on ice. Cells were washed and subsequently incubated with Alexa Fluor 546-conjugated goat anti-rabbit secondary antibody (1:1000) in HBSS 0.1% BSA for 1 h on ice, washed and then fixed with chilled PLP (periodate 0.2%,

lysine 1.4%, paraformaldehyde 2%) (37) for 20 min on ice. To stain nucleic acids, fixed cells were incubated with 300 nM DAPI in PBS for 5 min and washed before mounting onto microscope slides with Immu-mount. Alternatively, cells were fixed following incubation with primary anti-FLAG antibody and stored overnight at 4 °C in PBS before being blocked with PBS containing 10% BSA and incubated with Alexa Fluor 546-conjugated secondary antibody in PBS containing 3% BSA and mounted for microscopy.

To examine co-localization with EEA1 and LAMP1, HEK 293 cells were incubated with Alexa Fluor 647-conjugated α BTX in HBSS containing 0.1% BSA for 1 h on ice, then washed and transferred to cell culture medium at 37 °C for the specified time. At the end of the incubation period, cells were transferred to ice, fixed with chilled PLP and stored overnight at 4 °C in PBS. To detect endogenous EEA1 and LAMP1 proteins, cells were permeabilized with PBS containing 0.25% Triton X-100 for 5 min, blocked with PBS containing 10% BSA for 30 min, washed, and then incubated with anti-EEA1 or anti-LAMP1 antibodies (1:1000) in PBS containing 3% BSA for 1 h at room temperature. Primary antibody-labelled cells were incubated with Alexa Fluor 546-conjugated donkey anti-mouse IgG secondary antibody (1:1000) in PBS containing 3% BSA and 6% normal goat serum before washing and mounting cover slips to microscope slides. For HEK 293 cells co-transfected with RabGTPases, 500 nM Alexa Fluor 647 α BTX was added directly to cell cultures at 37 °C and cells were incubated in its presence for 2 h, before being washed and fixed on ice with chilled PLP. In HEK 293 cells co-transfected with flotillin 1-GFP and caveolin 1 α -GFP, cells were incubated with Alexa Fluor 647-conjugated α BTX in HBSS containing 0.1% BSA for 1 h on ice, then washed and transferred to cell culture medium for 2 h at 37 °C, following which they were returned to ice and fixed with chilled PLP.

3.3.7 Clathrin and Dynamin Inhibition

To determine if inhibition of clathrin-dependent endocytosis blocked receptor internalization, HEK 293 cells were co-transfected with FLAG- α 7 nAChR and HA-hRIC3 and either dominant negative dynamin 1 K44A or AP180-C, then labelled with 500 nM

Alexa Fluor 647-conjugated α BTX in HBSS containing 0.1% BSA for 1 h on ice, washed, and transferred to cell culture medium at 37 °C for 6 h. In some experiments, Alexa Fluor 633-conjugated transferrin was added to the cell culture media 20 min before the end of the incubation period to assess functional expression of dynamin 1 K44A or AP180-C. At the end of the incubation, cells were washed with ice-cold HBSS and fixed with chilled PLP on ice before mounting for microscopy.

3.3.8 Cytochalasin D Treatment and RhoGTPase Inhibition

To determine the effect of inhibition of actin polymerization on receptor internalization, HEK 293 cells co-transfected with FLAG- α 7 nAChR and HA-hRIC3 were incubated with 500 nM Alexa Fluor 647-conjugated α BTX in HBSS containing 0.1% BSA for 1h on ice, then washed and transferred to cell culture medium containing 2.5 μ M cytochalasin D or an equivalent volume of DMSO vehicle and incubated at 37 °C for 2 or 4 h. At the end of the incubation period, cells were washed with ice-cold HBSS, and incubated with rabbit anti-FLAG antibody in HBSS containing 0.1% BSA for 1 h on ice. Primary anti-FLAG antibody binding was detected by subsequently incubating cells with Alexa Fluor 546-conjugated goat anti-rabbit IgG secondary antibody in HBSS containing 0.1% BSA for 1 h on ice. Cells were washed and fixed with chilled PLP on ice for 20 min before mounting for microscopy. To assess the effects of over-expression of dominant negative RhoGTPases and RalGTPase on receptor internalization, HEK 293 cells co-transfected with FLAG- α 7 nAChR and HA-hRIC3 and either, YFP-RhoA T19N, YFP-Rac1 T17N, GFP-Cdc42 T17N, or YFP-RalA S28N were incubated with 500 nM Alexa Fluor 647-conjugated α BTX in HBSS containing 0.1% BSA for 1h on ice, then washed and transferred to cell culture medium at 37 °C for 4 h.

3.3.9 Co-localization with Flotillin 1 and Caveolin 1 α

HEK 293 cells co-transfected with FLAG- α 7 nAChR and HA-hRIC3 and either flotillin 1-GFP or caveolin 1 α -GFP were incubated with 500 nM Alexa Fluor 647-conjugated α BTX in HBSS containing 0.1% BSA for 1 h on ice, then washed and transferred to cell culture

medium at 37 °C for 2 h. At the end of the incubation period, cells were washed with ice-cold HBSS, then fixed with chilled PLP for 20 min on ice and mounted for microscopy.

3.3.10 Confocal Microscopy

Confocal microscopy was performed using a Zeiss LSM-510 META -NLO laser-scanning microscope with a Zeiss Plan-APOCHROMAT 63 × 1.4 DIC oil immersion lens. Alexa Fluor 546 fluorescence was detected by excitation with a HeNe 543 nm wavelength laser and 565 - 615 nm band-pass emission filter; Alexa Fluor 647 and Alexa Fluor 633 by excitation with a HeNe 633 nm laser and 650 - 710 nm band-pass emission filter, and GFP with an Argon laser with a 488 nm wavelength excitation filter and 500 - 550 nm band-pass emission filter. DAPI was detected by excitation with a multi-photon Chameleon Ti Sapphire laser pulsing photons at a wavelength of 870 nm and a 435 - 485 nm band-pass filter. In experiments examining the subcellular localization of Alexa Fluor 647-conjugated α BTX and Alexa Fluor 633-conjugated transferrin, emission fingerprints for each fluorochrome were obtained individually from separate control experiments in which HEK 293 cells had been treated with one fluorochrome-conjugated peptide or the other. Spectral signatures were carefully adjusted by comparison to the localization of each protein in the control samples to ensure that unmixing the overlapping spectra of the two fluorochromes did not alter the appearance or localization of each fluorochrome-conjugate in our experimental samples.

3.3.11 Criteria for Selection of Micrographs

In the experiments presented, we regarded each transiently transfected HEK 293 cell individually. The rationale for this approach is that we observed varying levels of heterologous protein expression following transfection of these cells, which could account for varying levels of fluorescent α BTX internalization and subsequent changes to FLAG immunofluorescence on the surface of cells. In most cases, experiments were repeated at least once (two independent experiments) or more on cells from different passages to ensure that observations were independent from factors that could affect protein expression or function in a given trial. In general, greater scientific rigour would

have been achieved by completing more than three independent experiments for each investigation. Experiments designed to assess the time course for protein internalization, co-localization, or the effects of dominant negative proteins were repeated to ensure that our observations were consistent from transfection to transfection and across cell passages. In protein co-localization experiments, we captured images from several cells, dependent upon the efficiency of transfection, to ensure that data reported are representative of the general population of cells from each transfection. For each experiment, we report the minimum and maximum number of representative micrographs recorded from each condition or time point, from one or more coverslip replicates, which reflected our overall observations and led to our findings.

3.4 Results

3.4.1 The Chaperone Protein, hRIC3 is Required for Functional Cell Surface Expression of $\alpha 7$ nAChR in HEK 293 Cells

Expression of the $\alpha 7$ nAChR in HEK 293 cells was problematic until the discovery of the protein RIC3, from the *Caenorhabditis elegans* gene, resistant to inhibitors of cholinesterase (*ric-3*) (38). RIC3 is a transmembrane protein resident in the ER of many neuronal cells and neuronal cell lines which co-ordinates the efficient assembly of $\alpha 7$ nAChR subunits into a functional receptor pentamer (39). Co-expression of *C. elegans* RIC3 or its human homologue, hRIC3, increases the responsiveness of $\alpha 7$ nAChR expressed in *Xenopus laevis* oocytes and facilitates functional expression of $\alpha 7$ nAChR in HEK 293 cells (27).

I first amplified and sub-cloned the full-length cDNA for the $\alpha 7$ nAChR subunit from a human universal cDNA library using primers based on the sequence in the GenBank database. DNA sequencing analysis revealed the coding sequence obtained is identical to NCBI Reference Sequence NM_000746.3, except for a silent mutation, adenine 933 to guanine, resulting in a codon change, ACA to ACG, and conservation of threonine 311. The FLAG epitope amino acid sequence was introduced into the extracellular carboxyl-

terminus of the $\alpha 7$ nAChR subunit by PCR to generate a FLAG epitope-tagged $\alpha 7$ nAChR, FLAG- $\alpha 7$ nAChR. Addition of the FLAG epitope to the receptor delayed the rate at which whole-cell calcium changed in response to the agonist nicotine (Appendix A).

To verify the requirement of co-expression with hRIC3 for functional expression of $\alpha 7$ nAChR in HEK 293 cells, we examined binding of fluorochrome-labelled α BTX and immunofluorescent staining of cells with anti-FLAG antibody in HEK 293 cells transfected with cDNA for FLAG- $\alpha 7$ nAChR subunit and HA-hRIC3 or FLAG- $\alpha 7$ nAChR subunit and empty vector DNA (Figure 3.1 A). Cells transfected with both FLAG- $\alpha 7$ nAChR subunit and HA-hRIC3 bound fluorescent α BTX. Cells expressing FLAG- $\alpha 7$ nAChR alone were detectable by immunofluorescent staining with anti-FLAG antibody on the cell surface (not permeabilized) and throughout the cell (permeabilized), but did not bind fluorescent α BTX. Cells transfected with FLAG- $\alpha 7$ nAChR subunit cDNA and empty vector DNA that were not permeabilized exhibited consistent surface anti-FLAG staining up and down throughout the Z-stack. This staining was less evident when scanning only a thin cross-section of plasma membrane at lower to mid Z, the upper most Z sections (top) of cells, which presented the greatest cross-sectional area of plasma membrane, provided the strongest fluorescent signal (Figure 3.1 A, FLAG (not permeabilized)). We did not observe binding of fluorescent α BTX or anti-FLAG immunofluorescence in cells that had been transfected with empty vector DNA alone (data not shown).

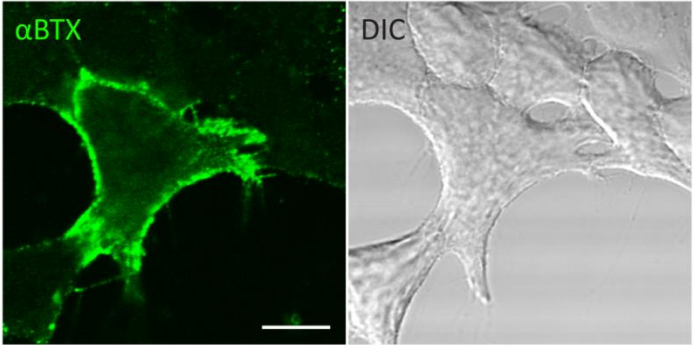
Immunoblotting of cell lysates from cells transfected in parallel to those labelled with fluorescent α BTX demonstrated co-expression of HA-hRIC3 protein in these cells following transfection (Figure 3.1 B). Anti-HA antibody directed toward the HA epitope on hRIC3 (apparent molecular weight 48 kDa) detected a single band resolving between the 46 and 58 kDa markers. Anti- $\alpha 7$ nAChR antibody or anti-FLAG antibody detected FLAG- $\alpha 7$ nAChR resolving as double bands above 46 kDa and higher molecular weight bands between 80 and 175 kDa. In comparison, anti- $\alpha 7$ nAChR antibody detected wild-type $\alpha 7$ nAChR resolving as double bands at slightly lower molecular weights than those for FLAG- $\alpha 7$ nAChR; the FLAG epitope amino acid sequence has an expected molecular

Figure 3.1 The chaperone protein, hRIC3 is required for functional cell surface expression of $\alpha 7$ nAChR in HEK 293 cells.

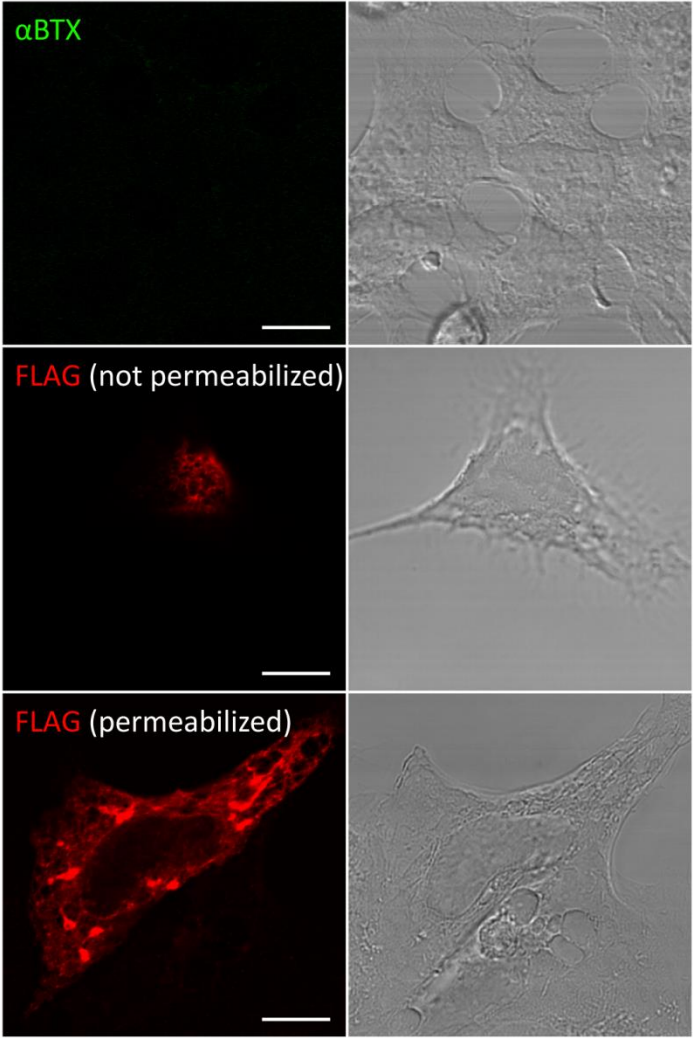
(A) HEK 293 cells transfected with FLAG- $\alpha 7$ nAChR subunit and HA-hRIC3 cDNA or FLAG- $\alpha 7$ nAChR subunit cDNA and empty vector DNA were incubated on ice with 500 nM Alexa Fluor 647- α BTX in 0.1% BSA HBSS for 1 h, washed, fixed with PLP, and mounted. To detect expression of FLAG- $\alpha 7$ nAChR subunit protein in the absence of co-transfection with HA-hRIC3 cDNA, cells were fixed with PLP and either left intact (not permeabilized), to label cell surface FLAG- $\alpha 7$ nAChR subunits, or treated with 0.25% Triton X-100 PBS (permeabilized), to label FLAG- $\alpha 7$ nAChR subunits throughout the cell, and incubated with anti-FLAG antibody and Alexa Fluor 546-conjugated secondary antibody. Images of Alexa Fluor 647- α BTX (green) or Alexa Fluor 546-conjugated secondary antibody (red) were captured from single z-sections or selected from a series of z-sections, captured as a stack, on a laser-scanning confocal microscope. FLAG (not permeabilized) represents the upper most Z section (top) of a cell, which presented the greatest cross-sectional area of plasma membrane and strongest fluorescent signal. Bar, 10 μ m. **(B)** Crude cell lysate from cells transfected in parallel to those in A, immunoblotted with anti-FLAG, anti- $\alpha 7$ nAChR, or anti-HA antibody and HRP-conjugated secondary antibody to detect expression of FLAG- $\alpha 7$ nAChR, wild-type $\alpha 7$ nAChR and FLAG- $\alpha 7$ nAChR, or HA-hRIC3 proteins respectively. Images are representative of 5 to 10 cells per treatment, per experiment, from two independent experiments; immunoblots are representative of two independent experiments.

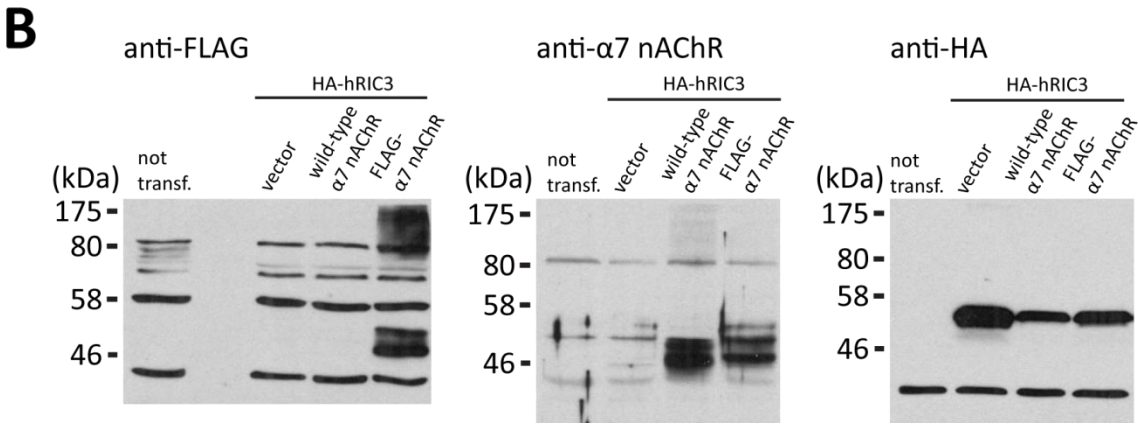
A

FLAG- $\alpha 7$ nAChR / hRIC3



FLAG- $\alpha 7$ nAChR / vector





weight of 1 kDa. Anti-FLAG, anti- $\alpha 7$ nAChR, or anti-HA antibodies did not detect bands resolving at these molecular weights in cells that were not transfected, and anti-FLAG and anti- $\alpha 7$ nAChR antibodies did not detect bands in cells transfected with HA-hRIC3 and empty vector DNA.

The cell surface expression of FLAG- $\alpha 7$ nAChR in HEK 293 cells in the absence of hRIC3 is supported by a preliminary cell surface biotinylation experiment in which FLAG- $\alpha 7$ nAChR is detectable in Neutravidin precipitates from cells expressing FLAG- $\alpha 7$ nAChR with or without co-transfection with HA-hRIC3 cDNA (Appendix B). In HEK-293 cells, transfected with FLAG- $\alpha 7$ nAChR cDNA and empty vector DNA, FLAG- $\alpha 7$ nAChR and HA-hRIC3 cDNA, or empty vector DNA and HA-hRIC3 cDNA, cell surface proteins were detected by reaction with EZ-Link sulfo-NHS-SS-biotin and subsequent precipitation with NeutrAvidin agarose. Sulfo-NHS-SS-biotin covalently binds preferentially to lysine amino acid residues to form biotinylated protein conjugates (40). It is not plasma membrane permeable and reacts with exposed lysine residues in extracellular polypeptides to biotinylate only cell surface proteins when incubated with intact cells (40). The $\alpha 7$ nAChR subunit contains 13 lysine residues in extracellular domains, potentially available for reaction with sulfo-NHS-SS-biotin, based on topological and transmembrane domain predictions provided by UniProt Knowledgebase reference P36544 (UniProt Consortium). The FLAG epitope, appended to the extracellular carboxyl-terminus of FLAG- $\alpha 7$ nAChR subunit, may provide an additional two lysine residues.

Immunoblotting with anti-FLAG antibody detected FLAG- $\alpha 7$ nAChR resolving as double bands circa 46 kDa and as higher molecular weight bands between 80 and 175 kDa in biotinylated fractions, containing only cell surface proteins, as well as crude cell lysates. FLAG- $\alpha 7$ nAChR immunoreactivity was noticeably increased, especially circa 46 kDa, in the biotinylated fraction of cells that were co-transfected with HA-hRIC3 cDNA.

3.4.2 α -Bungarotoxin Induces Internalization of the $\alpha 7$ nAChR

α BTX is an 8 kDa peptide isolated from the venom of the Many-banded krait, *Bungarus multicinctus* (41). It is an established subtype-selective nicotinic antagonist (42). $\alpha 7$ -, $\alpha 8$ -, and $\alpha 9$ -containing nAChR, muscle nAChR, and nAChR of *Torpedo californica* and *Electrophorus electricus* are the only nAChR that bind α BTX with near covalent affinity (42 - 48). When HEK 293 cells are co-transfected with plasmids encoding FLAG- $\alpha 7$ nAChR and HA-hRIC3, FLAG- $\alpha 7$ nAChR can be detected on the cell surface with fluorescent α BTX or anti-FLAG antibody. To investigate whether α BTX binding affects $\alpha 7$ nAChR internalization, we employed a pulse-chase paradigm (Figure 3.2).

Transfected HEK 293 cells were incubated on ice with a saturating concentration of fluorescent α BTX, washed, transferred to 37 °C for 0, 1, 2, 4, or 6 h, and then returned to ice and subsequently incubated with anti-FLAG antibody and fluorescent secondary antibody, directed toward the FLAG antibody, to detect the level of FLAG- $\alpha 7$ nAChR remaining on the cell surface. From 0 through 6 h, fluorescent α BTX was observed to internalize from the cell surface and gradually accumulate into intracellular puncta that accumulated in perinuclear regions (Figure 3.3 A, + α BTX). Coincident with the internalization of fluorescent α BTX was an apparent loss of cell surface levels of FLAG- $\alpha 7$ nAChR, detected by anti-FLAG antibody and secondary antibody fluorescence. In the absence of α BTX, the levels of FLAG- $\alpha 7$ nAChR on the cell surface did not appear to change over time at 37 °C (Figure 3.3 A, - α BTX). HEK 293 cells transfected with HA-hRIC3 cDNA and empty vector DNA did not bind anti-FLAG antibody and fluorescent secondary antibody or bind or accumulate internalized fluorescent α BTX after 0 or 6 h at 37 °C (Figure 3.3 B). To test whether anti-FLAG antibody was detecting the emergence of new $\alpha 7$ nAChR on the cell surface following α BTX-induced internalization, we incubated cells with fluorescent α BTX following a pulse-chase with unlabelled α BTX (Appendix C). HEK 293 cells transfected with cDNA for FLAG- $\alpha 7$ nAChR and HA-hRIC3 were incubated with a saturating concentration of unlabelled α BTX on ice, washed, transferred to 37 °C for 0 or 6 h, and then returned to ice and subsequently incubated

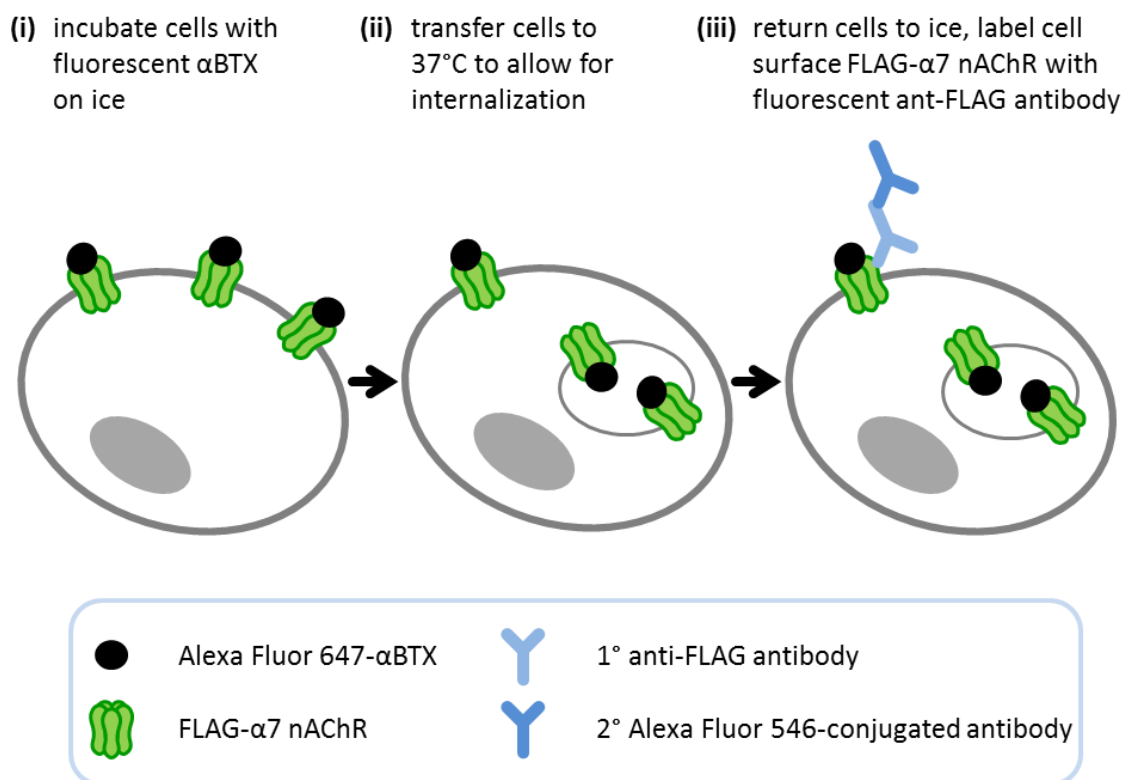
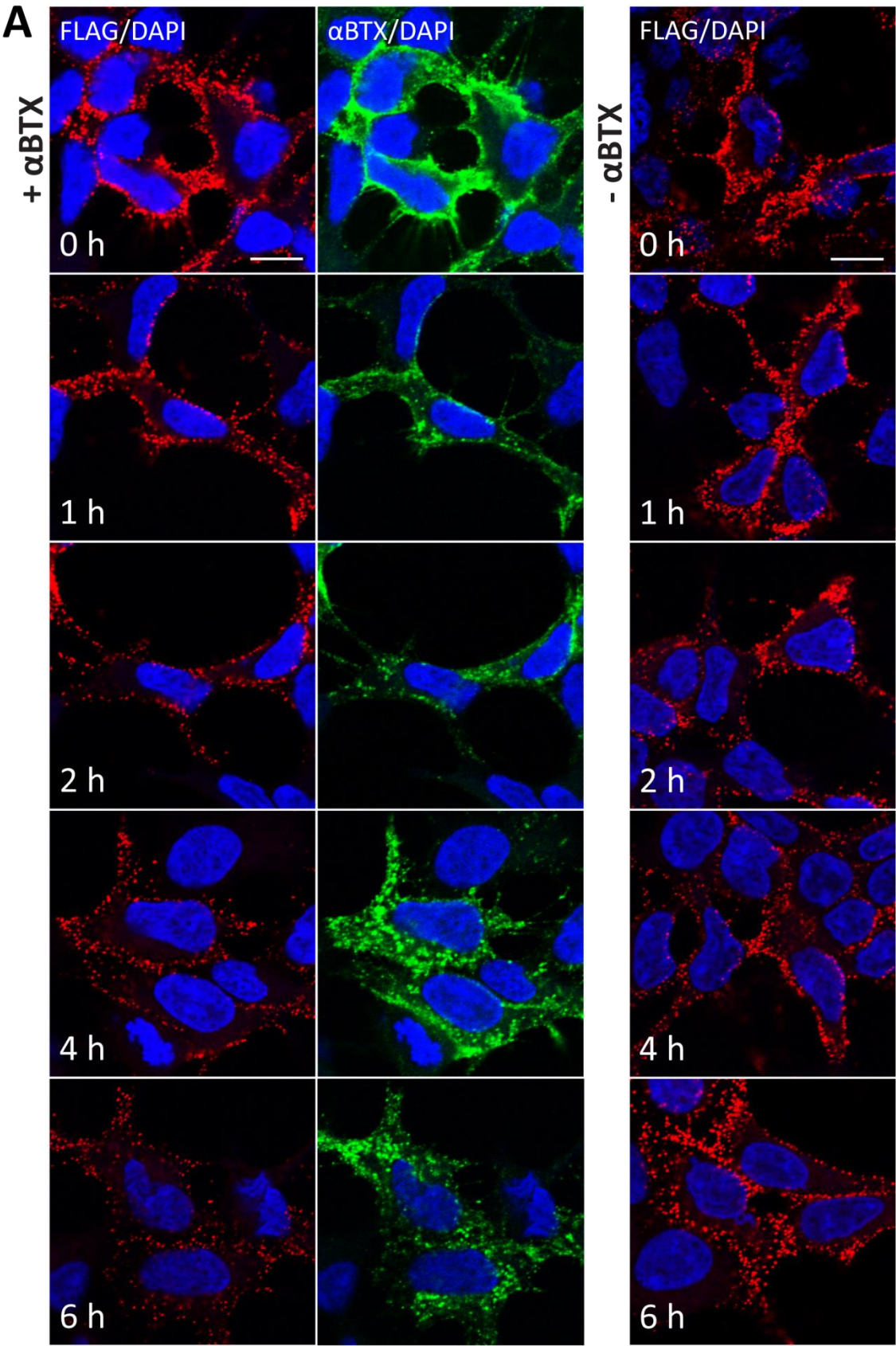


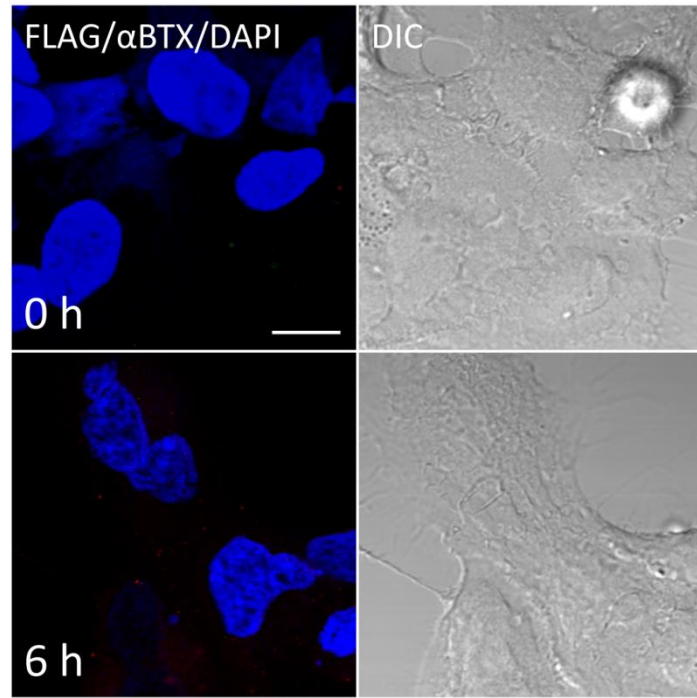
Figure 3.2 Pulse-chase method for investigating α BTX-induced internalization of α 7 nAChR.

(i) Transfected cells, seeded onto glass coverslips and maintained at 37 °C, were washed with chilled HBSS and transferred to ice to cool the cells and slow plasma membrane trafficking events. While on ice, the cells were incubated with 500 nM Alexa Fluor 647- α BTX in chilled HBSS 0.1% BSA for 1 h to label cell surface α 7 nAChR. **(ii)** Following surface labelling, cells were washed with chilled HBSS to remove unbound Alexa Fluor 647- α BTX and then transferred to warm cell culture medium and maintained at 37 °C for 0,1,2,4, or 6 h to allow receptor internalization events to occur. **(iii)** Cells were then returned to ice and washed with chilled HBSS to again slow trafficking events before sequential incubation with anti-FLAG antibody and Alexa Fluor 546-conjugated secondary antibody to label FLAG- α 7 nAChR that remained on the cell surface. Following antibody labelling, glass coverslips were fixed and mounted for confocal microscopy.

Figure 3.3 α BTX binding induces internalization of α 7 nAChR.

(A) HEK 293 cells transfected with FLAG- α 7 nAChR and HA-hRIC3 cDNA were incubated on ice for 1 h with (+ α BTX) or without (- α BTX) Alexa Fluor 647- α BTX, washed and transferred to 37 °C for 0, 1, 2, 4 or 6 h. At the end of the incubation, the cells were returned to ice and incubated with anti-FLAG antibody, followed by secondary Alexa Fluor 546-conjugated antibody directed against the anti-FLAG antibody. The cells were fixed with PLP and nuclei were stained with DAPI prior to mounting. Images of secondary Alexa Fluor 546-conjugated antibody (red), Alexa Fluor 647- α BTX (green), and DAPI (blue) were collected from single z-sections on a laser-scanning confocal microscope and colour combined. **(B)** HEK 293 cells transfected with empty vector DNA and HA-hRIC3 cDNA, chased with Alexa Fluor 647- α BTX for 0 or 6 h followed by antibody incubations as in A, were used to assess non-specific binding of Alexa Fluor 647- α BTX and anti-FLAG antibody. Images are representative of 5 to 30 cells per time point, per experiment, one to three cover slips per time point, from four independent experiments. Bar, 10 μ m.



B

with fluorescent α BTX. After 0 h, no cells bound fluorescent α BTX; after 6 h at 37 °C, a fraction of cells showed a small amount of fluorescent α BTX labelling.

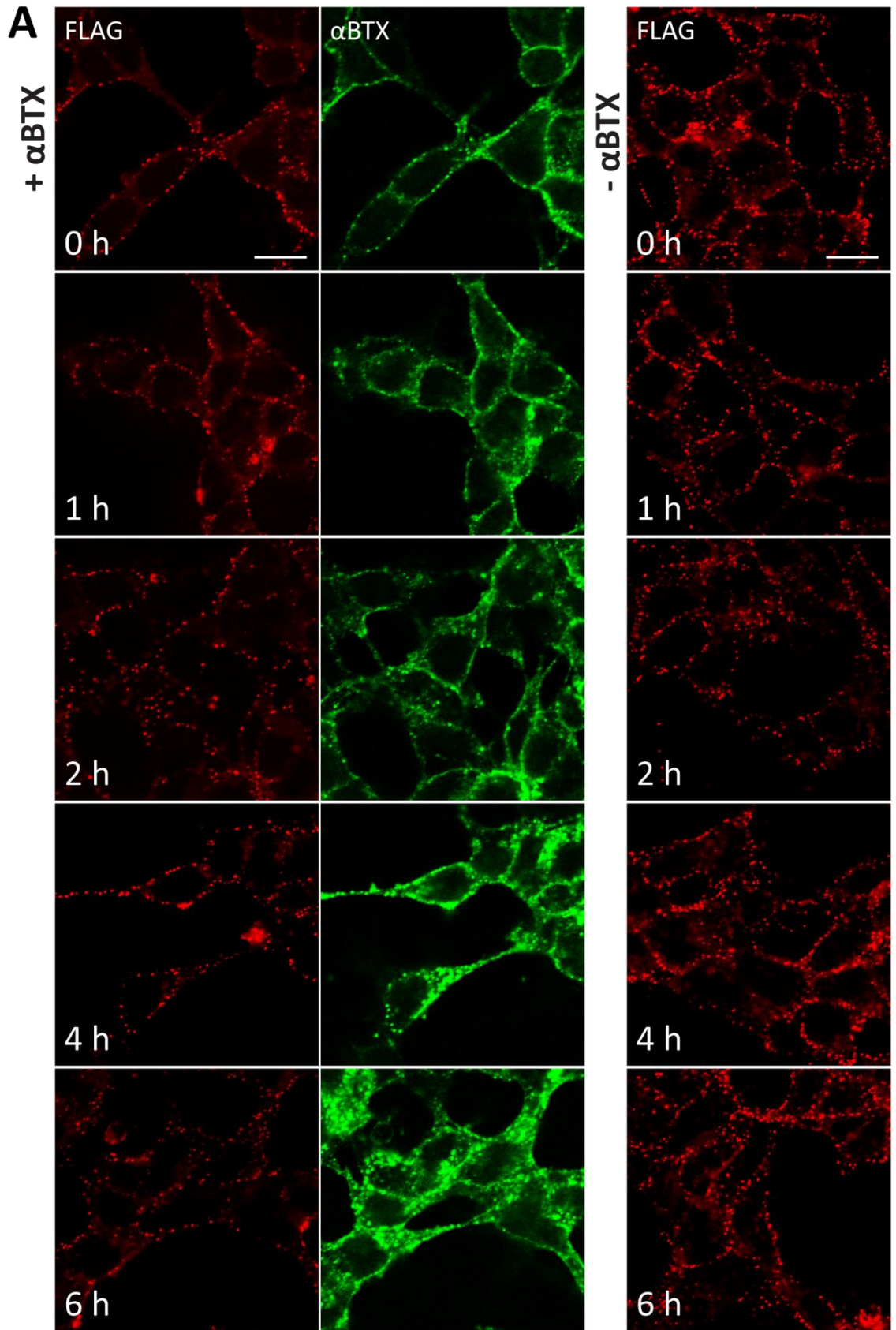
To investigate if α BTX induces internalization of α 7 nAChR in a cell line that endogenously expresses nAChR, we examined FLAG- α 7 nAChR endocytosis in SH-SY5Y cells. For the purpose of these experiments, we generated an SH-SY5Y cell line that stably expresses the FLAG- α 7 nAChR subunit, SH-SY5Y-FLAG- α 7, and a neomycin resistant control cell line, SH-SY5Y-Neo, which expresses the neomycin resistance gene. When SH-SY5Y-FLAG- α 7 cells were incubated with fluorescent α BTX on ice and transferred to 37 °C, fluorescent α BTX internalized as intracellular puncta similar to what was observed in HEK 293 cells (Figure 3.4 A, + α BTX). This indicates that both HEK 293 cells and SH-SY5Y-FLAG- α 7 cells exhibit α BTX induced internalization of the α 7 nAChR, suggesting the use of HEK 293 cells as a suitable model to study α BTX induced internalization of the receptor. However, changes to cell surface levels of FLAG- α 7 nAChR, detected by anti-FLAG antibody and secondary antibody fluorescence were not as apparent in SH-SY5Y-FLAG- α 7 cells as for HEK 293 cells. In the absence of α BTX, there was no change to cell surface anti-FLAG immunofluorescence over time at 37 °C (Figure 3.4 A, - α BTX). SH-SY5Y-Neo cells did not bind anti-FLAG antibody and fluorescent secondary antibody and did not bind or internalize fluorescent α BTX after 0 or 6 h at 37 °C (Figure 3.4 B). α BTX appears to induce internalization of the α 7 nAChR upon binding and lead to its accumulation in perinuclear regions of the cell.

3.4.3 α 7 nAChR- α BTX Complexes Traffic Through Late Endosomes to Lysosomes

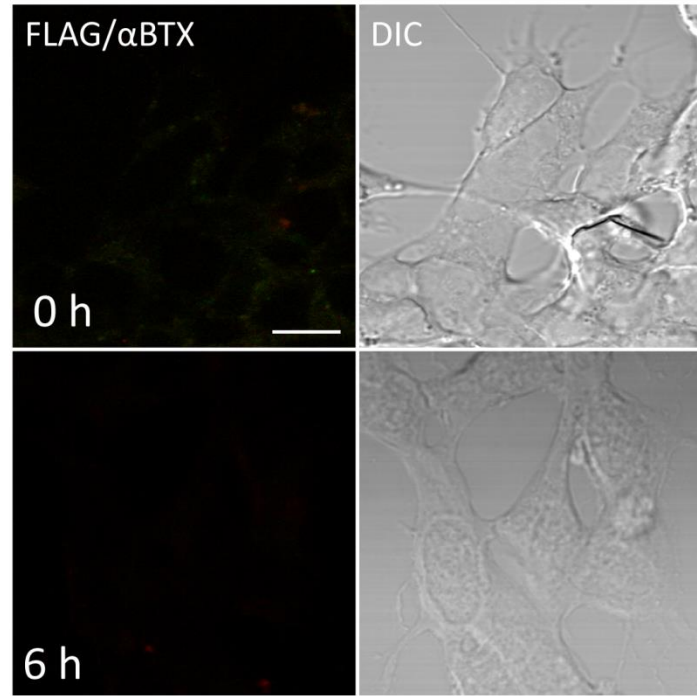
To investigate the fate of α 7 nAChR- α BTX complexes that have been internalized by endocytosis and identify which membrane compartments these complexes traffic through, we examined the kinetics of co-localization of fluorescent α BTX-labelled α 7 nAChR with early and late endosomal membrane markers. HEK 293 cells transfected with FLAG- α 7 nAChR and HA-hRIC3 cDNA were incubated on ice with fluorescent α BTX, washed, transferred to 37 °C for 0, 1, 2, 4 or 6 h, fixed, permeabilized, and then labelled

Figure 3.4 α BTX induces internalization of $\alpha 7$ nAChR in neuronal cells.

(A) SH-SY5Y-FLAG- $\alpha 7$ cells stably expressing FLAG- $\alpha 7$ nAChR were incubated on ice for 1 h with (+ α BTX) or without (- α BTX) Alexa Fluor 647- α BTX, washed and transferred to 37 °C for 0, 1, 2, 4 or 6 h. At the end of the incubation, the cells were returned to ice and incubated with anti-FLAG antibody, followed by secondary Alexa Fluor 546-conjugated antibody directed against the anti-FLAG antibody. Images of secondary Alexa Fluor 546-conjugated antibody (red) and Alexa Fluor 647- α BTX (green) were collected from single z-sections on a laser-scanning confocal microscope and colour combined. **(B)** Neomycin resistant SH-SY5Y cells, chased with Alexa Fluor 647- α BTX as in A for 0 or 6 h, were used as a control for non-specific binding of Alexa Fluor 647- α BTX and anti-FLAG antibody. Images are representative of 30 cells per time point, per experiment, one to two cover slips per time point, from two independent (+ α BTX) and a preliminary experiment (- α BTX). Bar, 10 μ m.



B



with antibodies directed toward early-endosomal autoantigen 1 (EEA1) or lysosomal-associated membrane protein 1 (LAMP1) and fluorescent secondary antibodies. EEA1 is involved in docking of vesicles to early endosomes (49 - 51). LAMP1 is a major lysosomal membrane protein required for maintaining lysosome integrity (52, 53). Fluorescent α BTX co-localized with EEA1 after 1 to 2 h, with some co-localized puncta visible as late as 4 h, while co-localization with LAMP1 only occurred after 2 h (Figure 3.5). After 2 h, fluorescent α BTX increasingly co-localized with LAMP1 positive vesicles from 4 to 6 h as α 7 nAChR- α BTX complexes appeared to accumulate in this membrane compartment. Lysosomes appear to represent the final destination for α 7 nAChR, following their removal from the cell surface in response to binding α BTX.

RabGTPases are small G-proteins that regulate the traffic of membrane-bound organelles to specific membrane compartments (54). We examined co-localization of fluorescent α BTX with the green fluorescent protein (GFP)-tagged RabGTPases, Rab4, Rab5, Rab7 and Rab11 to determine the involvement of these proteins in the trafficking of α 7 nAChR- α BTX complexes. Rab4, Rab5 and Rab11 are localized to early endosomes and participate in the endocytic recycling of membrane proteins, while Rab7 regulates the traffic of membrane organelles through late endosomes to lysosomes (55 - 61). HEK 293 cells transfected with FLAG- α 7 nAChR and HA-hRIC3 cDNA were incubated with fluorescent α BTX for 2 h at 37 °C to allow for the internalization and accumulation of α 7 nAChR- α BTX complexes. Fluorescent α BTX did not co-localize with GFP-Rab4, -Rab5, or -Rab11, suggesting that these complexes do not undergo recycling back to the cell surface (Figure 3.6). However, fluorescent α BTX did co-localize with GFP-Rab7 puncta, indicating that α 7 nAChR- α BTX complexes traffic through Rab7-positive late endosomes to lysosomes (Figure 3.6).

3.4.4 Canonical Endocytic Receptor Trafficking Motifs Do Not Alter Cell Surface Expression or Endocytosis of α 7 nAChR

The predicted amino acid sequence of the large intracellular loop between TM3 and TM4 of the human α 7 nAChR subunit (318 - 469) was identified from the UniProt

Figure 3.5 $\alpha 7$ nAChR- α BTX complexes traffic to late endosomes.

HEK 293 cells transfected with FLAG- $\alpha 7$ nAChR and HA-hRIC3 cDNA were incubated on ice for 1 h with Alexa Fluor 647- α BTX, washed and transferred to 37 °C for 0, 1, 2, 4, or 6 h. The cells were fixed, permeabilized, and labelled with antibodies directed towards specific markers EEA1 (early endosomes) and LAMP1 (lysosomes), followed by secondary Alexa Fluor 546-conjugated antibody. Images of Alexa Fluor 647- α BTX (green) and organelle markers (red) were collected from single z-sections on a laser-scanning confocal microscope and colour combined. Note that $\alpha 7$ nAChR- α BTX complexes co-localize initially with EEA1 and, after a chase of 4 or 6 h, localize extensively with LAMP1. Insets show magnified images of the areas indicated by an arrowhead for Alexa Fluor 647- α BTX (green) with EEA1 or LAMP1 (red) and an overlay of the two. Images are representative of 10 to 16 cells per time point, per experiment, from three (EEA1) or four (LAMP1) independent experiments. Bar, 10 μ m.

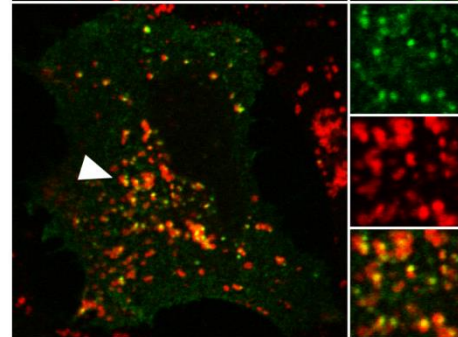
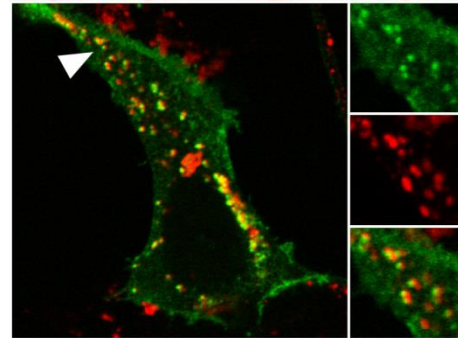
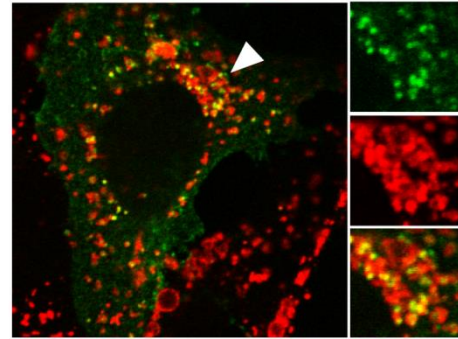
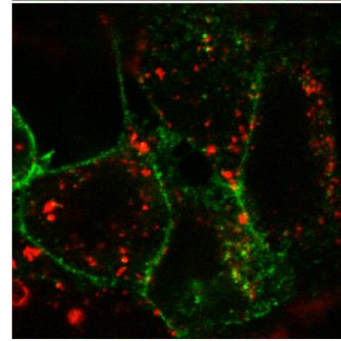
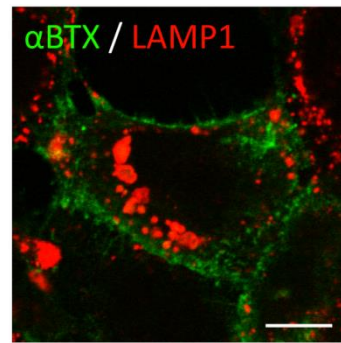
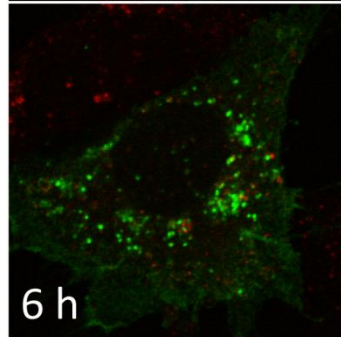
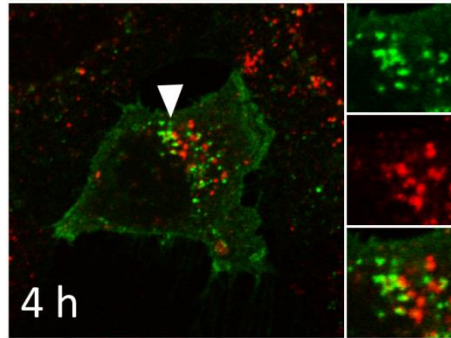
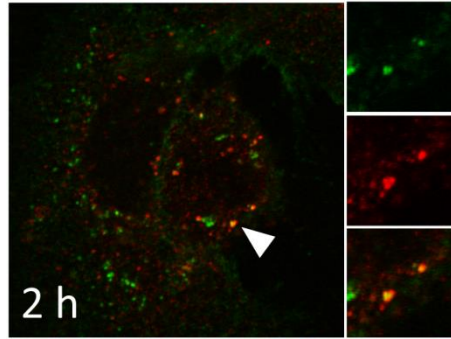
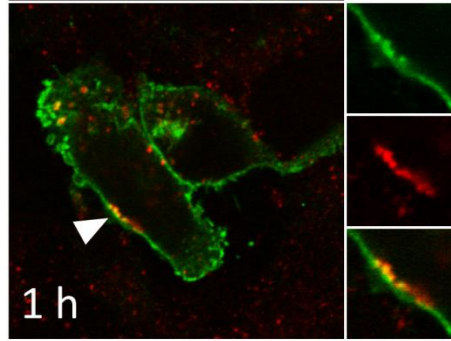
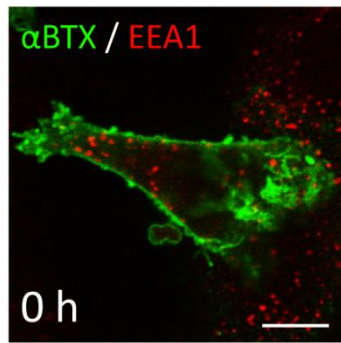
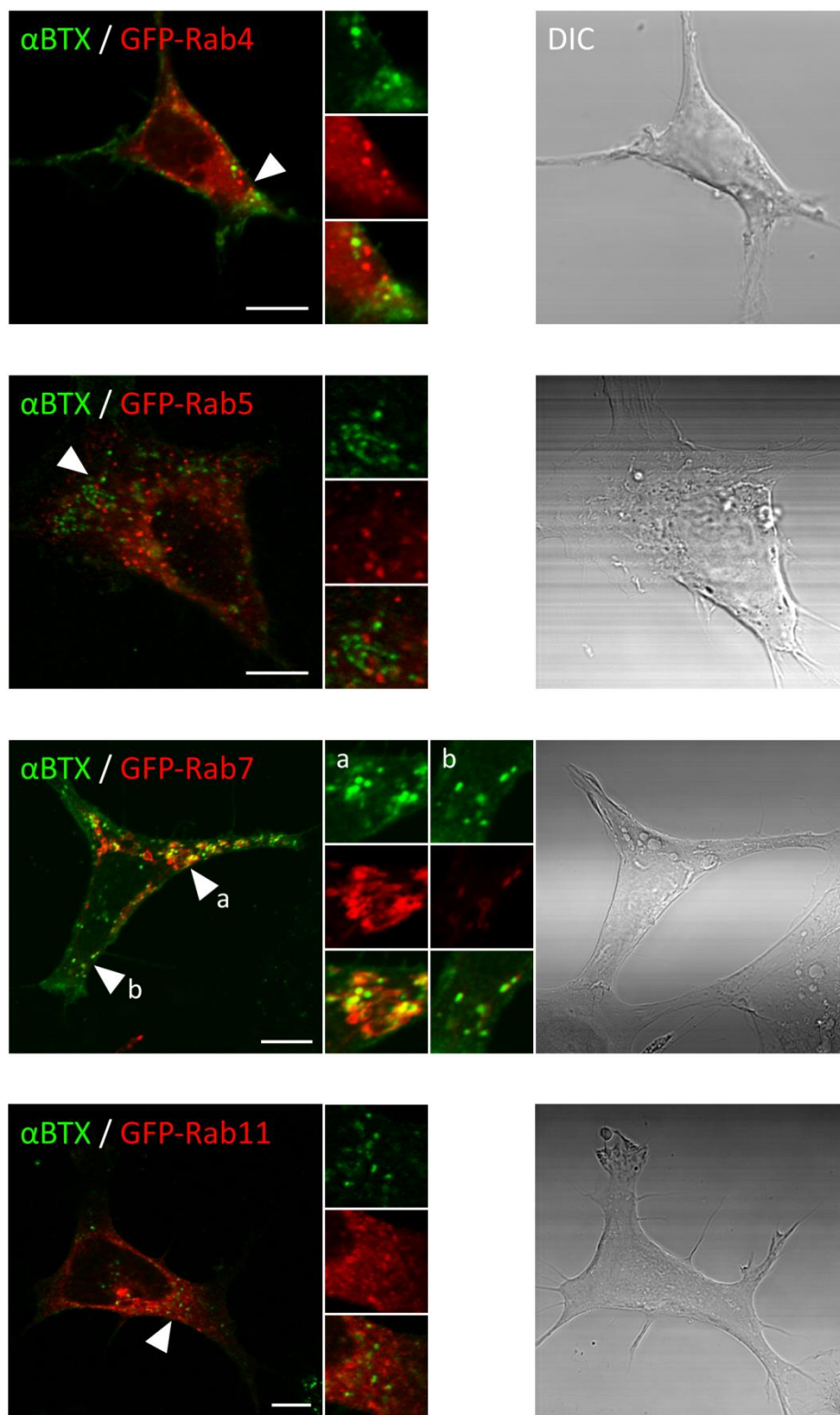


Figure 3.6 $\alpha 7$ nAChR- α BTX complexes traffic through late endosomes/lysosomes but not rapidly or slowly recycling endosomes or Rab5 positive early endosomes.

HEK 293 cells co-transfected with cDNA for FLAG- $\alpha 7$ nAChR, HA-hRIC3, and GFP-Rab4 (rapidly recycling endosomes), GFP-Rab5 (early endosomes), GFP-Rab7 (late endosomes/lysosomes), or GFP-Rab11 (slowly recycling endosomes) were incubated at 37 °C in the presence of Alexa Fluor 647- α BTX for 2 h. The cells were washed, fixed and mounted and images of Alexa Fluor 647- α BTX (green) and GFP (red) were collected from single z-sections on a laser-scanning confocal microscope and colour combined. Insets show magnified images of the areas indicated by an arrowhead for Alexa Fluor 647- α BTX (green) with GFP-tagged RabGTPases (red) and an overlay of the two. Images are representative of 5 to 10 cells per experiment, from two independent experiments. Bar, 10 μ m.



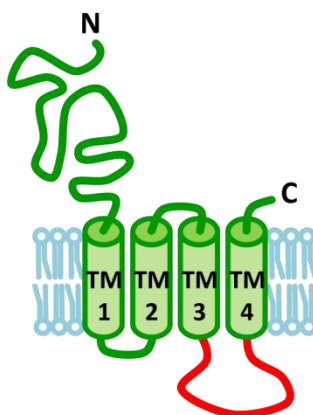
Knowledgebase reference P36544 (UniProt Consortium). From this sequence, I identified two short amino acid sequences that represent putative trafficking motifs that could be involved in regulating cell surface expression or endocytosis of the $\alpha 7$ nAChR (Figure 3.7 A). The sequence $_{386}\text{YIGF}_{389}$ fits the profile of a YXX Φ (Y, tyrosine; X, any amino acid, Φ , amino acid with a bulky hydrophobic side chain) signal that binds the μ subunits of adaptor protein complexes and mediates rapid internalization from the plasma membrane and can target proteins to the lysosome (62). The sequence $_{417}\text{DEHLL}_{421}$ is similar to the DXXLL signal present in transmembrane proteins that cycle between the *trans*-Golgi network and endosomes and bind the clathrin adaptor proteins, Golgi-localized, γ -ear-containing, ADP-ribosylation factor-binding proteins (62). We used site-directed mutagenesis to generate mutant isoforms of the FLAG- $\alpha 7$ nAChR subunit containing the mutations Y386A/F389A, Y386F/F389A, L420A/L421A, or D417A/L420A/L421A, then compared α BTX-induced internalization of these mutants to that of wild-type FLAG- $\alpha 7$ nAChR in HEK 293 cells co-transfected with HA-hRIC3 cDNA (Figure 3.7 B, C, and D). Mutations to these sequences did not appear to alter cell surface expression or α BTX-induced internalization of the $\alpha 7$ nAChR, as cell surface anti-FLAG immunofluorescence and the internalization of fluorescent α BTX did not appear to differ between wild-type and mutant isoforms of the receptor after 0, 4, or 6 h at 37 °C. This demonstrates that these two motifs do not play a role in the trafficking of $\alpha 7$ nAChR to the cell surface in HEK 293 cells or prevent α BTX-induced internalization of the receptor in these cells.

3.4.5 Endocytosis of $\alpha 7$ nAChR- α BTX Complexes is Independent of Clathrin

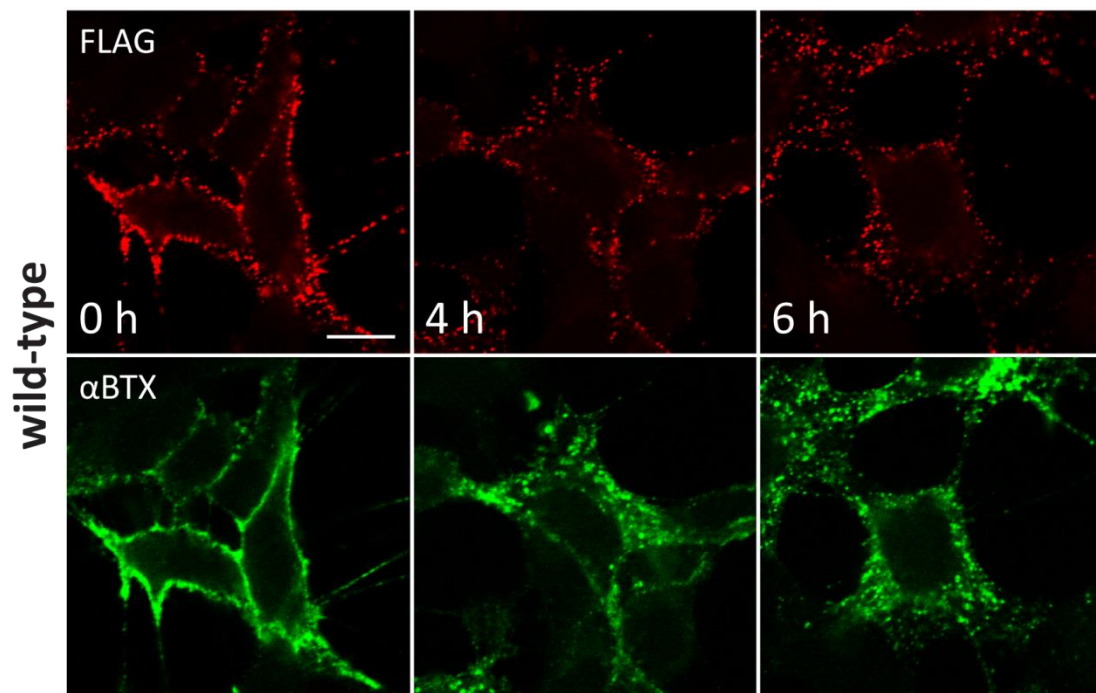
Some ligand-gated ion channels are internalized by a clathrin- and dynamin-dependent endocytic mechanism (19, 20, 63, 64). Transferrin receptor internalization is characteristic of the clathrin- and dynamin-dependent receptor endocytosis pathway (65 - 68). Clathrin- and dynamin-dependent receptor endocytosis can be blocked by the dominant negative mutant isoform of dynamin, dynamin K44A, and the carboxyl-terminal fragment of adaptor protein 180 (AP180-C) (69 - 71). GTPase defective

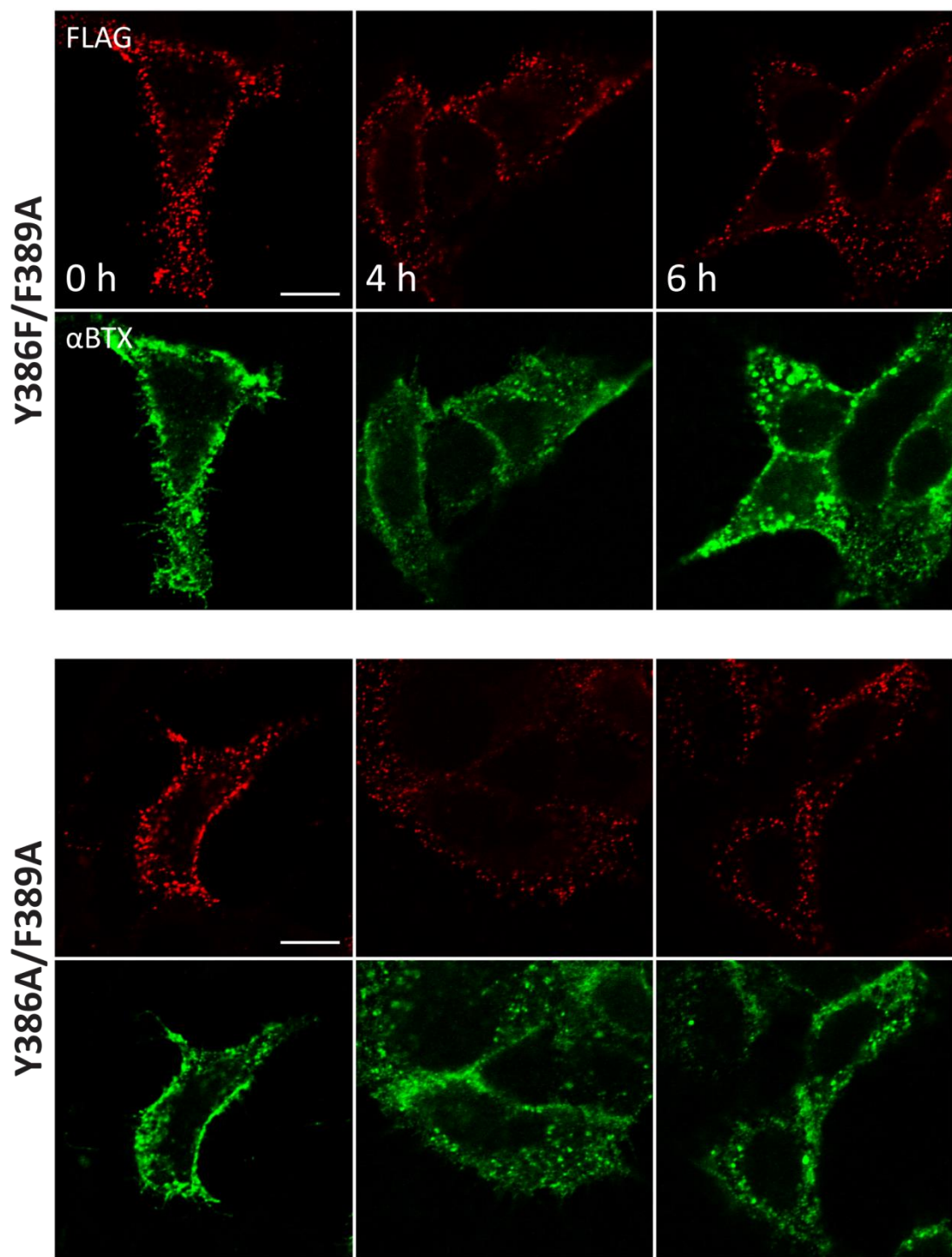
Figure 3.7 Canonical endocytic receptor trafficking motifs do not alter cell surface expression or endocytosis of $\alpha 7$ nAChR.

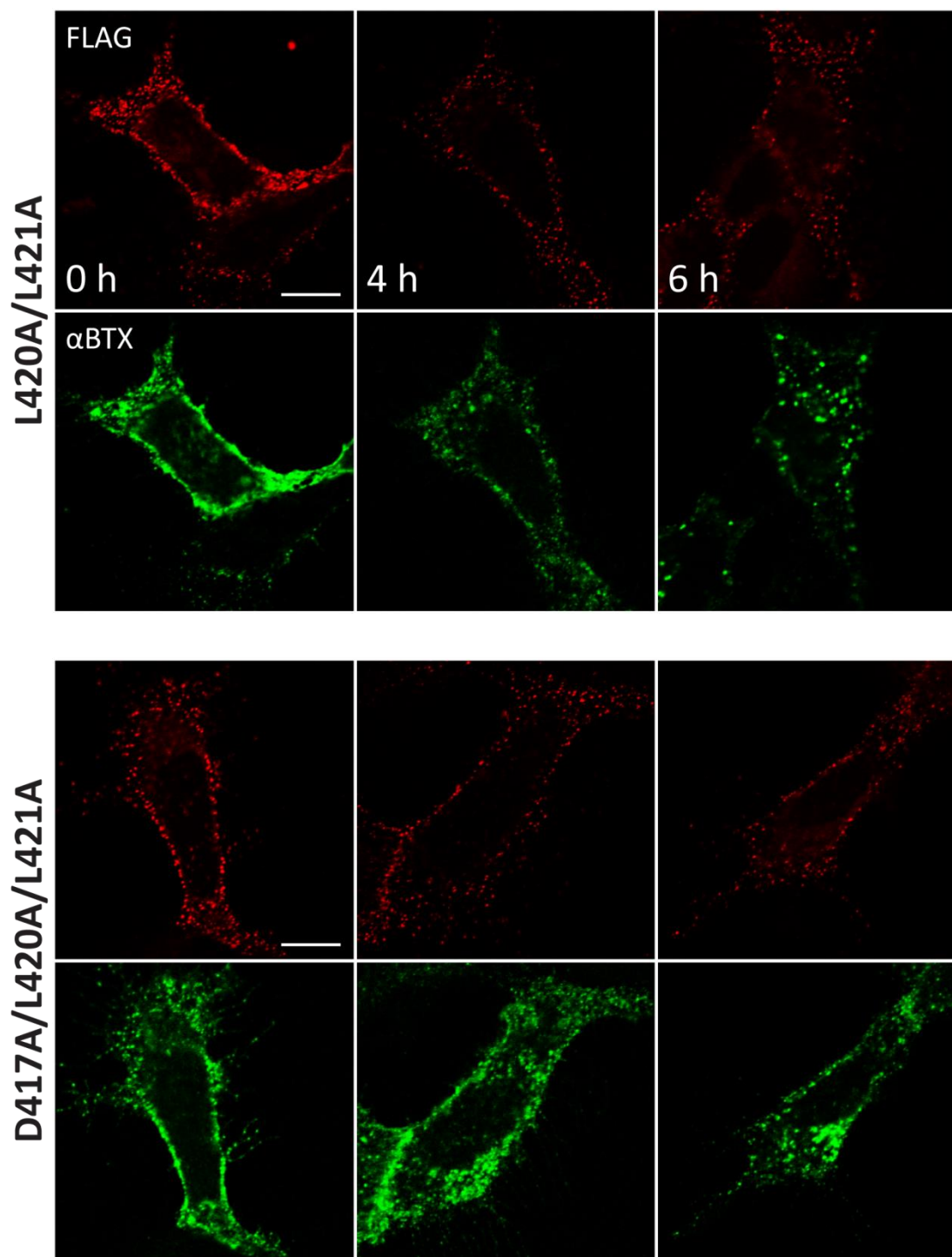
(A) Putative trafficking motifs were identified within the amino acid sequence of the large intracellular loop of the $\alpha 7$ nAChR subunit between TM3 and TM4, highlighted in red in the schematic. $_{386}\text{YIGF}_{389}$ (green) may represent a signal that binds the μ subunit of adaptor protein complexes and mediates rapid clathrin-dependent internalization from the plasma membrane. $_{417}\text{DEHLL}_{421}$ (yellow) may represent a signal that regulates cycling between the *trans*-golgi network and endosomes through binding GGA clathrin adaptor proteins. **(B, C, and D)** HEK 293 cells were transfected with cDNA for HA-hRIC3 and **(B)** wild-type FLAG- $\alpha 7$ nAChR or isoforms of FLAG- $\alpha 7$ nAChR containing mutations to **(C)** the putative adaptor protein binding motif $_{386}\text{YIGF}_{389}$ (Y386A/F389A or Y386F/F389A) or **(D)** the putative GGA binding motif $_{417}\text{DEHLL}_{421}$ (L420A/L421A or D417A/L420A/L421A). **(A, B and C)** Cells were incubated on ice for 1 h with Alexa Fluor 647- α BTX, washed and transferred to 37 °C for 0, 4, or 6 h. At the end of the incubation, the cells were stained to detect changes to surface levels of FLAG- $\alpha 7$ nAChR as described in Fig. 2. Images are representative of 5 to 20 cells per time point, per experiment, from three independent experiments. Bar, 10 μm .

A

HHHDPDGGKMPKWTRVILLNWCAWFLRMKRPGE	350
DKVRPACQHKQRRCSLASVEMSAVAPPPASNGNLLYIGFRGLDGVHCVPT	400
PDSGVVCGRMACSPTHDEHLLHGGQPPEGDPDLAKILEEVRYIANRFRCQ	450
DESEAVCSEWKFAACVVDR	469

B

C

D

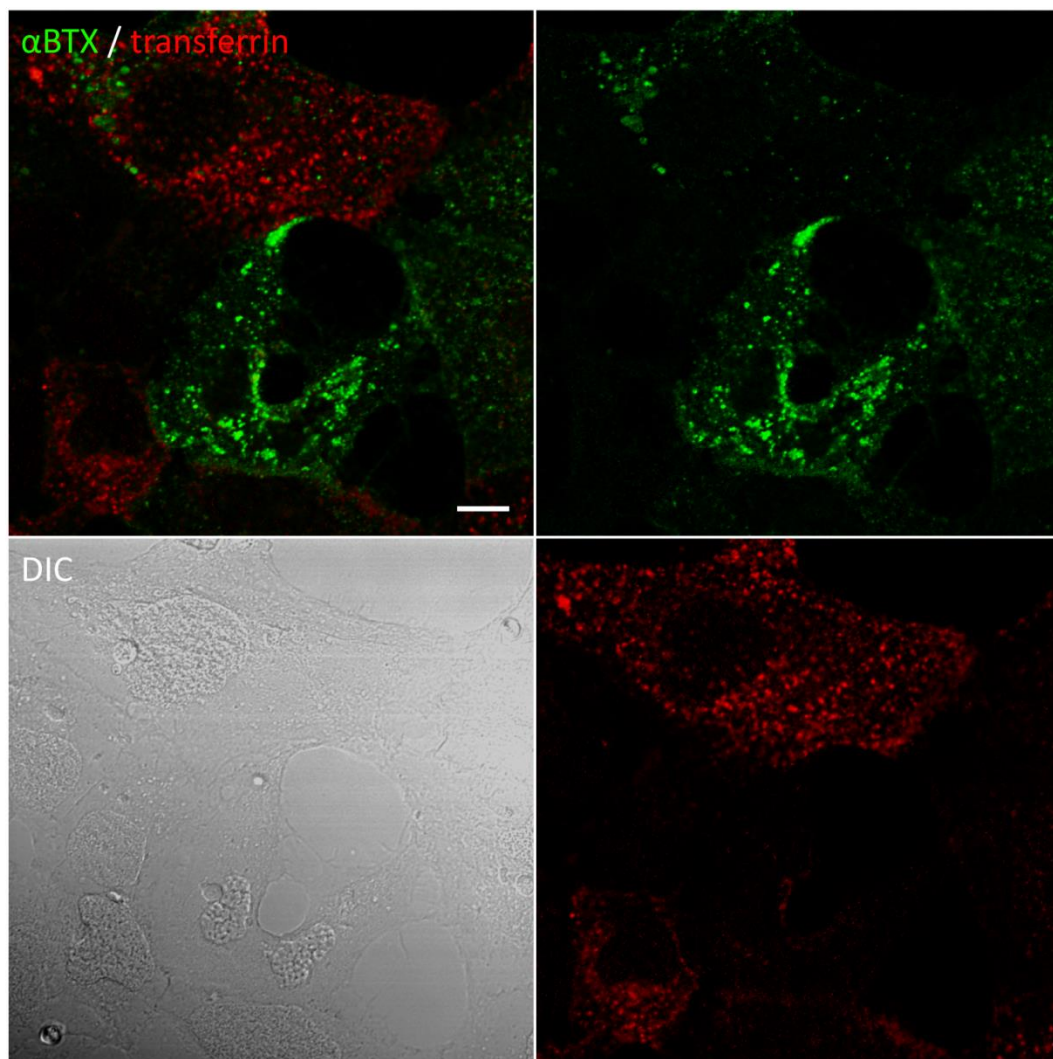
dynamin K44A inhibits the budding of clathrin vesicles from the plasma membrane (69, 70). AP180-C inhibits the formation of clathrin-coated pits that facilitate receptor internalization (71). Dynamin K44A and AP180-C both block transferrin receptor endocytosis (69 - 71). To determine if $\alpha 7$ nAChR- α BTX complexes undergo clathrin-dependent endocytosis, we examined internalization of fluorescent α BTX in cells co-transfected with FLAG- $\alpha 7$ nAChR and HA-hRIC3 cDNA and either dynamin 1 K44A or AP180-C (Figure 3.8). HEK 293 cells were transfected, incubated with fluorescent α BTX on ice and transferred to 37 °C for 6 h. To assess functional expression of dynamin 1 K44A or AP180-C protein, a fluorescent di-ferric transferrin conjugate was added to the cell culture medium 20 minutes prior to the end of the experiment. Cells co-expressing dynamin 1 K44A or AP180-C were indicated by a lack of fluorescent transferrin internalization; internalization of fluorescent α BTX was unaffected in these cells (Figure 3.8 A and B). We conducted four independent experiments on cells co-transfected with dynamin 1 K44A or AP180-C and employed transferrin internalization in our final experiment as a measure of the functional expression of these proteins; in any of the experiments we conducted we did not observe inhibition of fluorescent α BTX internalization. This suggests that the endocytosis of $\alpha 7$ nAChR- α BTX complexes does not occur through a clathrin- or dynamin-dependent mechanism.

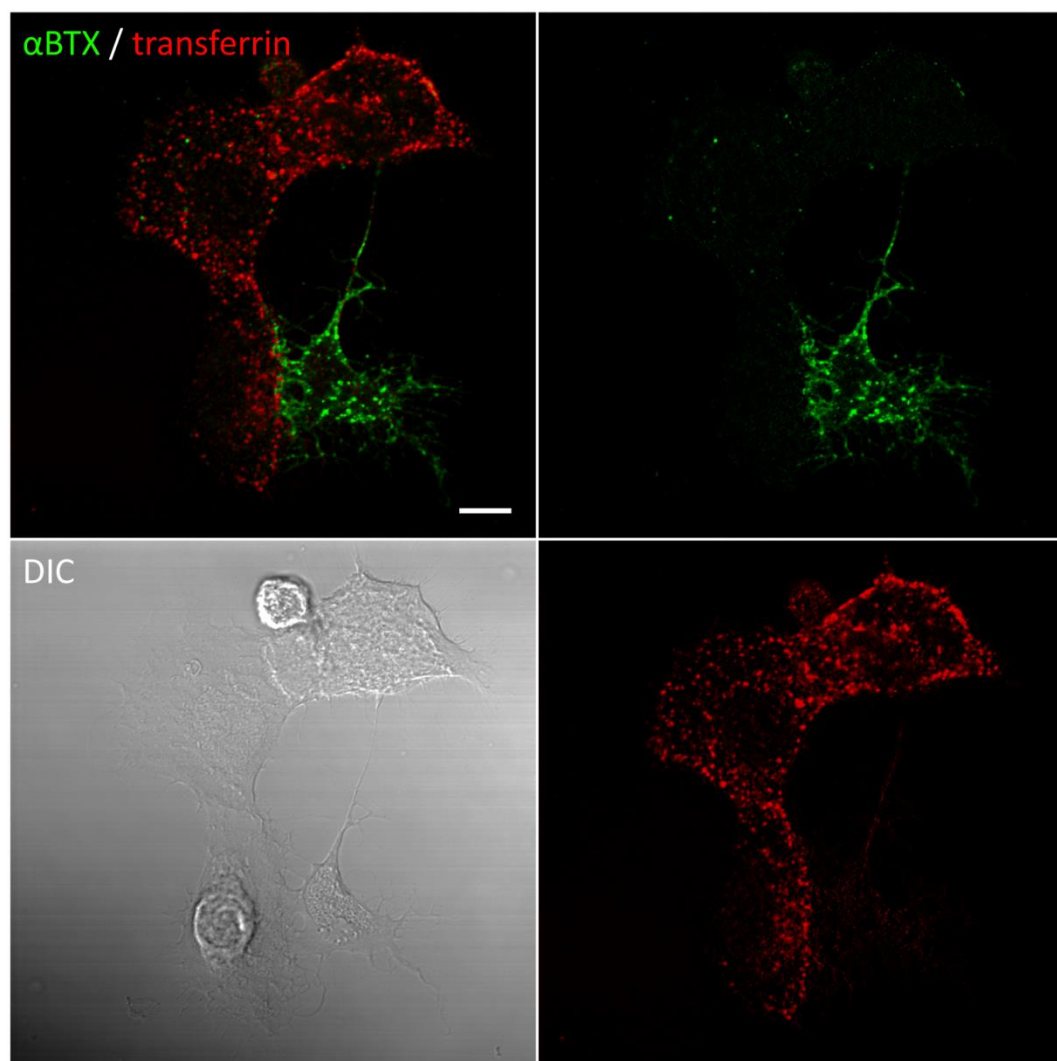
3.4.6 Inhibition of Actin Dynamics, RhoGTPases or RalGTPase Does Not Block $\alpha 7$ nAChR Endocytosis

Clathrin-independent endocytic mechanisms can induce changes to the actin cytoskeleton to facilitate endocytosis (72 - 74). We investigated the role of actin polymerization in the endocytosis of $\alpha 7$ nAChR- α BTX complexes by treating cells with cytochalasin D. Cytochalasin D is a plasma membrane-permeable inhibitor of actin polymerization that binds to the ends of actin filaments and prevents the addition of monomers (75). HEK 293 cells transfected with FLAG- $\alpha 7$ nAChR and HA-RIC3 cDNA were incubated on ice with fluorescent α BTX and transferred to 37 °C for 2 or 4 h in the presence of 2.5 μ M cytochalasin D or an equivalent concentration of DMSO vehicle. To label FLAG- $\alpha 7$ nAChR remaining in the plasma membrane, cells were returned to ice and

Figure 3.8 Endocytosis of $\alpha 7$ nAChR- α BTX complexes is independent of clathrin.

HEK 293 cells transfected with cDNA for FLAG- $\alpha 7$ nAChR and HA-hRIC3, and either **(A)** dominant-negative dynamin 1 K44A or **(B)** the C-terminal fragment of the adaptor protein AP180 (AP180-C) were incubated on ice for 1 h with Alexa Fluor 647- α BTX (green), washed, and transferred to 37 °C for 6 h. Twenty minutes before the end of the experiment, Alexa Fluor 633-transferrin (red) was added to the cell culture medium. For A and B , images are representative of 10 to 12 cells per time point, two cover slips per time point, from four independent experiments. Bar, 10 μ m.

A**dynamin 1 K44A**

B**AP180-C**

incubated with anti-FLAG antibody and fluorescent secondary antibody. Cytochalasin D clearly disrupted actin cytoskeleton dynamics, as evidenced by changes in cell morphology, but did not prevent the internalization of fluorescent α BTX (Figure 3.9 A). DMSO treatment did not affect cell morphology or internalization of fluorescent α BTX (Figure 3.9 A).

Rho family GTPases regulate actin dynamics and may function in distinct pathways of clathrin-independent endocytosis (72 - 74). We assessed the involvement of RhoGTPases in the internalization of α 7 nAChR- α BTX complexes in HEK 293 cells co-transfected with FLAG- α 7 nAChR and HA-RIC3 cDNA and cDNA for GFP-tagged dominant negative isoforms of the RhoGTPases, RhoA, Rac1, and Cdc42. Co-expression of RhoA T19N, Rac1 T17N, or Cdc42 T17N, did not prevent the internalization of fluorescent α BTX after 4 h at 37 °C (Figure 3.9 B).

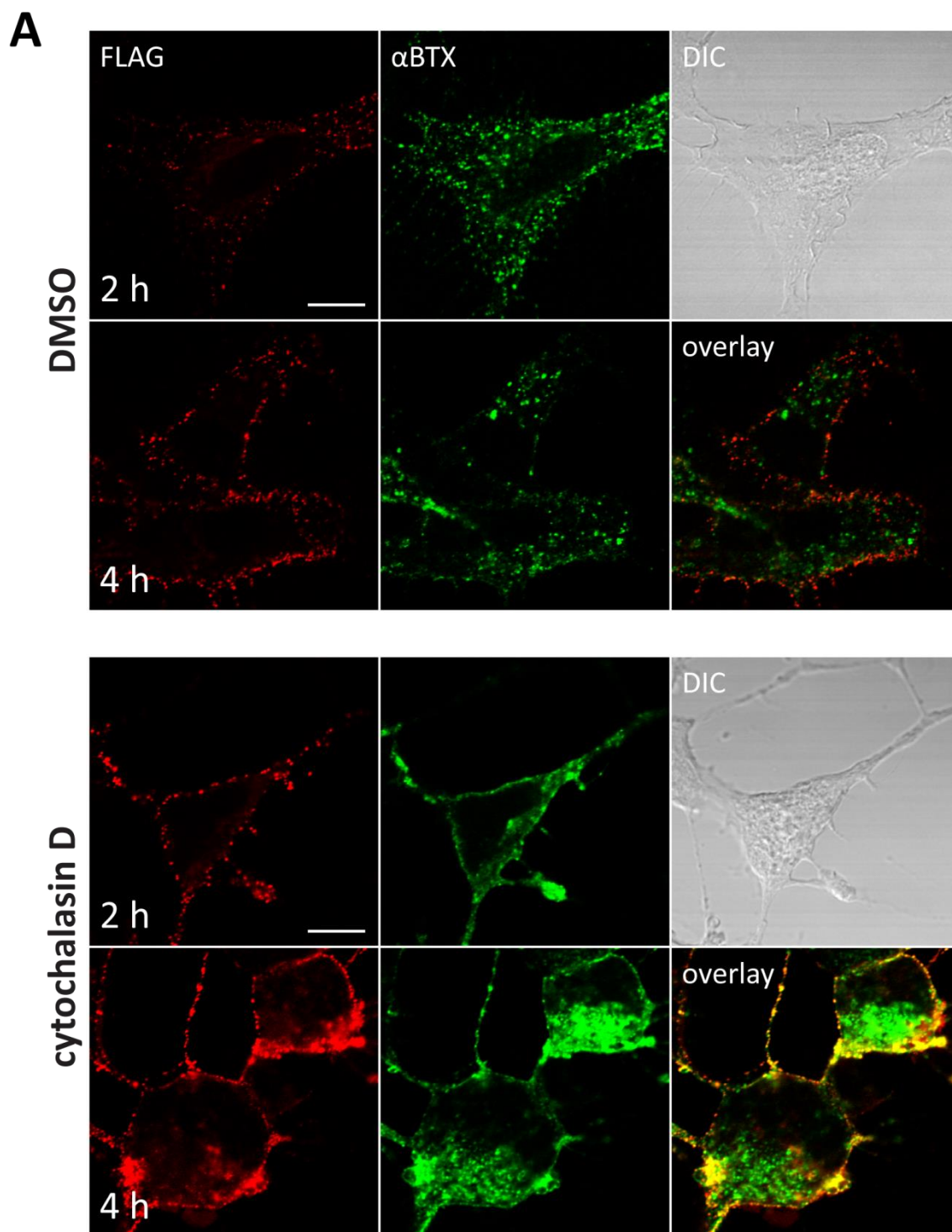
RalA is a member of the Ras family of GTPases which plays a role in the endocytosis of a variety of receptors and can act upstream of Rac1 and Cdc42 to affect actin dynamics (76, 77). We examined internalization of fluorescent α BTX in HEK 293 cells co-transfected with FLAG- α 7 nAChR and HA-RIC3 cDNA and cDNA for a yellow fluorescent protein (YFP)-tagged dominant negative isoform of RalA, RalA S28N (78, 79). Co-expression of RalA S28N did not prevent internalization of fluorescent α BTX after 4 h at 37 °C (Figure 3.9 B). These results suggest that inhibition of actin dynamics or small GTPases that regulate actin polymerization to facilitate endocytosis do not play a role in the internalization of α 7 nAChR- α BTX complexes.

3.4.7 α 7 nAChR- α BTX Complexes Endocytose Through Flotillin 1 and Caveolin 1 α Pathways

Flotillin 1 and caveolin 1 α are components of distinct pathways of clathrin-independent endocytosis that, in addition to clathrin, indicate separate plasma membrane regions involved in internalization (72, 80, 81). To determine the involvement of these proteins in the internalization of α 7 nAChR- α BTX complexes, we examined localization of fluorescent α BTX and GFP-tagged flotillin 1 or caveolin 1 α in HEK 293 cells. Cells

Figure 3.9 Inhibition of actin dynamics, RhoGTPases or RalGTPase does not block $\alpha 7$ nAChR endocytosis.

(A) HEK 293 cells transfected with FLAG- $\alpha 7$ nAChR and HA-hRIC3 cDNA were incubated on ice with Alexa Fluor 647- α BTX for 1 h, washed, and then transferred to 37 °C in the presence of cytochalasin D or DMSO vehicle for 2 or 4 h. At the end of the incubation, the cells were returned to ice and incubated with anti-FLAG antibody to label cell surface receptors, followed by Alexa Fluor 546-conjugated secondary antibody. Cells were fixed with PLP, mounted, and images of Alexa Fluor 546-conjugated secondary antibody (red) and Alexa Fluor 647- α BTX (green) were collected from single z-sections on a laser-scanning confocal microscope. **(B)** HEK 293 cells co-transfected with cDNA for FLAG- $\alpha 7$ nAChR, HA-hRIC3, and YFP- or GFP-tagged dominant-negative mutant isoforms of RhoGTPases (RhoA T19N, Rac1 T17N, and Cdc42 T17N) or RalGTPase (RalA S28N) were labelled with Alexa Fluor 647- α BTX as in A and chased at 37 °C for 4 h. Cells were fixed with PLP, mounted, and images of Alexa Fluor 647- α BTX (green) and YFP or GFP (red) were collected from single z-sections on a laser-scanning confocal microscope. For A, images are representative of 10 to 18 cells per time point, per treatment, per experiment, one to two cover slips per time point, from two independent experiments; for B, 5 to 17 cells, per treatment, per experiment, from four independent experiments. Bar, 10 μ m.



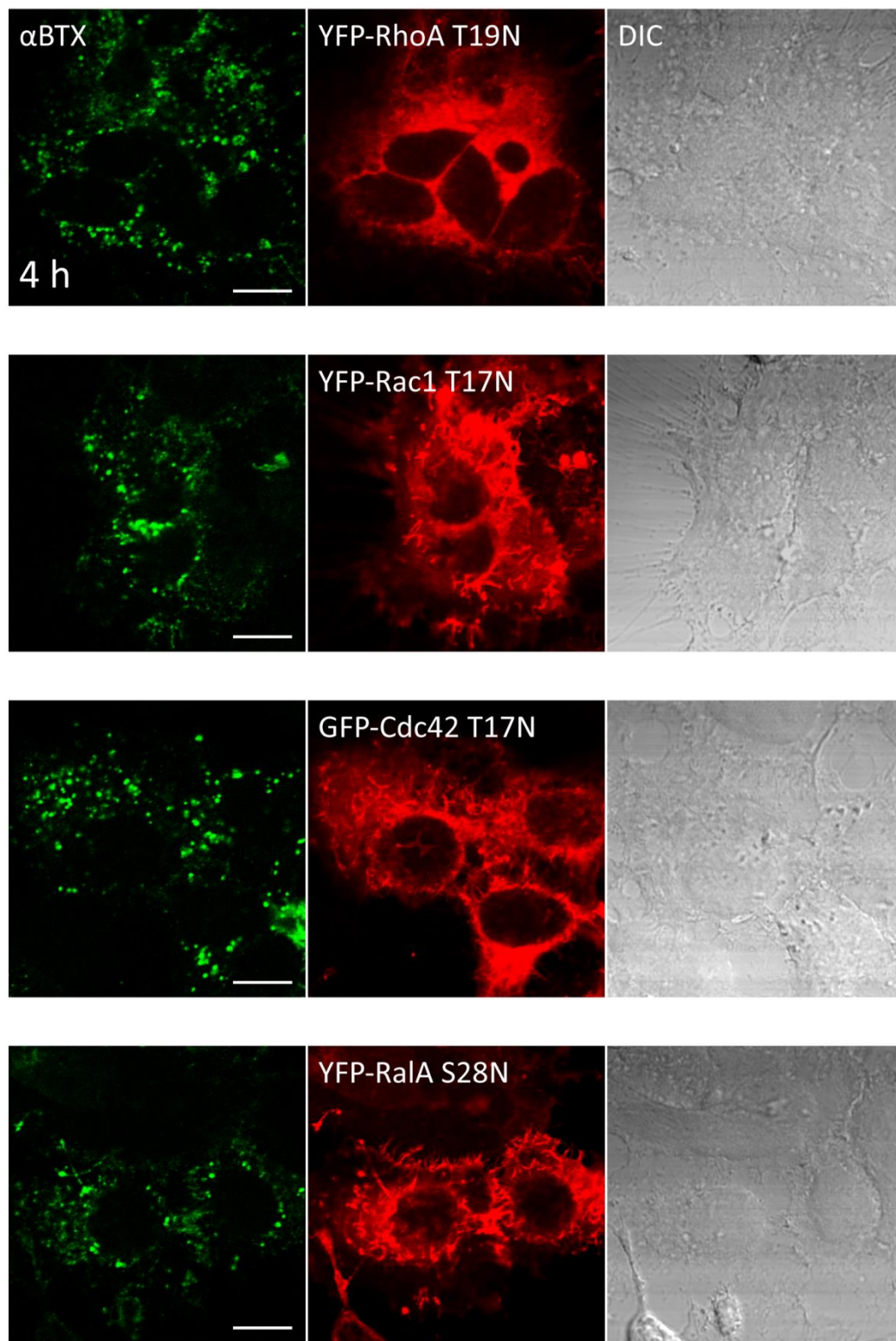
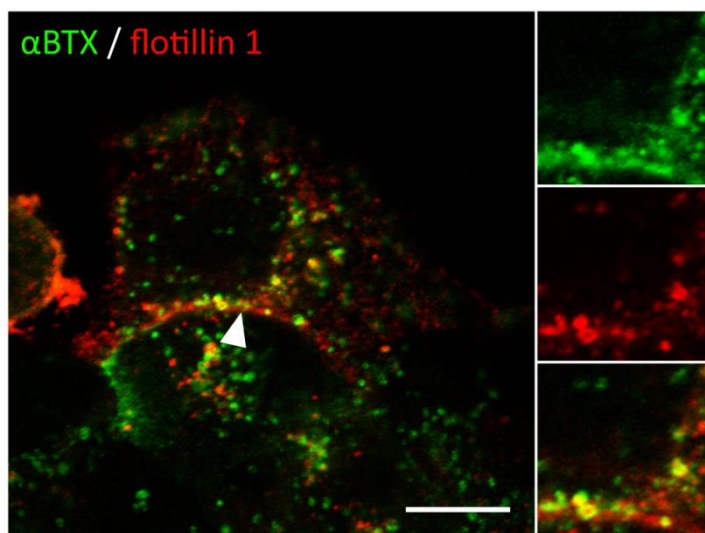
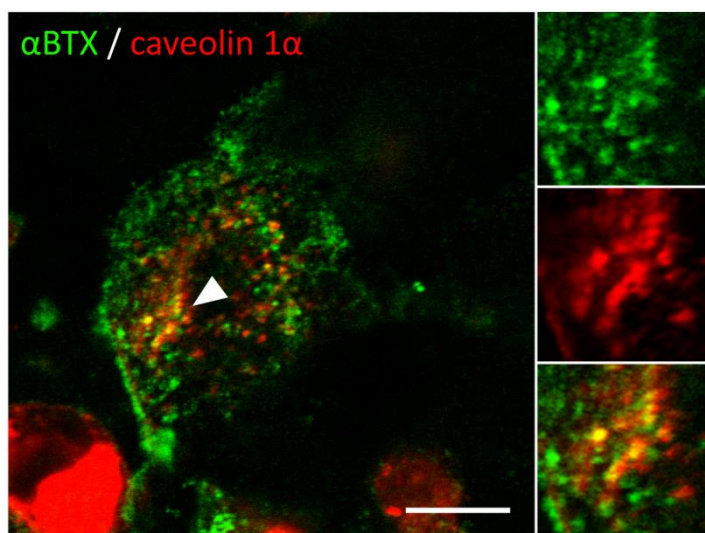
B

Figure 3.10 $\alpha 7$ nAChR- α BTX complexes internalize through flotillin 1 and caveolin 1 α pathways.

HEK 293 cells transfected with cDNA for FLAG- $\alpha 7$ nAChR, HA-hRIC3, and either **(A)** flotillin 1-GFP or **(B)** caveolin 1 α -GFP were incubated on ice for 1 h with Alexa Fluor 647- α BTX, washed and transferred to 37 °C for 2 h. Cells were fixed and mounted and images of Alexa Fluor 647- α BTX (green) and flotillin 1-, or caveolin 1 α -GFP (red) were collected from single z-sections on a laser-scanning confocal microscope and colour combined. Insets show magnified images of the area indicated by an arrowhead for Alexa Fluor 647- α BTX (green) with flotillin 1-, or caveolin 1 α -GFP (red) and an overlay of the two. Images are representative of 41 cells for A (flotillin 1-GFP) and 42 cells for B (caveolin 1 α -GFP) from a preliminary experiment. Bar, 10 μ m.

A**B**

transfected with FLAG- $\alpha 7$ nAChR, HA-hRIC3 and GFP-tagged flotillin 1 or GFP-tagged caveolin 1 α cDNA were incubated on ice with fluorescent α BTX and transferred to 37 °C for 2 h (Figure 3.10 A and B). Co-localization of fluorescent α BTX with flotillin 1 or caveolin 1 α , in punctate structures, was apparent in nearly all cells we observed. This suggests that these two proteins may represent pathways for internalization of $\alpha 7$ nAChR- α BTX complexes from the plasma membrane.

3.5 Discussion

Knowledge of mechanisms that regulate surface expression, endocytosis, or trafficking of $\alpha 7$ nAChR is currently limited. Some studies have identified specific sequences within the large intracellular loop of the $\alpha 7$ nAChR subunit that regulate the assembly of receptors and their insertion into the plasma membrane (82 - 84). Others have determined the necessity for post-translational modification (85) or the expression of tissue-specific component proteins, such as the chaperone protein hRIC3 (27), for functional expression of the $\alpha 7$ nAChR at the cell surface. Additional studies have determined a role for SNAREs, proteins that mediate vesicular fusion (86), in the dynamic cycling of the receptor in response to agonist stimulation (87) or tyrosine kinase activity (88). However, endocytic mechanisms that regulate cell surface levels of the $\alpha 7$ nAChR have yet to be described. In this study, we demonstrate that binding of the competitive antagonist α BTX induces internalization of the $\alpha 7$ nAChR and present a potential pathway for the traffic of $\alpha 7$ nAChR- α BTX complexes to degradative compartments of the cell.

We began our investigation by verifying that co-expression of the chaperone protein hRIC3 is required for functional expression of the $\alpha 7$ nAChR in HEK 293 cells. Our immunocytochemistry and biotinylation findings are in agreement with Williams et al. (27), in demonstrating that $\alpha 7$ nAChR can be expressed on the surface of HEK 293 cells in the absence of hRIC3, but that co-expression of hRIC3 with the $\alpha 7$ nAChR is required for α BTX binding. hRIC3 appears to be necessary for proper assembly of the $\alpha 7$ nAChR and functional expression of the receptor on the surface of HEK 293 cells.

We first compared α BTX-induced internalization of the $\alpha 7$ nAChR in HEK 293 cells with SH-SY5Y cells, a cell line with a neuronal phenotype (89, 90) that endogenously expresses hRIC3 (27). α BTX induced internalization of the $\alpha 7$ nAChR in both HEK 293 and SH-SY5Y cells, lead to the accumulation of $\alpha 7$ nAChR- α BTX complexes in perinuclear regions after several hours. Cell surface levels of the receptor following α BTX-induced internalization appeared to be down-regulated in HEK 293 cells over time, but similar changes were not observed in SH-SY5Y cells, perhaps due to the relative efficiency of receptor assembly exhibited by these two cell types (82). Although SH-SY5Y cells internalized α BTX at a rate similar to HEK 293 cells, SH-SY5Y cells may have a greater reserve of fully assembled receptors to replace those lost from the cell surface (82). In a preliminary experiment to examine the replacement of receptors on the surface of HEK 293 cells, we induced receptor internalization with unlabelled α BTX and stained for newly emerged receptors after 6 h. Only a fraction of cells showed a small amount of fluorescent α BTX labelling, suggesting that insertion of $\alpha 7$ nAChR into the plasma membrane in HEK 293 cells was a slow process. This also suggests that, when we are labelling cell surface receptors with anti-FLAG antibody and fluorescent secondary antibody to determine changes to cell surface levels, we are likely labelling receptors that remained on the surface of HEK 293 cells and have not yet internalized.

Following internalization, $\alpha 7$ nAChR- α BTX complexes trafficked to lysosomes from EEA1-positive early endosomes and Rab7-positive late endosomes. $\alpha 7$ nAChR- α BTX complexes transitioned from early endosomes to lysosomes from between 2 to 4 h and all internalized α BTX appeared to be in LAMP1-positive lysosomes after 6 h. This time-course is similar to that observed for α BTX-mediated down-regulation of the muscle nAChR in CHO cells (91). We did not find co-localization of α BTX with Rab 4 or Rab11-positive vesicles, suggesting that, once internalized, $\alpha 7$ nAChR complexes are not recycled back to the cell surface; rather they appear to be trafficked directly through Rab7-positive late endosomes to lysosomes for degradation. These results are in contrast to Kumari et al. (91), who observed that some muscle nAChR- α BTX complexes co-localized with Rab11; there is some evidence to suggest that α BTX-labelled nAChR

undergoes dynamic recycling at the neuromuscular junction (92, 93). Internalized α BTX did not co-localize with Rab 5, which seems to contradict with our observation that α BTX traffics through EEA1-positive vesicles early in the stages of receptor internalization. Although EEA1 is an important Rab5 effector, required for mediating fusion of early endosomes (50), it is evident that EEA1 can tether to endosomes independently of Rab5 (94).

The cell surface expression of several ionotropic receptors can be regulated by signal sequences contained within their cytosolic domains (63, 95 - 98). To determine whether the α 7 nAChR could be regulated in a similar manner, we identified two putative motifs that fit the criteria of sorting signals recognized in a large number of transmembrane proteins, $_{386}\text{YIGF}_{389}$, and $_{417}\text{DEHLL}_{421}$. Mutations to these signal sequences can lead to increased surface expression of the relevant receptors, as a result of the disruption of adaptor protein binding and the prevention of clathrin-mediated endocytosis (63, 95, 96, 98). When we generated mutant isoforms of the α 7 nAChR and compared their cell surface expression and α BTX-induced internalization to the wild-type protein, we did not observe a substantial difference between wild-type and mutant, demonstrating that $_{386}\text{YIGF}_{389}$ and $_{417}\text{DEHLL}_{421}$ sequences do not regulate cell surface expression of the receptor or alter α BTX-induced internalization.

To delineate a mechanism that regulates α BTX internalization, we investigated factors that are specific to clathrin-dependent and -independent endocytosis. The ineffectiveness of over-expression of dominant-negative dynamin 1 K44A and AP180-C demonstrate that α BTX induced internalization of the α 7 nAChR is a dynamin- and clathrin-independent process. α BTX induced internalization of the α 7 nAChR was not affected by treating cells with an inhibitor of actin polymerization, cytochalasin D, or over-expression of dominant negative isoforms of the RhoGTPases, RhoA, Rac1, or Cdc42, or over-expression of dominant negative RalA, suggesting that clathrin-independent mechanisms that recruit changes to the actin cytoskeleton and activity of these GTPases to facilitate endocytosis did not mediate this process. It appears that

internalization of $\alpha 7$ nAChR- α BTX complexes occurs independently of clathrin and dynamin, as well as cytoskeleton dynamics and RhoGTPase activity. In comparison, Kumari et al. (91) found that α BTX-induced internalization of the muscle nAChR was independent of dynamin, but required both actin polymerization and Rac1 activity. Both systems involve heterologous expression of nAChR, as HEK 293 cells and CHO cells do not endogenously express these proteins. However, the muscle nAChR is highly organized at neuromuscular junctions where coupling to the actin cytoskeleton maintains synaptic integrity (99, 100). In contrast, the $\alpha 7$ nAChR is expressed at perisynaptic and somatic locations (2 - 5, 7 - 12) and appear to function independently of cytoskeleton dynamics (101). Therefore, actin dynamics may not play a role in the internalization of the $\alpha 7$ nAChR in response to binding α BTX.

Clathrin-independent endocytosis can occur from lipid rafts within the plasma membrane that are enriched in either caveolins (caveolae) or flotillins (72, 80, 81). α BTX co-localized with flotillin 1 and caveolin 1 α puncta after internalization was allowed to proceed for 2 h, a time point at which α BTX is co-localized with EEA1 and in the process of becoming internalized. This suggests that flotillin 1 or caveolin 1 α -associated pathways may represent mechanisms for endocytosis of $\alpha 7$ nAChR- α BTX complexes. It is currently hypothesized that caveolins and flotillins represent distinct pathways for endocytosis (72, 80, 81). Despite this, it is apparent that the $\alpha 7$ nAChR can associate with either caveolin- or flotillin-positive lipid rafts, depending on the cell type (101, 102). This has also been demonstrated here.

HEK 293 cells endogenously express caveolins at negligible levels relative to their level of flotillin expression (103, 104). Caveolar-mediated endocytosis requires dynamin GTPase activity (105, 106), while flotillin-mediated endocytosis can occur both dependently (107, 108) and independently of dynamin (81). Given that we observed internalization of α BTX was not blocked by a dominant-negative isoform of dynamin, it seems likely that endocytosis of $\alpha 7$ nAChR- α BTX complexes occurs through a flotillin-associated pathway. However, since we observed co-localization of internalized α BTX

with both markers, endocytosis of the $\alpha 7$ nAChR through these pathways could be determined by the level of expression of caveolin and flotillin protein or the relative affinity of the receptor for localization to caveolae versus flotillin-enriched lipid rafts, which is currently unknown. Fractionation of intact cells followed by density gradient centrifugation is a widely used technique for separating subcellular membrane compartments, such as endocytic vesicles, for identifying subcellular organelles through which proteins traffic (109). Fractionation of transfected HEK-293 or SH-SY5Y-FLAG- $\alpha 7$ cells and density gradient centrifugation, following pulse-chase with α BTX, combined with immunoblotting for flotillin or caveolin (102) and FLAG epitope could have provided biochemical evidence in support of our localization experiment and help answer these questions.

We present here evidence in support of an endocytic pathway for the internalization of $\alpha 7$ nAChR in response to binding an irreversible competitive antagonist, α BTX. We propose a model in which α BTX induces internalization of the $\alpha 7$ nAChR alternatively through flotillin- or caveolin-associated endocytosis and trafficking of $\alpha 7$ nAChR- α BTX complexes through early and late endosomes to lysosomes (Figure 3.11). This occurs independently of clathrin, dynamin, actin polymerization, or RhoGTPase and RalGTPase activity and appears to be unique amongst ligand-gated ion channels.

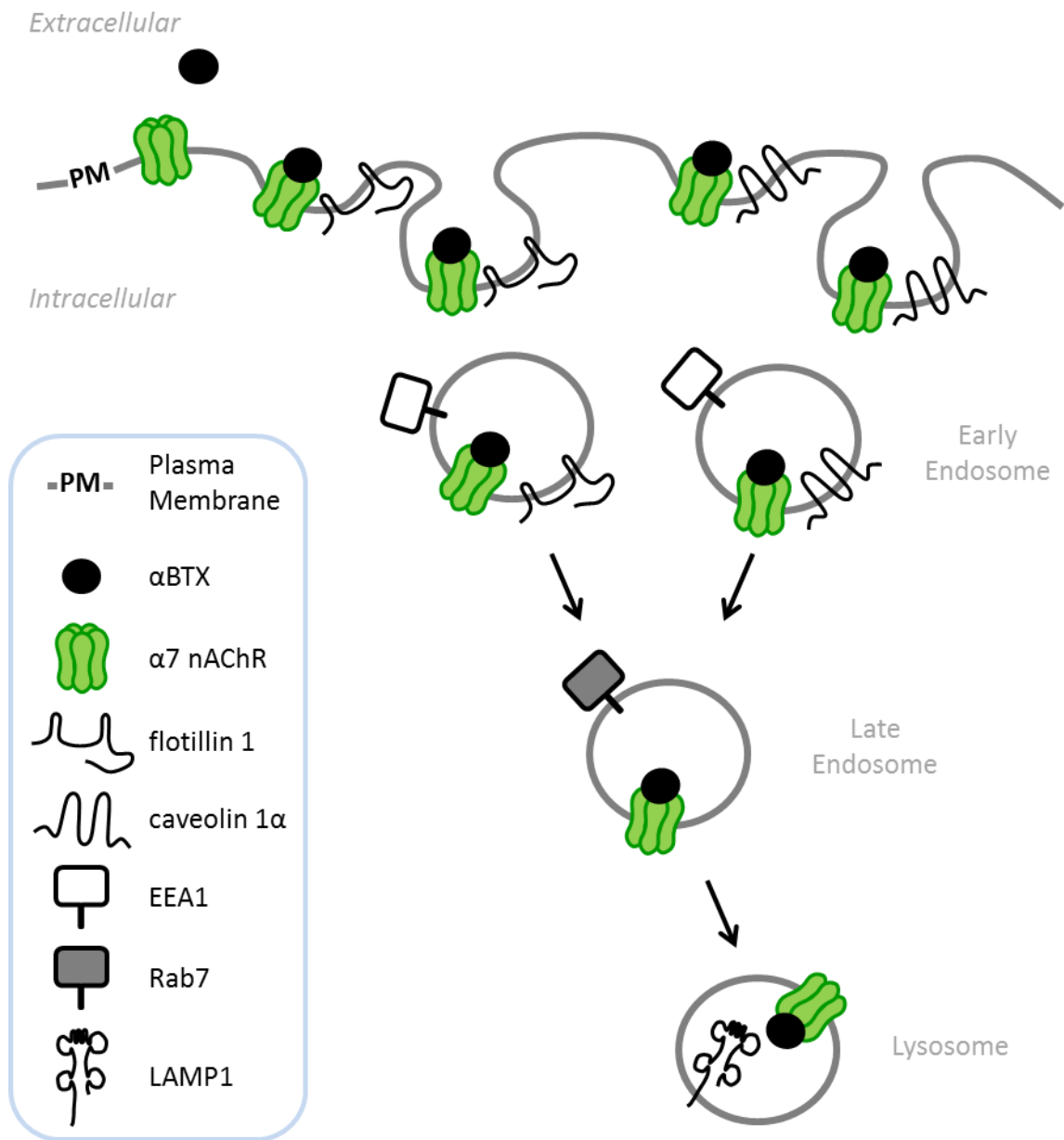


Figure 3.11 A Model for αBTX-induced internalization of the α7 nAChR.

αBTX binding induces endocytosis of α7 nAChR through alternate flotillin 1- or caveolin 1α-associated pathways and subcellular trafficking through EEA1-positive early endosomes and Rab7-positive late endosomes to LAMP1-positive lysosomes. Legend, inset.

3.6 References

1. Dajas-Bailador, F. and Wonnacott, S. (2004) Nicotinic acetylcholine receptors and the regulation of neuronal signalling. *Trends Pharmacol Sci* **25**: 317-24.
2. McGehee, D.S., Heath, M.J., Gelber, S., Devay, P., Role, L.W. (1995) Nicotine enhancement of fast excitatory synaptic transmission in CNS by presynaptic receptors. *Science* **269**: 1692-6.
3. Gray, R., Rajan, A.S., Radcliffe, K.A., Yakehiro, M., Dani, J.A. (1996) Hippocampal synaptic transmission enhanced by low concentrations of nicotine. *Nature* **383**: 713-716.
4. Fabian-Fine, R., Skehel, P., Errington, M.L., Davies, H.A., Sher, E., Stewart, M.G., Fine, A. (2001) Ultrastructural distribution of the alpha7 nicotinic acetylcholine receptor subunit in rat hippocampus. *J. Neurosci.* **21**: 7993-8003.
5. Jones, I.W., Barik, J., O'Neill, M.J., Wonnacott, S. (2004) Alpha bungarotoxin-1.4 nm gold: a novel conjugate for visualising the precise subcellular distribution of alpha 7* nicotinic acetylcholine receptors. *J. Neurosci. Methods* **134**: 65-74.
6. Xu, J., Zhu, Y., Heinemann, S.F. (2006) Identification of sequence motifs that target neuronal nicotinic receptors to dendrites and axons. *J. Neurosci.* **26**: 9780-9793.
7. Alkondon, M. and Albuquerque, E.X. (1993) Diversity of nicotinic acetylcholine receptors in rat hippocampal neurons. I. Pharmacological and functional evidence for distinct structural subtypes. *J. Pharmacol. Exp. Ther.* **265**: 1455-1473.
8. Frazier, C.J., Buhler, A.V., Weiner, J.L., Dunwiddie, T.V. (1998) Synaptic potentials mediated via alpha-bungarotoxin-sensitive nicotinic acetylcholine receptors in rat hippocampal interneurons. *J. Neurosci.* **18**: 8228-8235.

9. Frazier, C.J., Rollins, Y.D., Breese, C.R., Leonard, S., Freedman, R., Dunwiddie, T.V. (1998) Acetylcholine activates an alpha-bungarotoxin-sensitive nicotinic current in rat hippocampal interneurons, but not pyramidal cells. *J. Neurosci.* **18**: 1187-1195.
10. Hefft, S., Hulo, S., Bertrand, D., Muller, D. (1999) Synaptic transmission at nicotinic acetylcholine receptors in rat hippocampal organotypic cultures and slices. *J. Physiol.* **515 (Pt 3)**: 769-776.
11. Levy, R.B. and Aoki, C. (2002) Alpha7 nicotinic acetylcholine receptors occur at postsynaptic densities of AMPA receptor-positive and -negative excitatory synapses in rat sensory cortex. *J. Neurosci.* **22**: 5001-5015.
12. Khiroug, L., Giniatullin, R., Klein, R.C., Fayuk, D., Yakel, J.L. (2003) Functional mapping and Ca²⁺ regulation of nicotinic acetylcholine receptor channels in rat hippocampal CA1 neurons. *J. Neurosci.* **23**: 9024-9031.
13. Alkondon, M., Pereira, E.F., Albuquerque, E.X. (1998) Alpha-Bungarotoxin- and Methyllycaconitine-Sensitive Nicotinic Receptors Mediate Fast Synaptic Transmission in Interneurons of Rat Hippocampal Slices. *Brain Res.* **810**: 257-263.
14. Alkondon, M., Pereira, E.F., Cortes, W.S., Maelicke, A., Albuquerque, E.X. (1997) Choline is a selective agonist of alpha7 nicotinic acetylcholine receptors in the rat brain neurons. *Eur. J. Neurosci.* **9**: 2734-2742.
15. Jones, S. and Yakel, J.L. (1997) Functional nicotinic ACh receptors on interneurons in the rat hippocampus. *J. Physiol.* **504 (Pt 3)**: 603-610.
16. Ji, D., Lape, R., Dani, J.A. (2001) Timing and location of nicotinic activity enhances or depresses hippocampal synaptic plasticity. *Neuron* **31**: 131-141.
17. Radcliffe, K.A., Fisher, J.L., Gray, R., Dani, J.A. (1999) Nicotinic modulation of glutamate and GABA synaptic transmission of hippocampal neurons. *Ann. N. Y. Acad. Sci.* **868**: 591-610.

18. Kittler, J.T., Delmas, P., Jovanovic, J.N., Brown, D.A., Smart, T.G., Moss, S.J. (2000) Constitutive endocytosis of GABAA receptors by an association with the adaptin AP2 complex modulates inhibitory synaptic currents in hippocampal neurons. *J. Neurosci.* **20**: 7972-7977.
19. Carroll, R.C., Beattie, E.C., Xia, H., Luscher, C., Altschuler, Y., Nicoll, R.A., Malenka, R.C., von Zastrow, M. (1999) Dynamin-dependent endocytosis of ionotropic glutamate receptors. *Proc. Natl. Acad. Sci. U. S. A.* **96**: 14112-14117.
20. Nong, Y., Huang, Y.Q., Ju, W., Kalia, L.V., Ahmadian, G., Wang, Y.T., Salter, M.W. (2003) Glycine binding primes NMDA receptor internalization. *Nature* **422**: 302-307.
21. Ehlers, M.D. (2000) Reinsertion or degradation of AMPA receptors determined by activity-dependent endocytic sorting. *Neuron* **28**: 511-525.
22. Hutchison, C.A.,3rd, Phillips, S., Edgell, M.H., Gillam, S., Jahnke, P., Smith, M. (1978) Mutagenesis at a specific position in a DNA sequence. *J. Biol. Chem.* **253**: 6551-6560.
23. Graham, F.L., Smiley, J., Russell, W.C., Nairn, R. (1977) Characteristics of a human cell line transformed by DNA from human adenovirus type 5. *J. Gen. Virol.* **36**: 59-74.
24. Shaw, G., Morse, S., Ararat, M., Graham, F.L. (2002) Preferential transformation of human neuronal cells by human adenoviruses and the origin of HEK 293 cells. *FASEB J.* **16**: 869-871.
25. Cinar, H. and Barnes, E.M.,Jr. (2001) Clathrin-independent endocytosis of GABA(A) receptors in HEK 293 cells. *Biochemistry* **40**: 14030-14036.
26. Vina-Vilaseca, A., Bender-Sigel, J., Sorkina, T., Closs, E.I., Sorkin, A. (2011) Protein kinase C-dependent ubiquitination and clathrin-mediated endocytosis of the cationic amino acid transporter CAT-1. *J. Biol. Chem.* **286**: 8697-8706.

27. Williams, M.E., Burton, B., Urrutia, A., Shcherbatko, A., Chavez-Noriega, L.E., Cohen, C.J., Aiyar, J. (2005) Ric-3 promotes functional expression of the nicotinic acetylcholine receptor alpha7 subunit in mammalian cells. *J. Biol. Chem.* **280**: 1257-1263.
28. Ross, R.A., Spengler, B.A., Biedler, J.L. (1983) Coordinate morphological and biochemical interconversion of human neuroblastoma cells. *J. Natl. Cancer Inst.* **71**: 741-747.
29. Biedler, J.L., Helson, L., Spengler, B.A. (1973) Morphology and growth, tumorigenicity, and cytogenetics of human neuroblastoma cells in continuous culture. *Cancer Res.* **33**: 2643-2652.
30. Lukas, R.J., Norman, S.A., Lucero, L. (1993) Characterization of Nicotinic Acetylcholine Receptors Expressed by Cells of the SH-SY5Y Human Neuroblastoma Clonal Line. *Mol. Cell. Neurosci.* **4**: 1-12.
31. Peng, X., Katz, M., Gerzanich, V., Anand, R., Lindstrom, J. (1994) Human alpha 7 acetylcholine receptor: cloning of the alpha 7 subunit from the SH-SY5Y cell line and determination of pharmacological properties of native receptors and functional alpha 7 homomers expressed in *Xenopus* oocytes. *Mol. Pharmacol.* **45**: 546-554.
32. Ferguson, S.S., Downey, W.E., 3rd, Colapietro, A.M., Barak, L.S., Menard, L., Caron, M.G. (1996) Role of beta-arrestin in mediating agonist-promoted G protein-coupled receptor internalization. *Science* **271**: 363-366.
33. Bradford, M.M. (1976) A rapid and sensitive method for the quantitation of microgram quantities of protein utilizing the principle of protein-dye binding. *Anal. Biochem.* **72**: 248-254.
34. Laemmli, U.K. (1970) Cleavage of structural proteins during the assembly of the head of bacteriophage T4. *Nature* **227**: 680-685.

35. Barrantes, G.E., Rogers, A.T., Lindstrom, J., Wonnacott, S. (1995) alpha-Bungarotoxin binding sites in rat hippocampal and cortical cultures: initial characterisation, colocalisation with alpha 7 subunits and up-regulation by chronic nicotine treatment. *Brain Res.* **672**: 228-236.
36. Quik, M., Choremis, J., Komourian, J., Lukas, R.J., Puchacz, E. (1996) Similarity between rat brain nicotinic alpha-bungarotoxin receptors and stably expressed alpha-bungarotoxin binding sites. *J. Neurochem.* **67**: 145-154.
37. McLean, I.W. and Nakane, P.K. (1974) Periodate-lysine-paraformaldehyde fixative. A new fixation for immunoelectron microscopy. *J. Histochem. Cytochem.* **22**: 1077-1083.
38. Lansdell, S.J., Gee, V.J., Harkness, P.C., Doward, A.I., Baker, E.R., Gibb, A.J., Millar, N.S. (2005) RIC-3 enhances functional expression of multiple nicotinic acetylcholine receptor subtypes in mammalian cells. *Mol. Pharmacol.* **68**: 1431-1438.
39. Valles, A.S. and Barrantes, F.J. (2012) Chaperoning alpha7 neuronal nicotinic acetylcholine receptors. *Biochim. Biophys. Acta* **1818**: 718-729.
40. Cole, S.R., Ashman, L.K., Ey, P.L. (1987) Biotinylation: an alternative to radioiodination for the identification of cell surface antigens in immunoprecipitates. *Mol. Immunol.* **24**: 699-705.
41. Changeux, J.P., Kasai, M., Lee, C.Y. (1970) Use of a snake venom toxin to characterize the cholinergic receptor protein. *Proc. Natl. Acad. Sci. U. S. A.* **67**: 1241-1247.
42. Albuquerque, E.X., Pereira, E.F., Alkondon, M., Rogers, S.W. (2009) Mammalian nicotinic acetylcholine receptors: from structure to function. *Physiol. Rev.* **89**: 73-120.

43. Couturier, S., Bertrand, D., Matter, J.M., Hernandez, M.C., Bertrand, S., Millar, N., Valera, S., Barkas, T., Ballivet, M. (1990) A neuronal nicotinic acetylcholine receptor subunit (alpha 7) is developmentally regulated and forms a homo-oligomeric channel blocked by alpha-BTX. *Neuron* **5**: 847-856.
44. Seguela, P., Wadiche, J., Dineley-Miller, K., Dani, J.A., Patrick, J.W. (1993) Molecular cloning, functional properties, and distribution of rat brain alpha 7: a nicotinic cation channel highly permeable to calcium. *J. Neurosci.* **13**: 596-604.
45. Gerzanich, V., Anand, R., Lindstrom, J. (1994) Homomers of alpha 8 and alpha 7 subunits of nicotinic receptors exhibit similar channel but contrasting binding site properties. *Mol. Pharmacol.* **45**: 212-220.
46. Elgoyhen, A.B., Johnson, D.S., Boulter, J., Vetter, D.E., Heinemann, S. (1994) Alpha 9: an acetylcholine receptor with novel pharmacological properties expressed in rat cochlear hair cells. *Cell* **79**: 705-715.
47. Fertuck, H.C. and Salpeter, M.M. (1974) Localization of acetylcholine receptor by 125I-labeled alpha-bungarotoxin binding at mouse motor endplates. *Proc. Natl. Acad. Sci. U. S. A.* **71**: 1376-1378.
48. Raftery, M.A., Hunkapiller, M.W., Strader, C.D., Hood, L.E. (1980) Acetylcholine receptor: complex of homologous subunits. *Science* **208**: 1454-1456.
49. Mu, F.T., Callaghan, J.M., Steele-Mortimer, O., Stenmark, H., Parton, R.G., Campbell, P.L., McCluskey, J., Yeo, J.P., Tock, E.P., Toh, B.H. (1995) EEA1, an early endosome-associated protein. EEA1 is a conserved alpha-helical peripheral membrane protein flanked by cysteine "fingers" and contains a calmodulin-binding IQ motif. *J. Biol. Chem.* **270**: 13503-13511.
50. Christoforidis, S., McBride, H.M., Burgoyne, R.D., Zerial, M. (1999) The Rab5 effector EEA1 is a core component of endosome docking. *Nature* **397**: 621-625.

51. Callaghan, J., Simonsen, A., Gaullier, J.M., Toh, B.H., Stenmark, H. (1999) The endosome fusion regulator early-endosomal autoantigen 1 (EEA1) is a dimer. *Biochem. J.* **338 (Pt 2)**: 539-543.
52. Carlsson, S.R., Roth, J., Piller, F., Fukuda, M. (1988) Isolation and characterization of human lysosomal membrane glycoproteins, h-lamp-1 and h-lamp-2. Major sialoglycoproteins carrying polylactosaminoglycan. *J. Biol. Chem.* **263**: 18911-18919.
53. Saftig, P. and Klumperman, J. (2009) Lysosome biogenesis and lysosomal membrane proteins: trafficking meets function. *Nat. Rev. Mol. Cell Biol.* **10**: 623-635.
54. Zerial, M. and McBride, H. (2001) Rab proteins as membrane organizers. *Nat. Rev. Mol. Cell Biol.* **2**: 107-117.
55. van der Sluijs, P., Hull, M., Huber, L.A., Male, P., Goud, B., Mellman, I. (1992) Reversible phosphorylation--dephosphorylation determines the localization of rab4 during the cell cycle. *EMBO J.* **11**: 4379-4389.
56. Gorvel, J.P., Chavrier, P., Zerial, M., Gruenberg, J. (1991) Rab5 Controls Early Endosome Fusion in Vitro. *Cell* **64**: 915-925.
57. Bucci, C., Parton, R.G., Mather, I.H., Stunnenberg, H., Simons, K., Hoflack, B., Zerial, M. (1992) The small GTPase rab5 functions as a regulatory factor in the early endocytic pathway. *Cell* **70**: 715-728.
58. Sonnichsen, B., De Renzis, S., Nielsen, E., Rietdorf, J., Zerial, M. (2000) Distinct membrane domains on endosomes in the recycling pathway visualized by multicolor imaging of Rab4, Rab5, and Rab11. *J. Cell Biol.* **149**: 901-914.
59. Chavrier, P., Parton, R.G., Hauri, H.P., Simons, K., Zerial, M. (1990) Localization of low molecular weight GTP binding proteins to exocytic and endocytic compartments. *Cell* **62**: 317-329.

60. Bucci, C., Thomsen, P., Nicoziani, P., McCarthy, J., van Deurs, B. (2000) Rab7: a key to lysosome biogenesis. *Mol. Biol. Cell* **11**: 467-480.
61. Ullrich, O., Reinsch, S., Urbe, S., Zerial, M., Parton, R.G. (1996) Rab11 regulates recycling through the pericentriolar recycling endosome. *J. Cell Biol.* **135**: 913-924.
62. Bonifacino, J.S. and Traub, L.M. (2003) Signals for sorting of transmembrane proteins to endosomes and lysosomes. *Annu. Rev. Biochem.* **72**: 395-447.
63. Herring, D., Huang, R., Singh, M., Robinson, L.C., Dillon, G.H., Leidenheimer, N.J. (2003) Constitutive GABAA receptor endocytosis is dynamin-mediated and dependent on a dileucine AP2 adaptin-binding motif within the beta 2 subunit of the receptor. *J. Biol. Chem.* **278**: 24046-24052.
64. Man, H.Y., Lin, J.W., Ju, W.H., Ahmadian, G., Liu, L., Becker, L.E., Sheng, M., Wang, Y.T. (2000) Regulation of AMPA receptor-mediated synaptic transmission by clathrin-dependent receptor internalization. *Neuron* **25**: 649-662.
65. Pearse, B.M. (1982) Coated vesicles from human placenta carry ferritin, transferrin, and immunoglobulin G. *Proc. Natl. Acad. Sci. U. S. A.* **79**: 451-455.
66. Harding, C., Heuser, J., Stahl, P. (1983) Receptor-mediated endocytosis of transferrin and recycling of the transferrin receptor in rat reticulocytes. *J. Cell Biol.* **97**: 329-339.
67. Ciechanover, A., Schwartz, A.L., Lodish, H.F. (1983) The asialoglycoprotein receptor internalizes and recycles independently of the transferrin and insulin receptors. *Cell* **32**: 267-275.
68. Schmid, S.L. (1997) Clathrin-coated vesicle formation and protein sorting: an integrated process. *Annu. Rev. Biochem.* **66**: 511-548.

69. Damke, H., Baba, T., Warnock, D.E., Schmid, S.L. (1994) Induction of mutant dynamin specifically blocks endocytic coated vesicle formation. *J. Cell Biol.* **127**: 915-934.
70. Herskovits, J.S., Burgess, C.C., Obar, R.A., Vallee, R.B. (1993) Effects of mutant rat dynamin on endocytosis. *J. Cell Biol.* **122**: 565-578.
71. Ford, M.G., Pearse, B.M., Higgins, M.K., Vallis, Y., Owen, D.J., Gibson, A., Hopkins, C.R., Evans, P.R., McMahon, H.T. (2001) Simultaneous binding of PtdIns(4,5)P₂ and clathrin by AP180 in the nucleation of clathrin lattices on membranes. *Science* **291**: 1051-1055.
72. Doherty, G.J. and McMahon, H.T. (2009) Mechanisms of endocytosis. *Annu. Rev. Biochem.* **78**: 857-902.
73. Sandvig, K., Torgersen, M.L., Raa, H.A., van Deurs, B. (2008) Clathrin-independent endocytosis: from nonexisting to an extreme degree of complexity. *Histochem. Cell Biol.* **129**: 267-276.
74. Mayor, S. and Pagano, R.E. (2007) Pathways of clathrin-independent endocytosis. *Nat. Rev. Mol. Cell Biol.* **8**: 603-612.
75. Sampath, P. and Pollard, T.D. (1991) Effects of cytochalasin, phalloidin, and pH on the elongation of actin filaments. *Biochemistry* **30**: 1973-1980.
76. van Dam, E.M. and Robinson, P.J. (2006) Ral: mediator of membrane trafficking. *Int. J. Biochem. Cell Biol.* **38**: 1841-1847.
77. Feig, L.A. (2003) Ral-GTPases: approaching their 15 minutes of fame. *Trends Cell Biol.* **13**: 419-425.

78. Urano, T., Emkey, R., Feig, L.A. (1996) Ral-GTPases mediate a distinct downstream signaling pathway from Ras that facilitates cellular transformation. *EMBO J.* **15**: 810-816.
79. Jiang, H., Luo, J.Q., Urano, T., Frankel, P., Lu, Z., Foster, D.A., Feig, L.A. (1995) Involvement of Ral GTPase in v-Src-induced phospholipase D activation. *Nature* **378**: 409-412.
80. Hansen, C.G. and Nichols, B.J. (2009) Molecular mechanisms of clathrin-independent endocytosis. *J. Cell. Sci.* **122**: 1713-1721.
81. Glebov, O.O., Bright, N.A., Nichols, B.J. (2006) Flotillin-1 defines a clathrin-independent endocytic pathway in mammalian cells. *Nat. Cell Biol.* **8**: 46-54.
82. Mukherjee, J., Kuryatov, A., Moss, S.J., Lindstrom, J.M., Anand, R. (2009) Mutations of cytosolic loop residues impair assembly and maturation of alpha7 nicotinic acetylcholine receptors. *J. Neurochem.* **110**: 1885-1894.
83. Castelan, F., Mulet, J., Aldea, M., Sala, S., Sala, F., Criado, M. (2007) Cytoplasmic regions adjacent to the M3 and M4 transmembrane segments influence expression and function of alpha7 nicotinic acetylcholine receptors. A study with single amino acid mutants. *J. Neurochem.* **100**: 406-415.
84. Dineley, K.T. and Patrick, J.W. (2000) Amino acid determinants of alpha 7 nicotinic acetylcholine receptor surface expression. *J. Biol. Chem.* **275**: 13974-13985.
85. Drisdell, R.C., Manzana, E., Green, W.N. (2004) The role of palmitoylation in functional expression of nicotinic alpha7 receptors. *J. Neurosci.* **24**: 10502-10510.
86. Ungar, D. and Hughson, F.M. (2003) SNARE protein structure and function. *Annu. Rev. Cell Dev. Biol.* **19**: 493-517.

87. Liu, Z., Tearle, A.W., Nai, Q., Berg, D.K. (2005) Rapid activity-driven SNARE-dependent trafficking of nicotinic receptors on somatic spines. *J. Neurosci.* **25**: 1159-1168.
88. Cho, C.H., Song, W., Leitzell, K., Teo, E., Meleth, A.D., Quick, M.W., Lester, R.A. (2005) Rapid upregulation of alpha7 nicotinic acetylcholine receptors by tyrosine dephosphorylation. *J. Neurosci.* **25**: 3712-3723.
89. Ross, R.A., Spengler, B.A., Biedler, J.L. (1983) Coordinate morphological and biochemical interconversion of human neuroblastoma cells. *J. Natl. Cancer Inst.* **71**: 741-747.
90. Biedler, J.L., Roffler-Tarlov, S., Schachner, M., Freedman, L.S. (1978) Multiple neurotransmitter synthesis by human neuroblastoma cell lines and clones. *Cancer Res.* **38**: 3751-3757.
91. Kumari, S., Borroni, V., Chaudhry, A., Chanda, B., Massol, R., Mayor, S., Barrantes, F.J. (2008) Nicotinic acetylcholine receptor is internalized via a Rac-dependent, dynamin-independent endocytic pathway. *J. Cell Biol.* **181**: 1179-1193.
92. Bruneau, E., Sutter, D., Hume, R.I., Akaaboune, M. (2005) Identification of nicotinic acetylcholine receptor recycling and its role in maintaining receptor density at the neuromuscular junction in vivo. *J. Neurosci.* **25**: 9949-9959.
93. Bruneau, E.G. and Akaaboune, M. (2006) The dynamics of recycled acetylcholine receptors at the neuromuscular junction in vivo. *Development* **133**: 4485-4493.
94. Lawe, D.C., Chawla, A., Merithew, E., Dumas, J., Carrington, W., Fogarty, K., Lifshitz, L., Tuft, R., Lambright, D., Corvera, S. (2002) Sequential roles for phosphatidylinositol 3-phosphate and Rab5 in tethering and fusion of early endosomes via their interaction with EEA1. *J. Biol. Chem.* **277**: 8611-8617.

95. Zhang, S., Edelman, L., Liu, J., Crandall, J.E., Morabito, M.A. (2008) Cdk5 regulates the phosphorylation of tyrosine 1472 NR2B and the surface expression of NMDA receptors. *J. Neurosci.* **28**: 415-424.
96. Kastning, K., Kukhtina, V., Kittler, J.T., Chen, G., Pechstein, A., Enders, S., Lee, S.H., Sheng, M., Yan, Z., Haucke, V. (2007) Molecular determinants for the interaction between AMPA receptors and the clathrin adaptor complex AP-2. *Proc. Natl. Acad. Sci. U. S. A.* **104**: 2991-2996.
97. Huang, R., He, S., Chen, Z., Dillon, G.H., Leidenheimer, N.J. (2007) Mechanisms of homomeric alpha1 glycine receptor endocytosis. *Biochemistry* **46**: 11484-11493.
98. Royle, S.J., Bobanovic, L.K., Murrell-Lagnado, R.D. (2002) Identification of a non-canonical tyrosine-based endocytic motif in an ionotropic receptor. *J. Biol. Chem.* **277**: 35378-35385.
99. Strohlic, L., Cartaud, A., Cartaud, J. (2005) The synaptic muscle-specific kinase (MuSK) complex: new partners, new functions. *Bioessays* **27**: 1129-1135.
100. Wiesner, A. and Fuhrer, C. (2006) Regulation of nicotinic acetylcholine receptors by tyrosine kinases in the peripheral and central nervous system: same players, different roles. *Cell Mol. Life Sci.* **63**: 2818-2828.
101. Bruses, J.L., Chauvet, N., Rutishauser, U. (2001) Membrane lipid rafts are necessary for the maintenance of the (alpha)7 nicotinic acetylcholine receptor in somatic spines of ciliary neurons. *J. Neurosci.* **21**: 504-512.
102. Oshikawa, J., Toya, Y., Fujita, T., Egawa, M., Kawabe, J., Umemura, S., Ishikawa, Y. (2003) Nicotinic acetylcholine receptor alpha 7 regulates cAMP signal within lipid rafts. *Am. J. Physiol. Cell. Physiol.* **285**: C567-74.

103. Wang, L., Connelly, M.A., Ostermeyer, A.G., Chen, H.H., Williams, D.L., Brown, D.A. (2003) Caveolin-1 does not affect SR-BI-mediated cholesterol efflux or selective uptake of cholesteryl ester in two cell lines. *J. Lipid Res.* **44**: 807-815.
104. Wharton, J., Meshulam, T., Vallega, G., Pilch, P. (2005) Dissociation of insulin receptor expression and signaling from caveolin-1 expression. *J. Biol. Chem.* **280**: 13483-13486.
105. Oh, P., McIntosh, D.P., Schnitzer, J.E. (1998) Dynamin at the neck of caveolae mediates their budding to form transport vesicles by GTP-driven fission from the plasma membrane of endothelium. *J. Cell Biol.* **141**: 101-114.
106. Henley, J.R., Krueger, E.W., Oswald, B.J., McNiven, M.A. (1998) Dynamin-mediated internalization of caveolae. *J. Cell Biol.* **141**: 85-99.
107. Payne, C.K., Jones, S.A., Chen, C., Zhuang, X. (2007) Internalization and trafficking of cell surface proteoglycans and proteoglycan-binding ligands. *Traffic* **8**: 389-401.
108. Zhang, D., Manna, M., Wohland, T., Kraut, R. (2009) Alternate raft pathways cooperate to mediate slow diffusion and efficient uptake of a sphingolipid tracer to degradative and recycling compartments. *J. Cell. Sci.* **122**: 3715-3728.
109. de Araujo, M.E., Huber, L.A., Stasyk, T. (2008) Isolation of endocytic organelles by density gradient centrifugation. *Methods Mol. Biol.* **424**: 317-331.

Chapter 4

4 General Discussion

4.1 Conclusions

4.1.1 *Study One:* Oligomeric aggregates of amyloid β peptide 1-42 activate ERK/MAPK in SH-SY5Y cells via the $\alpha 7$ nicotinic receptor

- 1) A β 42 peptides aggregate into different structural forms under neutral and acidic pH. Neutral pH yields small globular oligomeric aggregates, with 3.0 to 3.8 nm height structures in abundance. Acidic pH yields elongated fibrillar structures tens of nanometres in length, comprised of oligomer-like subunits.
- 2) Oligomeric aggregates of A β 42 acutely activate the ERK/MAPK signalling pathway in human neuroblastoma cells at concentrations as low as 1 nM.
- 3) Fibrillar aggregates or non-aggregated A β 42 peptide do not activate the ERK/MAPK signalling pathway.
- 4) Activation of ERK/MAPK by oligomeric A β 42 is inhibited by MLA, an antagonist selective for the $\alpha 7$ nAChR.

4.1.2 *Study Two:* The $\alpha 7$ nicotinic receptor is internalized via a clathrin-independent, flotillin- or caveolin-associated endocytic pathway

- 1) Binding of the competitive antagonist α BTX causes internalization of the $\alpha 7$ nAChR.
- 2) Internalized $\alpha 7$ nAChR- α BTX complexes traffic through early and late endosomes to lysosomes.
- 3) Internalization is independent of clathrin and dynamin, and is not blocked by inhibition of actin polymerization or dominant negative RhoGTPases or dominant negative RalGTPase.
- 4) Flotillin 1 or caveolin 1 α may represent pathways for endocytosis.

4.2 Contributions to the Current State of Knowledge

The aim of the studies described in this thesis was to enhance our knowledge of the interaction of A β 42 peptides with the α 7 nAChR as well as factors which may regulate α 7 nAChR function. We present two distinct aspects of α 7 nAChR physiology; we identify a biologically important species of oligomeric A β 42 peptide aggregate capable of inducing signalling through the α 7 nAChR, and we determine a pathway for regulation of cell surface levels of the receptor in response to antagonist-induced receptor internalization.

In the study in Chapter 2, we compared the ability of different aggregates of A β 42 peptide to activate the ERK/MAPK signalling pathway. Following a previously established protocol, we pre-incubated synthetic A β 42 peptide to induce the formation of oligomers or fibrils. Characterization by AFM demonstrated that these preparations primarily contained oligomeric or fibrillar aggregates of A β 42 (Chapter 2, Figure 2.1). Oligomeric aggregates of A β 42 acutely activated ERK/MAPK at concentrations within the range of A β 42 measured in the CSF of AD subjects. Fibrillar aggregates or non-aggregated A β 42 did not activate ERK/MAPK. Induction of ERK1/2 phosphorylation by oligomeric A β 42 was inhibited by the α 7 nAChR-selective antagonist, MLA. In addition to fibrils, we observed a subpopulation of oligomers 2 nm in height, in fibrillar preparations. In oligomeric preparations, structures 3.0 - 3.8 nm in height were the most abundant, representing a biologically important oligomeric aggregate of A β 42 capable of inducing ERK/MAPK signalling through the α 7 nAChR.

Since the amyloid cascade hypothesis was proposed by Hardy and Higgins (1), suggesting that the generation and aggregation of A β peptides, particularly A β 42, were an initiating event in AD pathogenesis, considerable effort has been made to determine factors that contribute to the aggregation of these peptides and identify physiologically relevant species. Numerous studies have used AFM and/or SDS-PAGE to identify biologically important aggregates of A β 42 and equate their structure with receptor binding, cell signalling, toxicity, or membrane disruption. We employed AFM as a

method for characterizing our preparations because it provided a means for clearly distinguishing between different structural forms of A β 42 peptide. Using high resolution AFM, Mastrangelo and colleagues (2) determined that monomers of A β 42 peptide have an approximate height of 2 nm. Although the AFM instrument that we used likely introduced sample compression, thereby underestimating the true height of aggregates within our samples, we would propose that the globular structures we observed in abundance in oligomeric preparations of A β 42, with a height of 3.0 - 3.8 nm, were representative of dimers of A β 42 peptide. Also, given the distribution of aggregate sizes we observed, with subpopulations residing between 1.2 and 4.4 nm, that our oligomeric preparations contained a mixture of monomers and dimers.

In our fibrillar preparations of A β 42 peptide, we observed a subpopulation of oligomeric-like aggregates that appeared to represent distinct subunits of the greater fibrils. A recent study in a transgenic mouse model has proposed that plaques of A β 42 in the brain may act as reservoirs for the release of A β 42 oligomers (3). Plaques are thought to be primarily composed of A β 42 fibrils (4), our AFM analysis appears to support the hypothesis that these fibrils can disassemble into oligomeric species.

A β peptides have previously been observed to activate the ERK/MAPK signalling pathway through α 7 nAChR in hippocampus (5). An age-dependent increase in α 7 nAChR protein and coincident reduction in phosphorylated ERK2 protein in this brain region in a transgenic mouse model of AD may be a consequence of increased A β burden and the resulting chronic activation of α 7 nAChR-dependent signalling (5). The down-regulation of α 7 nAChR-dependent signalling is hypothesized to be a cellular mechanism that contributes to AD pathology (5). Given the evidence that α 7 nAChR largely plays a modulatory role in neurotransmission in the brain, by regulating the release of neurotransmitters (6 - 11), A β peptides likely have a complementary consequence in early stages of the disease process. Neurotransmitter release is enhanced by α 7 nAChR signalling through ERK/MAPK and increased ERK1/2-dependent phosphorylation of the synaptic vesicle co-ordinating protein, synapsin-1 (8), which

increases the proportion of vesicles available for release in the synaptic terminal (12). I would propose that oligomeric A β 42 may signal through α 7 nAChR and ERK/MAPK, as we have observed here, to synapsin-1 to alter activity of the neural network in the absence of cholinergic input, thereby contributing to disordered cognitive function in AD.

In the study described in Chapter 3, we investigated the pathway for internalization of the α 7 nAChR in response to binding the competitive antagonist, α BTX. α BTX binding induced internalization of α 7 nAChR- α BTX complexes that trafficked through early and late endosomes and accumulated in lysosomes (Chapter 3, Figure 3.4). Primary amino acid sequence analysis revealed two potential clathrin adaptor protein binding motifs within the large intracellular loop of the α 7 nAChR subunit. Site-directed mutagenesis experiments revealed these motifs did not alter internalization or subcellular trafficking of α 7 nAChR- α BTX complexes. Experiments employing over-expression of dominant negative dynamin 1 K44A or AP180-C did not block internalization, providing further evidence that internalization was independent of the clathrin endocytic machinery. Subsequent experiments, in which we disrupted clathrin-independent mechanisms of endocytosis, employing cytochalasin D to inhibit actin-polymerization or over-expression of dominant negative RhoGTPases or RalGTPase, did not have an effect on internalization either. Ultimately, co-localization experiments with flotillin 1 and caveolin 1 α revealed that these two lipid raft proteins represented pathways for endocytosis (Chapter 3, Figure 3.9). These experiments are the first to report internalization of the α 7 nAChR in response to binding α BTX and identify lipid raft proteins as the potential mediators.

Caveolins and flotillins represent distinct pathways for endocytosis (13 - 15) and are associated with separate lipid microdomains within the plasma membrane (15 - 19). These integral membrane proteins are differentially expressed and cell types that do not express caveolins often express flotillins as functional homologues in the organization of caveolae-like lipid rafts (19). The α 7 nAChR can be found in either caveolin- or flotillin-

positive lipid microdomains depending on the cell type (20, 21). However, caveolins are not expressed by brain neurons and flotillins are thought to be the primary integral membrane proteins associated with cholesterol-rich microdomains in brain neuronal plasma membranes (18, 22, 23). This evidence indicates that flotillins could represent the pathway for endocytosis of the $\alpha 7$ nAChR in the brain.

An important parallel can be drawn between factors that mediate endocytosis of flotillins and those which alter cell surface levels of the $\alpha 7$ nAChR. Endocytosis of flotillin 1 and flotillin 2 is regulated by activation of the tyrosine kinase, Fyn, leading to the redistribution of flotillins from the plasma membrane to late endosomes and lysosomes (24). Cell surface levels of the $\alpha 7$ nAChR in hippocampal neurons appear to be negatively regulated by tyrosine kinase activity that does not involve direct phosphorylation of the receptor, with tyrosine phosphorylation depressing $\alpha 7$ nAChR responses in brain slices to agonist stimulation (25).

Additionally, there is a relationship between the level of flotillin expression in the brain and the progression of AD, as flotillin levels increase with the development of senile plaque formation and the advancement of disease pathology (26). Increased A β 42 peptide production in transgenic mice leads to intracellular accumulation of A β 42 peptide in flotillin 1-positive endocytic vesicles (27). A β production appears to require flotillin-dependent clustering of the A β 42 precursor protein, APP, which promotes endocytosis and subsequent processing of APP into A β peptides (28). Increased levels of [3 H]-MLA binding as a measure of $\alpha 7$ nAChR protein in the frontal cortex are weakly correlated with A β plaque pathology in human subjects in the early stages of AD (29). Given the controversy surrounding the interaction between A β 42 peptides and the $\alpha 7$ nAChR, a shared pathway of endocytosis may account for some observations that the $\alpha 7$ nAChR mediates internalization of A β 42 peptides in neuronal cells (30).

Interestingly, a GPI-anchored cell surface molecule, lynx1, with a structure notably similar to α BTX and other elapid snake α -neurotoxins, has been identified in the brain (31). Lynx1 co-localizes with the $\alpha 7$ nAChR in many regions, including cortex,

hippocampus, amygdala, and thalamus (32). Studies in lynx 1 knock-out mice have revealed that lynx1 expression increases sensitivity of nAChRs to agonist stimulation, alters synaptic activity in the hippocampus, and enhances sensitivity of neurons to excitotoxicity, leading to neurodegeneration (33). Recombinant expression of α BTX in cells as a plasma membrane-tethered protein, as a model for lynx1 activity, retains its functions as an antagonist (34). Endogenous α -neurotoxin-like macromolecules in the brain may have a role in regulating $\alpha 7$ nAChR function.

4.3 Limitations of Research

The characterization of specific aggregate species of A β 42 peptides of particular biological relevance is a persistent and challenging problem. Although analysis by SDS-PAGE has been frequently used to characterize A β 42-containing solutions, this analysis does not reflect the nature of aggregates found in solution (35). AFM analysis relies upon the ability of samples to adsorb to the surface of a mica substrate. All species of aggregates within a solution containing A β 42 peptides may not be equally adsorbed to mica, thereby providing a misrepresentation of the true nature of the solution state of the peptide (36). Attempts have been made to circumvent these issues (35), but it is apparent that aggregates of A β 42 peptide in solution are likely in dynamic equilibrium and one can only infer from the method of analysis as to the true nature of the aggregates. However, AFM has been established as and remains a method for consistently discriminating between solutions containing oligomeric and fibrillar aggregates of A β 42 peptide (37).

Conducting experiments to examine the trafficking of transmembrane proteins is limited by evidence that demonstrates inhibition of one pathway for endocytosis, through over expression of dominant negative proteins for example (38), can lead to the up-regulation of an alternative endocytic mechanism. We have tried to overcome this by examining pathway specific markers in conjunction with the over-expression of dominant negative proteins; by comparing localization of internalized α BTX with that of transferrin, in the presence and absence of dominant negative proteins that disrupt

clathrin-dependent endocytosis. We also sought to examine the localization of endogenous proteins, EEA1 and LAMP1, to avoid artefacts that heterologous over-expression can create.

Experiments conducted in cell lines are not ideal, due to the possibility that cellular pathways or signalling mechanisms can be disrupted in comparison to their function in primary culture or *in vivo* (14). However, hippocampal neurons express limited amounts of $\alpha 7$ nAChR at the plasma membrane (39), and cell lines, as a model, often provide greater transfection efficiency and greater protein expression levels from which to ascertain clues as to how such proteins of low abundance may be regulated.

4.4 Suggestions for Future Studies

Many models have been proposed for the binding of A β 42 peptides to the $\alpha 7$ nAChR (40 - 42). However, the identification of a specific n-mer of A β 42 peptide that binds to the $\alpha 7$ nAChR as a ligand has yet to be identified in biochemical experiments. MALDI mass spectrometry of nAChR subunits has been performed successfully (43, 44). Cross-linking of $\alpha 7$ nAChR and bound A β 42 peptide oligomers, followed by MALDI mass spectrometry of these isolated complexes could provide a definitive answer as to the composition of these oligomers.

Further studies would be necessary to fully elucidate the mechanism of α BTX-induced internalization of the $\alpha 7$ nAChR. Knock-down of endogenous caveolin or flotillin expression through transfection with siRNA (15, 45) could determine if these lipid raft proteins were required for receptor internalization. Immunostaining with antibody directed against endogenous flotillin (19), in conjunction with the same for endogenous endosomal and lysosomal markers, such as EEA1 and LAMP1, to determine their localization with internalized $\alpha 7$ nAChR- α BTX complexes, could determine if flotillin and the $\alpha 7$ nAChR traffic together through intracellular membrane compartments.

4.5 Significance of the Research

The studies presented in this thesis further our knowledge of distinct aspects of $\alpha 7$ nAChR physiology. Oligomeric aggregates of A β 42 peptide are identified as the principal structural form of the peptide capable of activating intracellular signalling through the $\alpha 7$ nAChR. This has direct implications in AD pathology in that it reinforces the widely held hypothesis that small oligomers of A β 42 peptide, rather than A β 42 fibrils, represent the biologically active form of the peptide and that oligomeric A β 42-mediated signalling through $\alpha 7$ nAChR may play a role in the disease process. The studies also describe internalization of the $\alpha 7$ nAChR in response to binding the competitive antagonist, α BTX. This is the first time antagonist-induced internalization of the $\alpha 7$ nAChR has been reported. A unique pathway for endocytosis of the receptor is proposed, providing new insight into mechanisms that can regulate cell surface expression of the receptor.

4.6 References

1. Hardy, J.A. and Higgins, G.A. (1992) Alzheimer's disease: the amyloid cascade hypothesis. *Science* **256**: 184-185.
2. Mastrangelo, I.A., Ahmed, M., Sato, T., Liu, W., Wang, C., Hough, P., Smith, S.O. (2006) High-resolution atomic force microscopy of soluble Abeta42 oligomers. *J. Mol. Biol.* **358**: 106-119.
3. Koffie, R.M., Meyer-Luehmann, M., Hashimoto, T., Adams, K.W., Mielke, M.L., Garcia-Alloza, M., Micheva, K.D., Smith, S.J., Kim, M.L., Lee, V.M., Hyman, B.T., Spires-Jones, T.L. (2009) Oligomeric amyloid beta associates with postsynaptic densities and correlates with excitatory synapse loss near senile plaques. *Proc. Natl. Acad. Sci. U. S. A.* **106**: 4012-4017.
4. Glenner, G.G. (1989) Amyloid beta protein and the basis for Alzheimer's disease. *Prog. Clin. Biol. Res.* **317**: 857-868.
5. Dineley, K.T., Westerman, M., Bui, D., Bell, K., Ashe, K.H., Sweatt, J.D. (2001) Beta-amyloid activates the mitogen-activated protein kinase cascade via hippocampal alpha7 nicotinic acetylcholine receptors: In vitro and in vivo mechanisms related to Alzheimer's disease. *J Neurosci* **21**: 4125-33.
6. Gray, R., Rajan, A.S., Radcliffe, K.A., Yakehiro, M., Dani, J.A. (1996) Hippocampal synaptic transmission enhanced by low concentrations of nicotine. *Nature* **383**: 713-716.
7. Jones, I.W., Barik, J., O'Neill, M.J., Wonnacott, S. (2004) Alpha bungarotoxin-1.4 nm gold: a novel conjugate for visualising the precise subcellular distribution of alpha 7* nicotinic acetylcholine receptors. *J. Neurosci. Methods* **134**: 65-74.
8. Dickinson, J.A., Kew, J.N., Wonnacott, S. (2008) Presynaptic alpha 7- and beta 2-containing nicotinic acetylcholine receptors modulate excitatory amino acid release

- from rat prefrontal cortex nerve terminals via distinct cellular mechanisms. *Mol. Pharmacol.* **74**: 348-359.
9. Quarta, D., Naylor, C.G., Barik, J., Fernandes, C., Wonnacott, S., Stolerman, I.P. (2009) Drug discrimination and neurochemical studies in alpha7 null mutant mice: tests for the role of nicotinic alpha7 receptors in dopamine release. *Psychopharmacology (Berl)* **203**: 399-410.
 10. Livingstone, P.D., Srinivasan, J., Kew, J.N., Dawson, L.A., Gotti, C., Moretti, M., Shoaib, M., Wonnacott, S. (2009) Alpha7 and Non-Alpha7 Nicotinic Acetylcholine Receptors Modulate Dopamine Release in Vitro and in Vivo in the Rat Prefrontal Cortex. *Eur. J. Neurosci.* **29**: 539-550.
 11. Barik, J. and Wonnacott, S. (2006) Indirect modulation by alpha7 nicotinic acetylcholine receptors of noradrenaline release in rat hippocampal slices: interaction with glutamate and GABA systems and effect of nicotine withdrawal. *Mol. Pharmacol.* **69**: 618-628.
 12. Greengard, P., Valtorta, F., Czernik, A.J., Benfenati, F. (1993) Synaptic vesicle phosphoproteins and regulation of synaptic function. *Science* **259**: 780-785.
 13. Doherty, G.J. and McMahon, H.T. (2009) Mechanisms of endocytosis. *Annu. Rev. Biochem.* **78**: 857-902.
 14. Hansen, C.G. and Nichols, B.J. (2009) Molecular mechanisms of clathrin-independent endocytosis. *J. Cell. Sci.* **122**: 1713-1721.
 15. Glebov, O.O., Bright, N.A., Nichols, B.J. (2006) Flotillin-1 defines a clathrin-independent endocytic pathway in mammalian cells. *Nat. Cell Biol.* **8**: 46-54.
 16. Lang, D.M., Lommel, S., Jung, M., Ankerhold, R., Petrusch, B., Laessing, U., Wiechers, M.F., Plattner, H., Stuermer, C.A. (1998) Identification of reggie-1 and reggie-2 as plasmamembrane-associated proteins which cocluster with

activated GPI-anchored cell adhesion molecules in non-caveolar micropatches in neurons. *J. Neurobiol.* **37**: 502-523.

17. Bickel, P.E., Scherer, P.E., Schnitzer, J.E., Oh, P., Lisanti, M.P., Lodish, H.F. (1997) Flotillin and epidermal surface antigen define a new family of caveolae-associated integral membrane proteins. *J. Biol. Chem.* **272**: 13793-13802.
18. Kokubo, H., Helms, J.B., Ohno-Iwashita, Y., Shimada, Y., Horikoshi, Y., Yamaguchi, H. (2003) Ultrastructural localization of flotillin-1 to cholesterol-rich membrane microdomains, rafts, in rat brain tissue. *Brain Res.* **965**: 83-90.
19. Volonte, D., Galbiati, F., Li, S., Nishiyama, K., Okamoto, T., Lisanti, M.P. (1999) Flotillins/cavatellins are differentially expressed in cells and tissues and form a hetero-oligomeric complex with caveolins in vivo. Characterization and epitope-mapping of a novel flotillin-1 monoclonal antibody probe. *J. Biol. Chem.* **274**: 12702-12709.
20. Oshikawa, J., Toya, Y., Fujita, T., Egawa, M., Kawabe, J., Umemura, S., Ishikawa, Y. (2003) Nicotinic acetylcholine receptor alpha 7 regulates cAMP signal within lipid rafts. *Am. J. Physiol. Cell. Physiol.* **285**: C567-74.
21. Bruses, J.L., Chauvet, N., Rutishauser, U. (2001) Membrane lipid rafts are necessary for the maintenance of the (alpha)7 nicotinic acetylcholine receptor in somatic spines of ciliary neurons. *J. Neurosci.* **21**: 504-512.
22. Cameron, P.L., Ruffin, J.W., Bollag, R., Rasmussen, H., Cameron, R.S. (1997) Identification of caveolin and caveolin-related proteins in the brain. *J. Neurosci.* **17**: 9520-9535.
23. Wu, C., Butz, S., Ying, Y., Anderson, R.G. (1997) Tyrosine kinase receptors concentrated in caveolae-like domains from neuronal plasma membrane. *J. Biol. Chem.* **272**: 3554-3559.

24. Riento, K., Frick, M., Schafer, I., Nichols, B.J. (2009) Endocytosis of flotillin-1 and flotillin-2 is regulated by Fyn kinase. *J. Cell. Sci.* **122**: 912-918.
25. Cho, C.H., Song, W., Leitzell, K., Teo, E., Meleth, A.D., Quick, M.W., Lester, R.A. (2005) Rapid upregulation of alpha7 nicotinic acetylcholine receptors by tyrosine dephosphorylation. *J. Neurosci.* **25**: 3712-3723.
26. Kokubo, H., Lemere, C.A., Yamaguchi, H. (2000) Localization of flotillins in human brain and their accumulation with the progression of Alzheimer's disease pathology. *Neurosci. Lett.* **290**: 93-96.
27. Rajendran, L., Knobloch, M., Geiger, K.D., Dienel, S., Nitsch, R., Simons, K., Konietzko, U. (2007) Increased Abeta production leads to intracellular accumulation of Abeta in flotillin-1-positive endosomes. *Neurodegener Dis.* **4**: 164-170.
28. Schneider, A., Rajendran, L., Honsho, M., Gralle, M., Donnert, G., Wouters, F., Hell, S.W., Simons, M. (2008) Flotillin-dependent clustering of the amyloid precursor protein regulates its endocytosis and amyloidogenic processing in neurons. *J. Neurosci.* **28**: 2874-2882.
29. Ikonomic, M.D., Wecker, L., Abrahamson, E.E., Wu, J., Counts, S.E., Ginsberg, S.D., Mufson, E.J., Dekosky, S.T. (2009) Cortical alpha7 nicotinic acetylcholine receptor and beta-amyloid levels in early Alzheimer disease. *Arch. Neurol.* **66**: 646-651.
30. Nagele, R.G., D'Andrea, M.R., Anderson, W.J., Wang, H.Y. (2002) Intracellular accumulation of beta-amyloid(1-42) in neurons is facilitated by the alpha 7 nicotinic acetylcholine receptor in Alzheimer's disease. *Neuroscience* **110**: 199-211.
31. Miwa, J.M., Ibanez-Tallon, I., Crabtree, G.W., Sanchez, R., Sali, A., Role, L.W., Heintz, N. (1999) lynx1, an endogenous toxin-like modulator of nicotinic acetylcholine receptors in the mammalian CNS. *Neuron* **23**: 105-114.

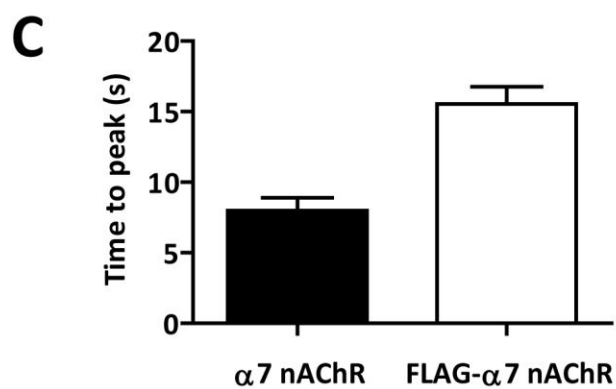
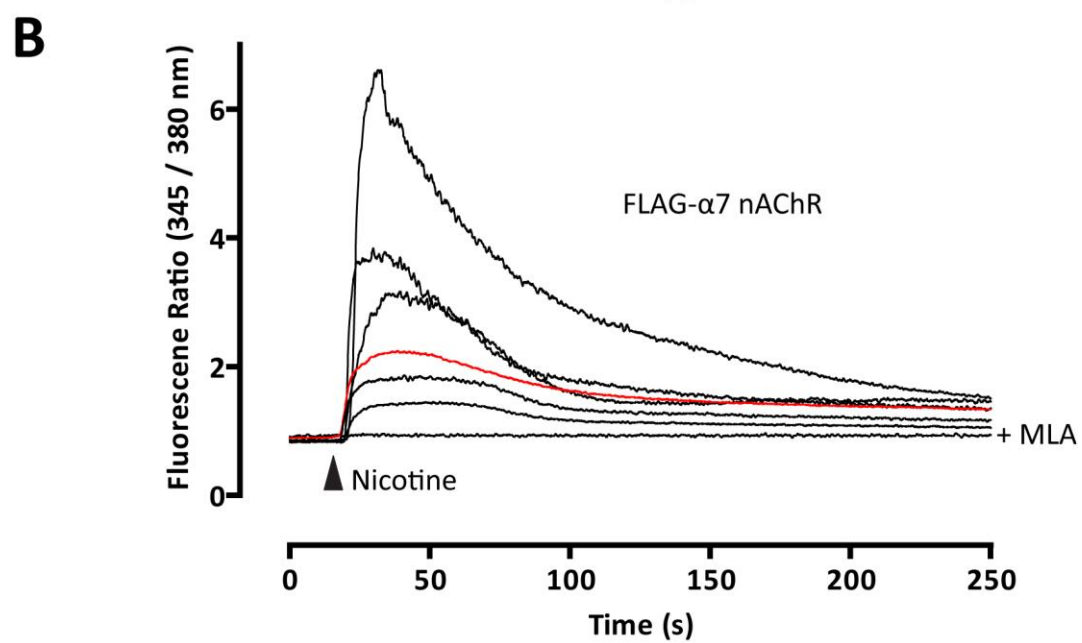
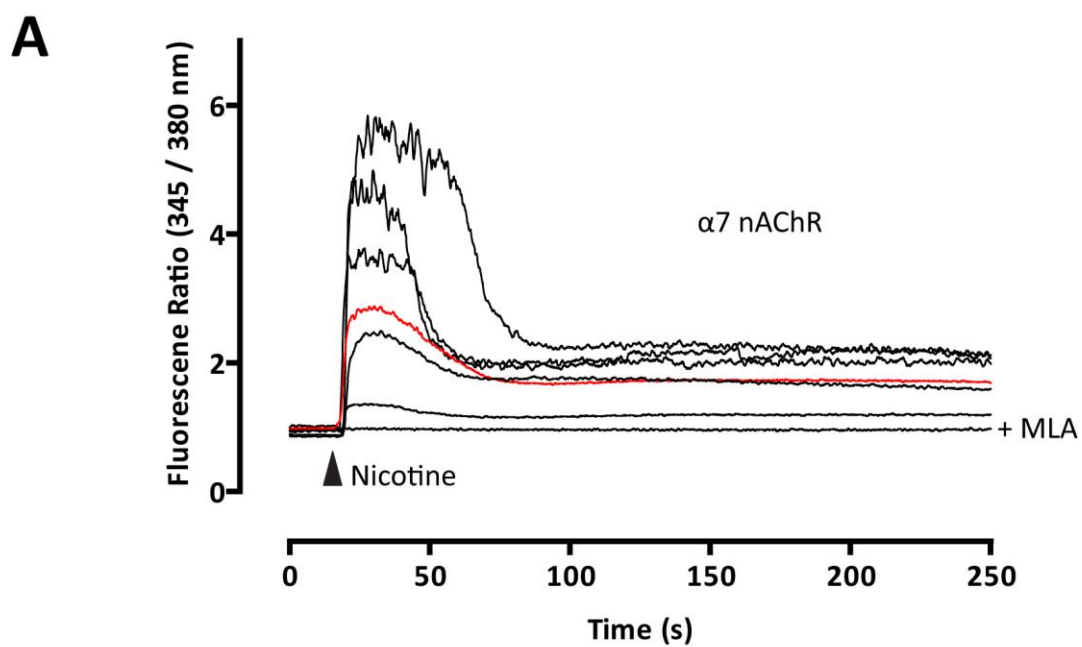
32. Ibanez-Tallon, I., Miwa, J.M., Wang, H.L., Adams, N.C., Crabtree, G.W., Sine, S.M., Heintz, N. (2002) Novel modulation of neuronal nicotinic acetylcholine receptors by association with the endogenous prototoxin lynx1. *Neuron* **33**: 893-903.
33. Miwa, J.M., Stevens, T.R., King, S.L., Caldarone, B.J., Ibanez-Tallon, I., Xiao, C., Fitzsimonds, R.M., Pavlides, C., Lester, H.A., Picciotto, M.R., Heintz, N. (2006) The prototoxin lynx1 acts on nicotinic acetylcholine receptors to balance neuronal activity and survival in vivo. *Neuron* **51**: 587-600.
34. Ibanez-Tallon, I., Wen, H., Miwa, J.M., Xing, J., Tekinay, A.B., Ono, F., Brehm, P., Heintz, N. (2004) Tethering naturally occurring peptide toxins for cell-autonomous modulation of ion channels and receptors in vivo. *Neuron* **43**: 305-311.
35. Hepler, R.W., Grimm, K.M., Nahas, D.D., Breese, R., Dodson, E.C., Acton, P., Keller, P.M., Yeager, M., Wang, H., Shughrue, P., Kinney, G., Joyce, J.G. (2006) Solution state characterization of amyloid beta-derived diffusible ligands. *Biochemistry* **45**: 15157-67.
36. Ding, T.T. and Harper, J.D. (1999) Analysis of amyloid-beta assemblies using tapping mode atomic force microscopy under ambient conditions. *Methods Enzymol.* **309**: 510-525.
37. B., S.W., Jr, Dahlgren, K.N., Krafft, G.A., LaDu, M.J. (2003) In vitro characterization of conditions for amyloid-beta peptide oligomerization and fibrillogenesis. *J Biol Chem* **278**: 11612-22.
38. Damke, H., Baba, T., van der Bliek, A.M., Schmid, S.L. (1995) Clathrin-independent pinocytosis is induced in cells overexpressing a temperature-sensitive mutant of dynamin. *J. Cell Biol.* **131**: 69-80.
39. Mielke, J.G. and Mealing, G.A. (2009) Cellular distribution of the nicotinic acetylcholine receptor alpha7 subunit in rat hippocampus. *Neurosci. Res.* **65**: 296-306.

40. Espinoza-Fonseca, L.M. and Trujillo-Ferrara, J.G. (2006) Fully flexible docking models of the complex between alpha7 nicotinic receptor and a potent heptapeptide inhibitor of the beta-amyloid peptide binding. *Bioorg. Med. Chem. Lett.* **16**: 3519-3523.
41. Espinoza-Fonseca, L.M. (2004) Molecular docking of four beta-amyloid1-42 fragments on the alpha7 nicotinic receptor: delineating the binding site of the Abeta peptides. *Biochem Biophys Res Commun* **323**: 1191-6.
42. Espinoza-Fonseca, L.M. (2004) Base docking model of the homomeric alpha7 nicotinic receptor-beta-amyloid(1-42) complex. *Biochem Biophys Res Commun* **320**: 587-91.
43. Lukas, R.J., Tubbs, K.A., Krivoshein, A.V., Bieber, A.L., Nelson, R.W. (2002) Mass spectrometry of nicotinic acetylcholine receptors and associated proteins as models for complex transmembrane proteins. *Anal. Biochem.* **301**: 175-188.
44. Kasheverov, I., Utkin, Y., Weise, C., Franke, P., Hucho, F., Tsetlin, V. (1998) Reverse-phase chromatography isolation and MALDI mass spectrometry of the acetylcholine receptor subunits. *Protein Expr. Purif.* **12**: 226-232.
45. Galvez, B.G., Matias-Roman, S., Yanez-Mo, M., Vicente-Manzanares, M., Sanchez-Madrid, F., Arroyo, A.G. (2004) Caveolae are a novel pathway for membrane-type 1 matrix metalloproteinase traffic in human endothelial cells. *Mol. Biol. Cell* **15**: 678-687.

Appendices

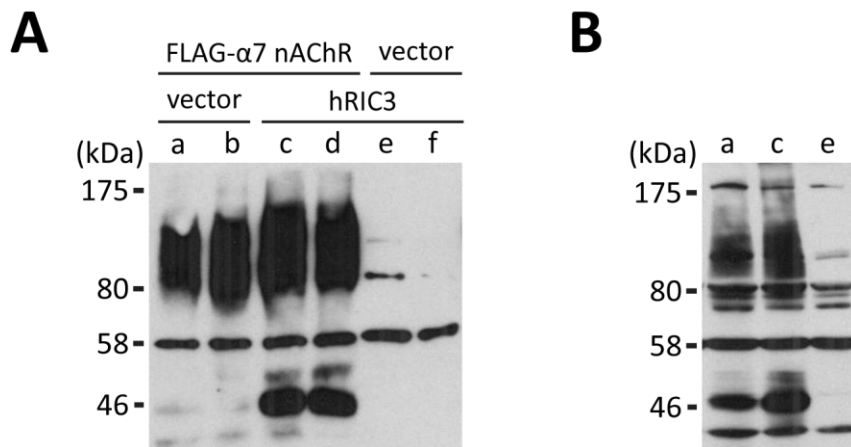
Appendix A. Addition of the FLAG epitope to the $\alpha 7$ nAChR subunit slows receptor-dependent Ca^{2+} responses to the agonist nicotine.

(A – C) HEK 293 cells co-transfected with cDNA for HA-hRIC3 and either wild-type $\alpha 7$ nAChR or FLAG- $\alpha 7$ nAChR subunit were loaded with the Ca^{2+} -sensitive dye fura-2, perfused with HEPES buffered Krebs-Ringer's solution, and whole-cell fluorescence emission of fura-2 (510 nm) was monitored at alternating excitation wavelengths (345 and 380 nm). An increase in the ratio of fluorescence emission at excitations 345 / 380 nm indicated an increase in intracellular Ca^{2+} . Nicotine (1 mM) was applied for 0.5 s (arrowhead). The $\alpha 7$ nAChR antagonist MLA (10 μM) was included in perfusion buffer prior to application of nicotine (+ MLA). **(A)** Changes observed in five different HEK 293 cells transfected with wild-type $\alpha 7$ nAChR subunit and HA-hRIC3 cDNA. Tracings are superimposed to illustrate the variability in responses observed between cells and between transfections. Average tracing from 20 cells (red). **(B)** Changes observed in five different cells transfected with FLAG- $\alpha 7$ nAChR subunit and HA-hRIC3 cDNA. Average tracing from 30 cells (red). **(C)** Time to peak response as measured by the difference between the time of application of nicotine and the time when fluorescence ratio reached maximum. Bars represent mean \pm SEM, $n = 20$ cells for wild-type $\alpha 7$ nAChR subunit and $n = 30$ cells for FLAG- $\alpha 7$ nAChR subunit, from four independent experiments.



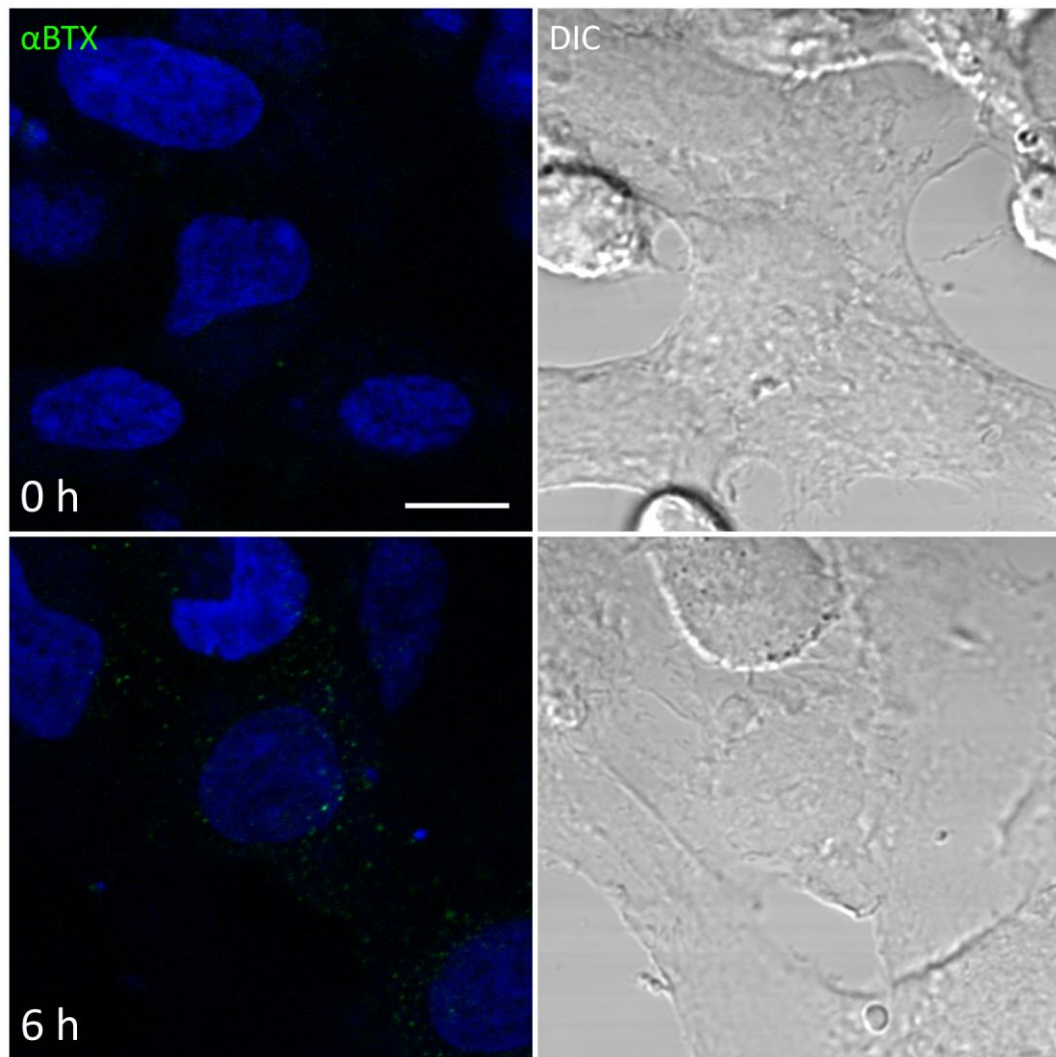
Appendix B. Cell surface biotinylation of HEK 293 cells transfected with FLAG- α 7 nAChR cDNA with or without co-transfection with HA-hRIC3 cDNA.

HEK-293 cells were transfected with FLAG- α 7 nAChR cDNA and empty vector DNA; FLAG- α 7 nAChR and HA-hRIC3 cDNA, or empty vector DNA and HA-hRIC3 cDNA. Eighteen hours after transfection, cells were transferred to ice and incubated with EZ-Link sulfo-NHS-SS-biotin (1.5 mg/mL) in HBSS for 1 h. To quench unreacted sulfo-NHS-SS-biotin, cells were subsequently washed and incubated with chilled HBSS containing glycine (100 mM) for 30 min. Cells were then lysed and equal amounts of protein from each transfection (400 μ g) were made up to equal volumes in lysis buffer (500 μ L) and rotated with NeutrAvidin agarose beads (100 μ L of slurry; biotin binding capacity of 1 - 2 mg/mL) at 4 °C for 1 h to precipitate sulfo-NHS-SS-biotin bound proteins. NeutrAvidin beads were washed with lysis buffer and biotinylated proteins were eluted by heating in Laemmli sample buffer. **(A)** Precipitated biotinylated proteins immunoblotted with anti-FLAG antibody and HRP-conjugated secondary antibody. Lanes (a) and (b), HEK 293 cells transfected with FLAG- α 7 nAChR subunit cDNA and empty vector DNA; lanes (c) and (d), cells co-transfected with FLAG- α 7 nAChR subunit and HA-hRIC3 cDNA, lanes (e) and (f), cells co-transfected with empty vector DNA and HA-hRIC3 cDNA. **(B)** Crude lysate fractions from lanes (a), (c) and (e), immunoblotted for FLAG epitope. Immunoblots are from a preliminary experiment.



Appendix C. De novo cell surface $\alpha 7$ nAChR following α BTX-induced receptor internalization.

HEK 293 cells transfected with cDNA for FLAG- $\alpha 7$ nAChR and HA-hRIC3 were incubated on ice for 1 h with unlabelled α BTX, washed, and transferred to 37 °C for 0 or 6 h. At the end of the incubation, the cells were returned to ice and incubated with Alexa Fluor 647- α BTX for 1 h to detect the appearance of new receptors on the cell surface. Nuclei were stained with DAPI prior to fixing and mounting. Images of Alexa Fluor 647- α BTX (green) and DAPI (blue) were collected from single z-sections on a confocal microscope and colour combined. Images are representative of 16 to 18 cells per time point, from three cover slips, a preliminary experiment. Bar, 10 μ m.



Appendix D. Permission for reproduction from *Neurochemistry International*

The copyright policy of Elsevier, the publisher of *Neurochemistry International* is as follows^b:

How authors can use their own journal articles

Authors can use their articles for a wide range of scholarly, non-commercial purposes as outlined below. These rights apply for all Elsevier authors who publish their article as either a subscription article or an open access article.

We require that all Elsevier authors always include a full acknowledgement and, if appropriate, a link to the final published version hosted on Science Direct.

For open access articles these rights are separate from how readers can reuse your article as defined by the author's choice of Creative Commons user license options.

Authors can use either their accepted author manuscript or final published article for:

- ✓ Inclusion in a thesis or dissertation

^b <http://www.elsevier.com/journal-authors/author-rights-and-responsibilities#author-use>

Curriculum Vitae

Name: Kirk F Young

Education: The University of Western Ontario
Schulich School of Medicine and Dentistry
Department of Pharmacology and Toxicology
London, Ontario, Canada
1998 – 2002 B.M.Sc (Hons)

Honours and Awards: Ontario Graduate Scholarship in Science and Technology
2003 – 2004

Mogenson Trust Graduate Student Travel Award
2004

Canadian Institutes of Health Research Summer Program on
Aging
2006

Work Experience: Undergraduate Research Assistant
Laboratory of Professor Kem A. Rogers
Department of Anatomy and Cell Biology
Schulich School of Medicine and Dentistry
The University of Western Ontario
2001 – 2002

Undergraduate Research Assistant
Laboratory of Professor R. Jane Rylett
Robarts Research Institute
Department of Physiology and Pharmacology
Schulich School of Medicine and Dentistry
The University of Western Ontario
2002

Graduate Research Assistant
Laboratory of Professor R. Jane Rylett
Robarts Research Institute
Department of Physiology and Pharmacology
Schulich School of Medicine and Dentistry
The University of Western Ontario
2002 – 2010

Teaching:

Teaching Assistantship
The University of Western Ontario
Physiology 310 – Mammalian Physiology
2002 – 2003

Teaching Assistantship
The University of Western Ontario
Physiology 310 – Mammalian Physiology
2003 – 2004

Teaching Assistantship
The University of Western Ontario
Pharmacology 357 – Fundamentals of Pharmacology and
Toxicology (Laboratory)
2004 – 2005

Teaching Assistantship
The University of Western Ontario
Physiology 130 – Human Physiology
2005 – 2006

Teaching Assistantship
The University of Western Ontario
Physiology 314a – Cellular Physiology
2006

Teaching Assistantship
The University of Western Ontario
Physiology 468b – Cellular and Molecular Neurobiology
2007

Professional Activity:

Cell Biology Research Group
Robarts Research Institute
2002 – 2010

Invited Speaker
Robarts Research and MaRS 'Rush Hour Research' Fundraiser
2006

Invited Speaker
Robarts Research Presentation of the J. Allyn International
Prize in Medicine
2006, 2007

Publications:

Young KF and Rylett RJ (2004) Oligomeric Amyloid- β 1-42 Activates Extracellular Signal Regulated Kinases ERK1 and ERK2 of The Mitogen Activated Protein Kinase Pathway in SH-SY5Y Human Neuroblastoma Cells. *Neurobiology of Aging* 25(S2):150.

Young KF and Rylett RJ (2007) Endocytosis and Trafficking of α 7 Nicotinic Acetylcholine Receptors. Program No. 575.2/K2. 2007 Neuroscience Meeting Planner. San Diego, CA: Society for Neuroscience, 2007. Online.

Young KF and Rylett RJ (2008) Activation of α 7 Nicotinic Acetylcholine Receptors Attenuates Constitutive Internalization. Abstract No. C-B3036. Montreal, QC, Canada: 2nd Annual Canadian Neuroscience Meeting, 2008. Online.

Young KF, Pasternak SH, and Rylett RJ (2009) Oligomeric Aggregates of Amyloid β Peptide 1-42 Activate ERK/MAPK in SH-SY5Y Cells via the α 7 Nicotinic Receptor. *Neurochemistry International* 55: 796-801.

Beraldo FH, Arantes CP, Santos TG, Queiroz NG, Young K, Rylett RJ, Markus RP, Prado MA, and Martins VR (2010) Role of α 7 Nicotinic Acetylcholine Receptor in Calcium Signaling Induced by Prion Protein Interaction with Stress-Inducible Protein 1. *Journal of Biological Chemistry* 285(47): 36542-50.

Presentations:

Young, KF and Rylett RJ. Human Lysine Deficient 1 Kinase Interacts with Choline Acetyltransferase in Human Neuroblastoma IMR 32 Cells. London, ON, Canada: University of Western Ontario Pharmacology and Toxicology Programme Poster Day, 2002.

Young, KF and Rylett RJ. Oligomeric Amyloid- β 1-42 Activates Extracellular Signal Regulated Kinases ERK1 and ERK2 of the Mitogen Activated Protein Kinase Pathway in SH-SY5Y Human Neuroblastoma Cells. Philadelphia, PA, USA: The 9th International Conference on Alzheimer's Disease and Related Disorders, 2004.

Young, KF and Rylett RJ. Endocytosis and Trafficking of α 7 Nicotinic Acetylcholine Receptors. Program No. 575.2/K2. 2007 Neuroscience Meeting Planner. San Diego, CA: Society for Neuroscience, 2007.

Young, KF and Rylett RJ. Activation of α 7 Nicotinic Acetylcholine Receptors Attenuates Constitutive Internalization. Abstract No. C-B3036. Montreal, QC, Canada: 2nd Annual Canadian Neuroscience Meeting, 2008.